AN ABSTRACT OF THE THESIS OF

Chung-Chu Teng for the degree of Master of Ocean Engineering in Civil Engineering presented on March 10, 1983

Title: HYDRODYNAMIC FORCES ON A HORIZONTAL CYLINDER UNDER WAVES AND CURRENT

Redacted for Privacy

ABSTRACT APPROVED: Dr. John H. Nath

By assuming the linear superposition principle to be valid, the hydrodynamic forces on a horizontal cylinder under waves and current are examined. In this study, towing a cylinder in waves is used to simulate a cylinder under waves and current. The experimental technique is proved valid through theoretical considerations and experimental investigations. For large current velocity (or high tow speed), the drag coefficient for waves and current approaches that for steady flow. If the current is large enough, these two values are nearly identical.

In addition, the behavior of force coefficients for a horizontal cylinder in waves only with moderately large Reynolds number, Keulegan-Carpenter number and frequency parameter is examined. The

results show that the forces on a horizontal cylinder in waves are smaller than those for planar oscillatory flow.

Whether the total acceleration or local acceleration should be used in the inertia term is a debatable point for using the Morison equation. To study this problem, the similarities and differences between these two accelerations for different water depths and wave heights are examined. The results show there is no evident difference in force prediction if the related force coefficients are used.

To check the suitability of this data for determining C_d and/or C_m, an indicator, RR, is developed for the horizontal smooth cylinder in waves and current.

HYDRODYNAMIC FORCES ON A HORIZONTAL CYLINDER UNDER WAVES AND CURRENT

by

Chung-Chu Teng

A THESIS

submitted to

Oregon State University

in partial fulfillment of
the requirements for the
degree of

Master of Ocean Engineering

Commencement June 1983

APPROVED:

Redacted for Privacy

Professor of Civil Engineering in Charge of Major

Redacted for Privacy

Head of Department of Civil Engineering

Redacted for Privacy

Dean of Graduate School

Date thesis is presented March 10, 1983

Typed by Word Processing Specialists for Chung-Chu Teng

ACKNOWLEDGEMENTS

The author would like to express his sincere gratitude to his major professor, Dr. John H. Nath, for his guidance, encouragement and support throughout this study. Acknowledgements must be made to Dr. Robert T. Hudspeth and Dr. Charles K. Sollitt for their review and advice on the writing of this thesis.

During the study, the author received graduate research assistantship funds from the American Petroleum Institute, National Science Foundation, OSU Sea Grant Program and NOAA Data Buoy Program. Their support is gratefully acknowledged.

The author would also like to express his thanks to his brother Chung-Chian, his sisters Nai-Jan and Ming-Hwa, his cousin Louise Yu and some friends in OSU for their concern and encouragement.

This thesis and the greatest thanks are dedicated to his parents, Pao-Shin and Mien-Yuan, for their love and patience throughout all these years.

TABLE OF CONTENTS

LIST OF FIGURES

LIST OF FIGURES
(Continued)

LIST OF FIGURES
(Continued)

LIST OF TABLES

HYDRODYNAMIC FORCES ON A HORIZONTAL CYLINDER UNDER WAVES AND CURRENT

1. INTRODUCTION

1.1 Horizontal Cylinder in Waves

Wave induced forces on cylinders have been investigated mostly for vertical cylinders or horizontal cylinders in planar oscillatory flow. Little research has been done on horizontal cylinders in waves in spite of the common use of horizontal members in many offshore structures and ocean pipelines.

The significant difference between a horizontal cylinder in waves and a vertical cylinder (or a horizontal cylinder subjected to planar oscillatory flow) is that the former experiences orbital motion of the fluid particles around the axis of the cylinder.

In wavy flow, the wake formed over a horizontal cylinder will rotate around the cylinder. It will be swept back and forth in an oscillatory way only for cylinders near the sea bottom or in shallow water. The stagnation point on the cylinder will rotate around the horizontal cylinder as the waves pass.

For vertical smooth cylinders, the vertical force component parallel to the cylinder axis is probably negligible compared to the in-line force and the transverse vortex force. However, for the horizontal cylinder, the vertical force component due to the orbital motion of the water particle is significant.

The presence of a vertical velocity will affect the hydrodynamic force. By increasing the ratio of water particle velocity amplitudes, w_m/u_m, where w_m is the maximum vertical velocity and u_m is the maximum horizontal velocity, the drag force and drag coefficient for the horizontal cylinder will be reduced. Maull and Norman (1978) examined the hydrodynamic forces on the horizontal cylinder under waves, and showed the above results. Ramberg and Niedzweki (1982) obtained the same trend and their results agreed well with those from Maull and Norman, which will be shown later.

From preliminary studies by Sarpkaya (1982) for cylinders oscillating normal to harmonic planar flow, Sarpkaya and Isaacson (1981) state that the force coefficients, C_d and C_m, for $w_m/u_m=1$ and $K=20$ are about one half of those for $w_m/u_m=0$. Thus, the use of force coefficients from planar oscillatory flow may overpredict the actual forces on a stationary horizontal cylinder in waves by as much as 100%. This conclusion was also indicated by Ramberg and Niedzwecki (1982). It was shown that a similar trend was experienced for experimentation reported in Nath (1982) and reiterated herein.

1.2 Current Effect

In the open sea, there are currents generated by wind, earth gravity, tide and waves. Ocean waves in general propagate on currents, not on still water. There are two major categories when the waves and current problem is studied. What are the kinematics and

dynamics in the flow field when, (i) a wave train of given height and period propagates from still water into a current field; and (ii) a wave height and period are specified in the combined state with the current. It is known that the characteristics change [for category (i)] due to the hydrodynamic interactions when a wave encounters a current. That is, if the current is in the direction of the wave, the wave amplitude decreases and the wave length increases. But, if the current opposes the waves, the wave length decreases and the amplitude increases, making the wave steeper (Longuet-Higgins and Stewart, 1961). Due to some certain difficulties, very few papers in the open literature have discussed how to separate current from waves when the waves and current condition is given [category (ii)]. But, if the linear superposition principle is assumed, it will be easier to separate the current velocity from the waves. When dealing with the waves and current problem one should state clearly the coordinate systems involved. There are three coordinate systems that can be used to describe the flow field under waves and current: (1) stationary (fixed) coordinate system, (2) coordinate system moving with the surface current velocity, and (3) coordinate system moving with the wave celerity.

An excellent review on the interaction of wave and currents was presented by Peregrine (1976) who gave appropriate physical and mathematical details on almost all kinds of conditions for wave-current interaction.

Hydrodynamic forces on marine structures are directly related to the kinematics and dynamics of water particles, and are significantly affected by the presence of currents. Hedges (1979) and Dalrymple (1973) indicated that neglecting the current in a wave field can give rise to a significant error in the evaluation of the kinematics and in the wave force analysis. Tung and Huang (1973) examined the combined effects with spectral analysis. They concluded that the presence of a current can bring considerable change to the hydrodynamic forces and omission of the current will cause underestimates because the force spectral peak with current is greater than without current.

In the past, the phenomenon of wave-current interaction was usually ignored because it was not fully understood. Because it is difficult to generate currents in conjunction with laboratory waves, we do not have much experimental data to test existing interaction theories. In addition, forces on cylinders from waves and current are also difficult to evaluate. In the present study, towing a cylinder in the wave tank is used as an alternative to providing a current with waves. It will be seen that this is equivalent to the superposition principle.

Frequently, the Morison equation is used by superimposing the current velocity on the wave-induced horizontal water particle velocity for predicting hydrodynamic forces from waves and current. There is a bias to the wake structure because of the mean flow. It affects the time-dependent forces, thence the force coefficients. So, the

force coefficients for waves and current may be different from those obtained under planar oscillatory flow (Sarpkaya, 1976) wavy flows (Nath, 1982) and ocean tests (Kim and Hibbard, 1975) and need to be determined.

1.3 Scope of the Present Study

The main consideration of this study is the hydrodynamic force on a horizontal circular cylinder under waves and current [category (ii) defined above]. The force coefficients for a horizontal cylinder, either in waves or under waves and current, are determined experimentally for Reynolds number up to 5×10^5. Some differences of wave force coefficients between a horizontal cylinder in waves and in planar oscillatory flow (or a vertical cylinder in waves) are shown. Whether the wave and force data are well-conditioned for determining the drag and/or the inertia coefficient should be determined before these coefficients are adopted. A method with associated criteria is proposed for evaluating the suitability of the data under waves and wave plus current.

The kinematics for the linear superposition of waves and current are compared to those for waves plus towing on the basis of theory and experimentation. The results for waves plus towing can be used for waves and current <u>if the linear superposition principle is assumed</u>.

The differences between using total acceleration and local acceleration in the inertia term are examined for both waves only and the waves and current condition.

2. THEORETICAL CONSIDERATIONS

2.1 Combined Flow Field under Waves and Current

When the Morison equation is used to predict hydrodynamic forces on offshore structures, the kinematics related to the design wave and current condition need to be known. Force coefficients determined from experimental measurements are very dependent on the flow kinematics used. In this section, the combined flow field under waves and current is discussed.

The combined flow field is considered with respect to the fixed coordinate axes and the coordinates moving with the current velocity U (see Fig. 2-1). When the current is in the direction of the waves,

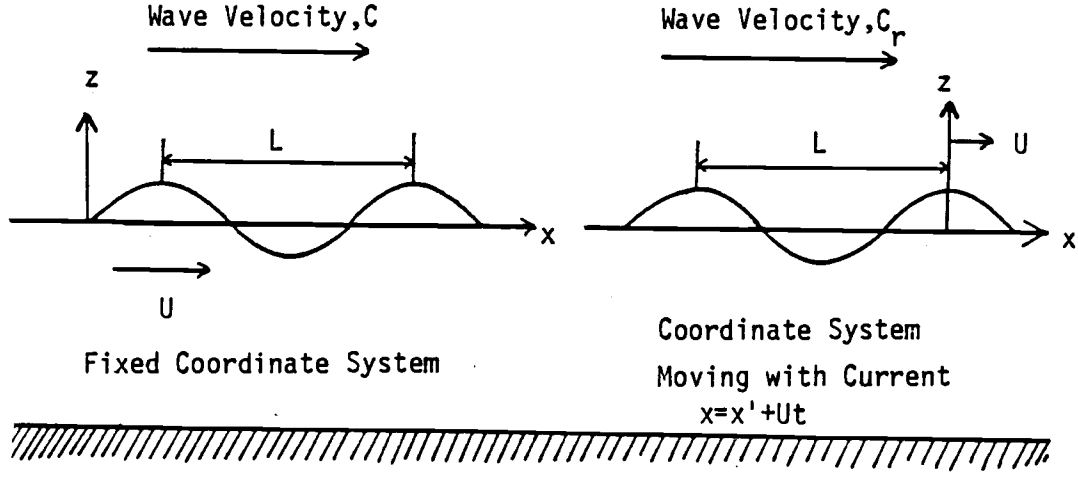

Fig. 2-1 Definition Sketch for Waves and Current

the wave celerity relation between these two coordinate systems is:

$$C = C_r + U \tag{2.1}$$

in which C is the wave celerity with respect to the fixed coordinates and C_r is the relative wave celerity with respect to coordinates moving with U (or quasi-still water).

By introducing $C = L/T$ and $C_r = L/T_r$, the following expression can be obtained.

$$\omega = \sigma + kU \tag{2.2}$$

in which ω is the frequency with respect to the fixed coordinates, σ is the frequency with respect to the moving coordinates and $k = 2\pi/L$ is the wave number.

For generality, Eq. (2.2) can be written as

$$\sigma = \omega \pm kU \tag{2.3}$$

in which the negative sign is taken when current follows with the waves and the positive sign is taken as the current opposes the waves.

If linear wave theory is applied, the dispersion relation of this flow field can be obtained as follows:

$$\sigma^2 = (\omega \pm kU)^2 = gk \tanh kh \tag{2.4}$$

When evaluating the kinematics and dynamics under the combined flow field of waves and current [for category (ii), with specified wave height and wave period], there are two possible considerations: (1) including the interactive effect and (2) considering the linear superposition principle.

Considering the interactive effect, Dalrymple (1973) proposed a stream function model for nonlinear waves on shear currents in which the shear current can be represented with a linear or bilinear (formed by two straight lines) velocity profile. The stream function perturbation series for the linear current model was assumed as

$$\Psi(x,z) = (C-U_b)z - \frac{(U_s-U_b)(h+z)^2}{2h} + \sum_{n=2}^{NN+1} X(n) \sinh \frac{2\pi(n-1)(h+z)}{L} \cos \frac{2\pi(n-1)x}{L} \qquad (2.5)$$

in which the X(n)s are unknowns and NN represents the order of the wave theory. The current velocity in U_b and U_s are at the bottom and surface respectively. Dalrymple (1973) defined an objective function (OF) with two Lagrangain multipliers, λ_1 and λ_2.

$$OF = E_1 + \lambda_1 E_2 + \lambda_2 E_3$$

$$= \frac{2}{L} \int_0^{L/2} [Q(x)-\bar{Q}]^2 dx + \lambda_1 \frac{2}{L} \int_0^{L/2} \eta(x)dx + \lambda_2 [\eta(0)-\eta(\frac{L}{2}) - H] \tag{2.6}$$

in which Q is the Bernoulli constant, $\bar{Q} = \frac{2}{L} \int_0^{L/2} Q(x)dx$, and η is the free surface elevation. By minimizing the OF, with respect to $L, \Psi(x,\eta)$, λ_1, λ_2 and all the $X(n)$s, small corrections to these unknown coefficients, may be found and then are added to the previous iterative estimates for the unknowns. The process must be iterated a number of times for proper convergence. After evaluating the stream function, $\Psi(x,z)$, the components of water particle velocity under waves and current can be found by

$$u = - \frac{\partial \Psi}{\partial z} + C \tag{2.7}$$

$$w = \frac{\partial \Psi}{\partial x} \tag{2.8}$$

in which the derivative of Ψincludes the interactive effect.

Neglecting the interactive effect, the linear superposition principle can be used to predict the kinematics under waves and current. The kinematics are then expressed as

$$u(x,z,t) = U(z,t) + u_w(x,z,t) \tag{2.9}$$

and

$$w(x,z,t) = w_w(x,z,t) \tag{2.10}$$

in which the u_w and w_w are the kinematics caused by waves alone and can be obtained by using one of two different methods. One method is by using the wave period from the fixed coordinate system in conjunction with the still water condition. The other method is to use the moving coordinate system (quasi-still water) in order to evaluate u_w and w_w. The second method should yield a better estimate for L than the former one.

Although the importance of the interactive effect of the waves and current has been known for a long time (c.f. Longuet-Higgins and Stewart 1961, Dalrymple 1973, Tung and Huang 1973), the linear superposition principle is still widely used for both research (c.f. Bishop 1978, Dean 1979, Bernitsas 1979) and the design of offshore structures. The reasons researchers and designers use the simple superposition principle instead of some other theory are:

(I) The complex fluid-mechanic phenomenon, where the interaction of waves and current is taken into consideration, may not be fully

understood, and for laboratory studies it is difficult to generate waves and current simultaneously. In addition, it is difficult to verify the accuracy of, thence the validity of, existing wave-current theories.

(II) From the engineering design point of view, the linear superposition principle may be sufficient and valid with a suitable factor of safety and design experience.

(III) When an analytical theory or equation is derived, the current effect will be easily observed by using the superposition principle. Also, it is convenient for deriving. For other models, the current effect is implicit in the combined kinematics.

(IV) With measured force data only, the current velocity can be evaluated if the superposition principle is assumed (see Dalrymple 1973).

Dalrymple (1973) compared the horizontal velocity profile predicted by his stream function shear current model to that by the superposition principle where the wave kinematics from still water (fixed coordinates) were added to the current. (That is, the wave period was NOT modified to that in quasi-still water.) He found the differences between these two are small in deep water (1.1% under wave crest and 11.1% under wave trough) and the error becomes larger for shallow water (13.9% under wave crest and 29.5% under trough in his example).

In this study, linear superposition principle is used.

2.2 Modified Morison Equation

Morison et al (1950) proposed a mathematical equation to calculate the forces on a vertical pile exerted by unbroken surface waves, the so-called Morison equation. This equation represents a sum of drag force (F_D) and inertia force (F_I).

$$F = C_d \frac{1}{2} \rho D u|u| + C_m \frac{\rho \pi D^2}{4} \frac{\partial u}{\partial t} \tag{2.11}$$

where F = horizontal force per unit length

D = pile diameter

ρ = water mass density

C_d = drag coefficient

C_m = inertia coefficient

u = horizontal component of water particle velocity

$\frac{\partial u}{\partial t}$ = horizontal component of water particle local acceleration

Wave Forces on a Horizontal Cylinder

The Morison equation can be extended to evaluate wave forces on a horizontal cylinder. Under this circumstance, the elliptical orbits of water particles should be considered, so the vector form is utilized to describe the hydrodynamic forces on a horizontal cylinder. The kinematics and related forces are assumed to be aligned as shown in Fig. 2-2.

Because the direction and period of the lift force are ambiguous

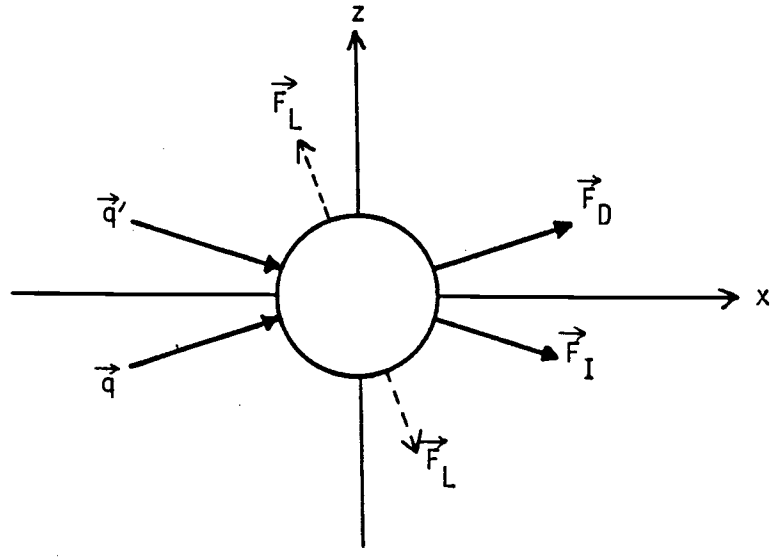

Fig. 2-2 Kinematics and Forces on a Horizontal Cylinder

the lift force is ignored in the following and its effects are considered to be included into the drag and inertia components.

The vector form of the Morison equation can be expressed as follows (see Nath, 1982):

$$\vec{F} = \vec{F}_D + \vec{F}_I$$

$$= C_d \frac{1}{2} \rho D \vec{q} \mid \vec{q} \mid + C_m \frac{\rho \pi D^2}{4} \vec{q}' \qquad (2.12)$$

where $\vec{q} = \vec{u} + \vec{w}$, $\vec{q}' = \vec{u}' + \vec{w}'$, u and w are the horizontal and vertical components of velocity, u′ and w′ are the two components of

acceleration (the total, or material derivative of the velocity). The drag and inertia component of the hydrodynamic forces can be decomposed into the horizontal (x) and vertical (z) components respectively.

$$\vec{F} = \vec{F}_{Dx} + \vec{F}_{Dz} + \vec{F}_{Ix} + \vec{F}_{Iz}$$

$$= C_d \frac{1}{2} \rho D \vec{u} |\vec{q}| + C_d \frac{1}{2} \rho D \vec{w} |\vec{q}| + C_m \frac{\rho \pi D^2}{4} \vec{u}' + C_m \frac{\rho \pi D^2}{4} \vec{w}'$$

$$= \vec{F}_x + \vec{F}_z = \vec{F}_D + \vec{F}_I \qquad (2.13)$$

where $\vec{F}_D = \vec{F}_{Dx} + \vec{F}_{Dz}$ and $\vec{F}_I = \vec{F}_{Ix} + \vec{F}_{Iz}$. After rearranging, we have

$$F_x = C_d \frac{1}{2} \rho D \, u \, |\vec{q}| + C_m \frac{\rho \pi D^2}{4} u' \qquad (2.14)$$

$$F_z = C_d \frac{1}{2} \rho D w \, |\vec{q}| + C_m \frac{\rho \pi D^2}{4} w' \qquad (2.15)$$

and $F = (F_x^2 + F_z^2)^{\frac{1}{2}}$.

Sarpkaya and Isaacson (1981, pp. 297) cautioned that the writing of the Morison equation in vector form, i.e. Eq. (2.12), does not necessarily imply that the behavior of the wake can be correctly represented because of the neglect of the higher harmonics, which occur from vortex shedding and other turbulence.

Hydrodynamic Forces under Waves and Current

If a uniform and steady current, U, is introduced to the wave field, we can modify the vector form of the Morison equation for the case of a horizontal cylinder subjected to waves and current. In the present study, the current is assumed to be in the direction of wave propagation as sketched in Fig. 2-3.

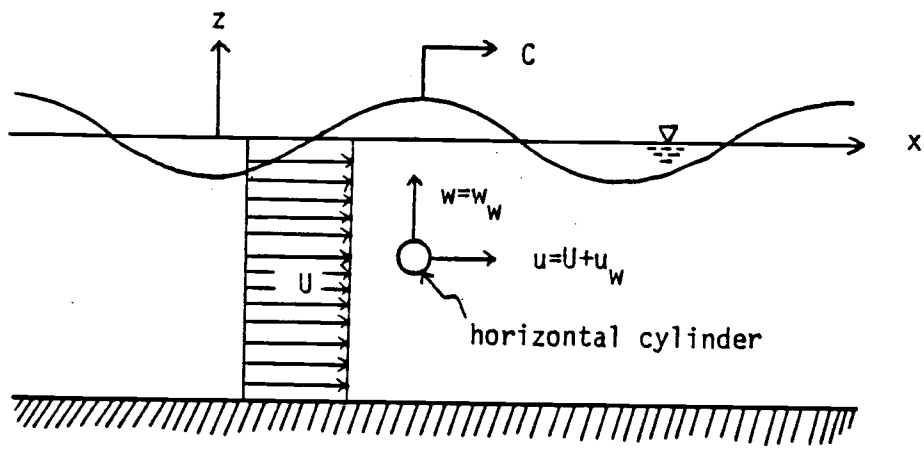

Fig. 2-3 Definition Sketch for a Horizontal Cylinder under Waves and Current

Since the linear superposition principle is assumed, we have the following water particle velocity components as described in Eq. (2.9) and Eq. (2.10) for a uniform and steady current.

$$u(x,z,t) = U + u_w(x,z,t) \tag{2.16}$$

$$w(x,z,t) = w_w(xz,t) \tag{2.17}$$

and $\vec{q} = \vec{u} + \vec{w}$ (2.18)

in which u_w and w_w are water particle velocities induced by waves only.

Also, if the total acceleration is used instead of the local acceleration in the inertia force, the acceleration will be modified by introducing a current in the wave field as follows

$$u' = \frac{\partial u_w}{\partial t} + (u_w + U)\frac{\partial u_w}{\partial x} + w_w \frac{\partial u_w}{\partial z} \tag{2.19}$$

$$w' = \frac{\partial w_w}{\partial t} + (u_w + U)\frac{\partial w_w}{\partial x} + w_w \frac{\partial w_w}{\partial z} \tag{2.20}$$

and

$$\vec{q}' = \frac{D\vec{q}}{Dt} = \vec{u}' + \vec{w}'$$

$$= \frac{\partial \vec{q}}{\partial t} + u\frac{\partial \vec{q}}{\partial x} + w\frac{\partial \vec{q}}{\partial z}$$

$$= \frac{\partial \vec{q}}{\partial t} + u_w\frac{\partial \vec{q}}{\partial x} + U\frac{\partial \vec{q}}{\partial x} + w_w\frac{\partial \vec{q}}{\partial z} \tag{2.21}$$

With the above relations, the hydrodynamic forces on a horizontal cylinder under waves and current can be described by

$$\vec{F} = C_d \frac{\rho D\vec{q}}{z}|\vec{q}| + C_m \frac{\rho\pi D^2}{4}\vec{q}' \tag{2.22}$$

in which $|\vec{q}| = (u^2 + w^2)^{\frac{1}{2}}$.

Eq. (2.22) can be decomposed into the horizontal (x) and vertical (z) component as Eq. (2.14) and Eq. (2.15).

2.3. Dimensional Analysis

Some insight into the appropriateness of the Morison equation and the force acting on a submerged cylinder by waves and current can be gained through dimensional analysis. The instantaneous force per unit length, F, on a stationary horizontal circular cylinder under waves and current whose propagating direction is perpendicular to the cylinder axis is

$$F = f(D, \varepsilon, \rho, \nu, H, T, L, h, U, u_{wm}, w_{wm}, e, d, g, t) \qquad (2.23)$$

where the cylinder is characterized by its diameter and roughness height, D and ε respectively. The pertinent fluid properties are the density, ρ, and the kinematic viscosity, ν. If the fluid flow field is under waves and current, it may be completely characterized by the wave height, H, wave period, T (with respect to the fixed coordinate system), wave length, L, water depth, h, and the current velocity, U. The maximum horizontal and vertical component of the wave water particle velocities, u_{wm} and w_{wm}, are considered for quasi-still water and depend only on H, h and L. The distance from the ocean bottom to the lowest point of the cylinder is denoted by e. The distance between the highest point of the cylinder and the still water surface is denoted by d. Note that h=d+e+D.

The linear superposition principle is assumed. The current is also assumed to be steady and uniform. The maximum total horizontal velocity, i.e., $u_m = u_{wm} + U$ if the current is in the direction of waves, could be used instead of the maximum horizontal velocity induced by waves only in the parametric analysis. Thus, Eq. (2.23) can be rewritten as

$$F = f\ (D,\ \varepsilon,\ \rho,\ \nu,\ H,\ T,\ L,\ h,\ u_m,\ w_{wm},\ U,\ e,\ d,\ g,\ t) \qquad (2.24)$$

Through dimensional analysis, one possible set of dimensionless parameters is

$$\frac{F}{\rho D u_{wm}^2} = f_1\left(\frac{u_m D}{\nu},\ \frac{H}{L},\ \frac{D}{L},\ \frac{u_m T}{D},\ \frac{h}{L},\ \frac{\varepsilon}{D},\ \frac{e}{D},\ \frac{d}{D},\ \frac{w_{wm}}{u_m},\ \frac{u_m}{\sqrt{gd}},\ \frac{U}{u_m},\ \frac{t}{T}\right) \qquad (2.25)$$

Nath and Yamamoto (1974) summarized and graphed the results from Havelock (1936) and Ogilvie (1963). They concluded that the free surface effects for the forces on a horizontal cylinder are negligible if the submergence is greater than about four cylinder diameters, i.e., $d>4D$. In this study, the horizontal cylinder is submerged deeper than 4D, so d/D and $u_m/\sqrt{gd}$ can be ignored. Sarpkaya (1977) showed that the effect of wall-proximity is to increase the force coefficients for relative gaps e/D less than about 0.5, i.e., $e/D < 0.5$. Also, it can be observed from the experimental data obtained by Yamamoto and Nath (1976) that there is no significant

difference in force coefficients if e/D>1.0, especially for large Reynolds numbers (say $R>1x10^5$). The parameter e/D can be removed from Eq. (2.25) because e/D always is greater than 1.0 in this study. The parameters H/L and h/L can be used for determining the water particle velocity amplitudes u_m and w_m. Because the cylinder considered is slender, i.e., D<20L, D/L can be ignored. Now, Eq. (2.25) can be reduced to

$$\frac{F}{\rho D u_{wm}^2} = f_2\left(\frac{u_m D}{\nu}, \frac{u_m T}{D}, \frac{\varepsilon}{D}, \frac{U}{u_m}, \frac{w_{wm}}{u_m}, \frac{t}{T}\right) \tag{2.26}$$

or

$$\frac{F}{\rho D u_{wm}^2} = f_2\left(R, K, \frac{\varepsilon}{D}, \frac{U}{u_m}, \frac{w_m}{u_m}, \frac{t}{T}\right) \tag{2.27}$$

in which R is the Reynolds number, K is the Keulegan-Carpenter number, ε/D is the relative roughness, U/u_m is the ratio of the current to the maximum horizontal velocity, w_m/u_m is the water particle velocity ratio, and t/T is the time history.

Combining Eq. (2.22) and Eq. (2.27), we have

$$C_d = f_d\left(R, K, \frac{\varepsilon}{D}, \frac{U}{u_m}, \frac{w_{wm}}{u_m}\right) \tag{2.28}$$

$$C_m = f_m\left(R, K, \frac{\varepsilon}{D}, \frac{U}{u_m}, \frac{w_{wm}}{u_{wm}}\right) \tag{2.29}$$

The time-variation term, t/T, is ignored in the above relation because the force coefficients C_d and C_m are considered in the present study to be time-averaged values over one wave cycle.

The velocity in the Reynolds number and Keulegan-Carpenter number can be noted as q_m, which is the maximum value of the total velocity vector. But, the total water particle velocity is maximum at the time of the maximum horizontal component. Thus, $q_m = u_m$, so u_m is used in R and K instead of q_m for convenience.

In order to examine the current effect on hydrodynamic forces, the current velocity and wave-induced water particle velocity (in quasi still water) can be considered separately. Every non-dimensional parameter in Eq. (2.26) including the maximum velocity u_m can be decomposed into two components concerned with u_{wm} and U respectively, i.e., $u_m = u_{wm} + U$. Thus, more dimensionless parameters can be derived which could measure the behavior of the force coefficients.

$$\frac{F}{\rho D u_{wm}^2} = f_3\left(\frac{UD}{\nu}, \frac{u_{wm}D}{\nu}, \frac{UT}{D}, \frac{u_{wm}T}{D}, \frac{U}{u_{wm}}, \frac{w_{wm}}{u_{wm}}\right) \tag{2.30}$$

The first parameter on the right hand side is the Reynolds number under the influence of current only. The third parameter can be termed the "Verley-Moe number" (VM) after being used by them (1978). In the VM number, U/D is proportional to the eddy shedding frequency if a steady current is considered rather than waves, and

$1/T = n$ is the wave frequency. Thus, the VM number represents the ratio of wave period and wake developvement time. Combining the second and the fourth parameter, the parameter $D^2/\upsilon T = \beta$, which is termed the "frequency parameter" by Sarpkaya (1976), is obtained. This parameter is the ratio of the Reynolds number and the Keulagen-Carpenter number, i.e., $\beta = R/K$. The fifth parameter U/u_{wm} can be used to examine the effect of current velocity to the wave-induced velocity. The last parameter w_m/u_m is an index of the water particle orbital shape effect.

2.4. Force Coefficients Dependence on Governing Parameters

The parametric dependencies of force coefficients from previous studies are reviewed and discussed in this section.

For steady current, Achenbach (1971) described the variation of the drag coefficient with Reynolds number. The nature of steady flow past a hydrodynamically smooth circular cylinder is composed of sub-critical, critical, supercritical and post-critical regions as indicated in Fig. 2-4. Roughness generally increased the rate of boundary layer growth, the skin friction and the effective diameter. The effects of roughness on the drag coefficient of a cylinder in steady flow reported by Miller (1977) are shown in Fig. 2-5. The smooth cylinder (an effective roughness of $\varepsilon/D=0.0004$) and sand roughened cylinder with $\varepsilon/D=0.02$ test results from Nath (1983) are superimposed. As relative roughness increases, (i) the critical Reynolds

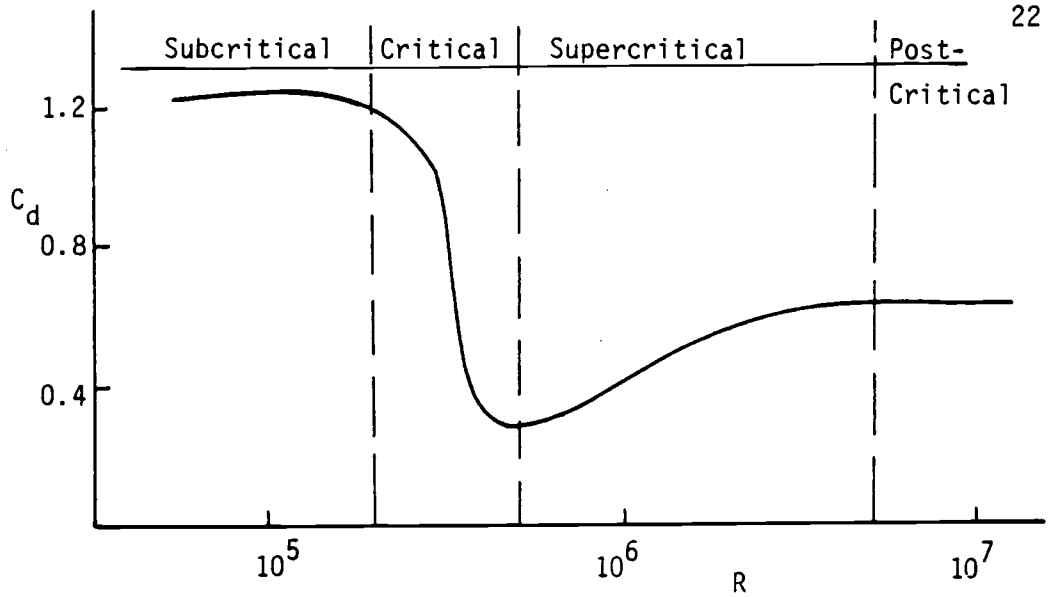

Fig. 2-4 Drag Coefficients for a Smooth Cylinder in Steady Flow (From Achenback 1971)

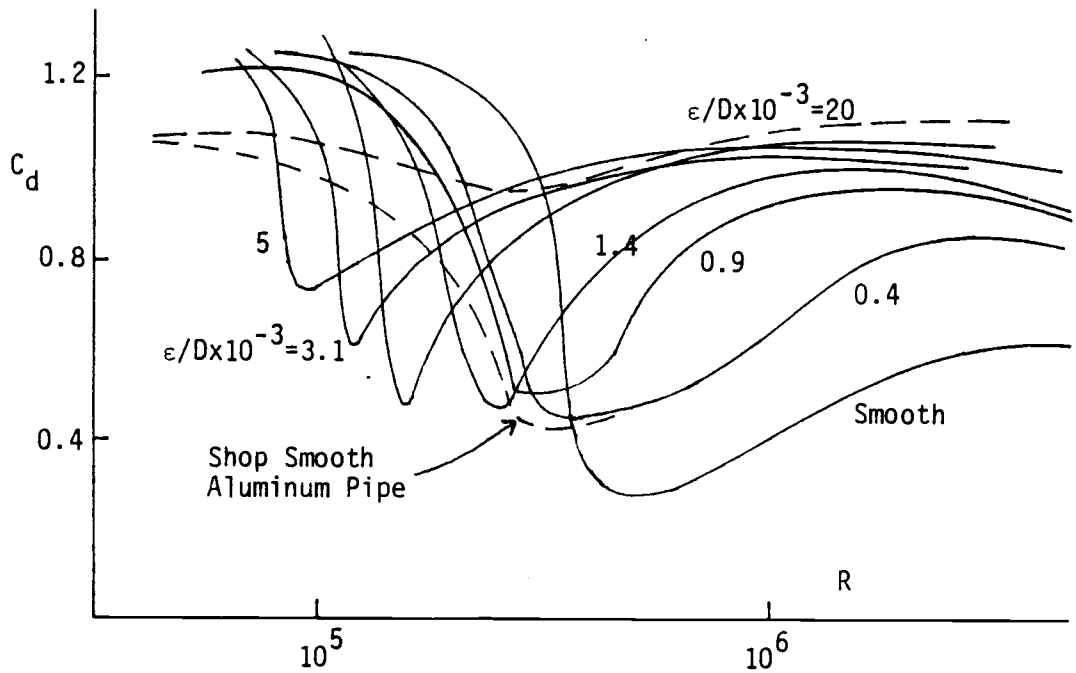

Fig. 2-5 Roughness Effect on Drag Coefficients for Steady Flow (———:from Miller 1977; -----:from Nath 1983)

number (where drag coefficient falls steeply) decreases, (ii) the minimum drag coefficient increases, and (iii) the drag coefficient at high Reynolds number increases.

For oscillatory flow, a lot of experiments and studies verify the variation of C_d and C_m as functions of the Reynolds number and Keulegan-Carpenter number. The study carried out by Sarpkaya (1976) is probably the most comprehensive and detailed. Typical results for a smooth cylinder in his study are shown is Fig. 2-6. The dependence of C_d and C_m on the frequency parameter β was first presented in his study as shown in Fig. 2-7.

Yamamoto and Nath (1976) and Garrison et al. (1977, 1980) conducted their experiments by oscillating a cylinder sinusoidally in still water to investigate the influence of R and K. Their results are plotted in Fig. 2-8. To calculate C_d and C_m, Keulegan and Carpenter used the Fourier-averaged method, Garrison used the least square method, and Yamamoto and Nath evaluated C_d at the maximum velocity and C_m at maximum acceleration. Although different techniques were used, consistent results are seen in the figure. The analytical consistency of C_d and C_m value determined from different techniques is shown in Appendix A.

Sarpkaya (1976) also presented force coefficient data obtained with sand roughened cylinders. His results are shown in Fig. 2-9. The significant effects of relative roughness can be easily observed.

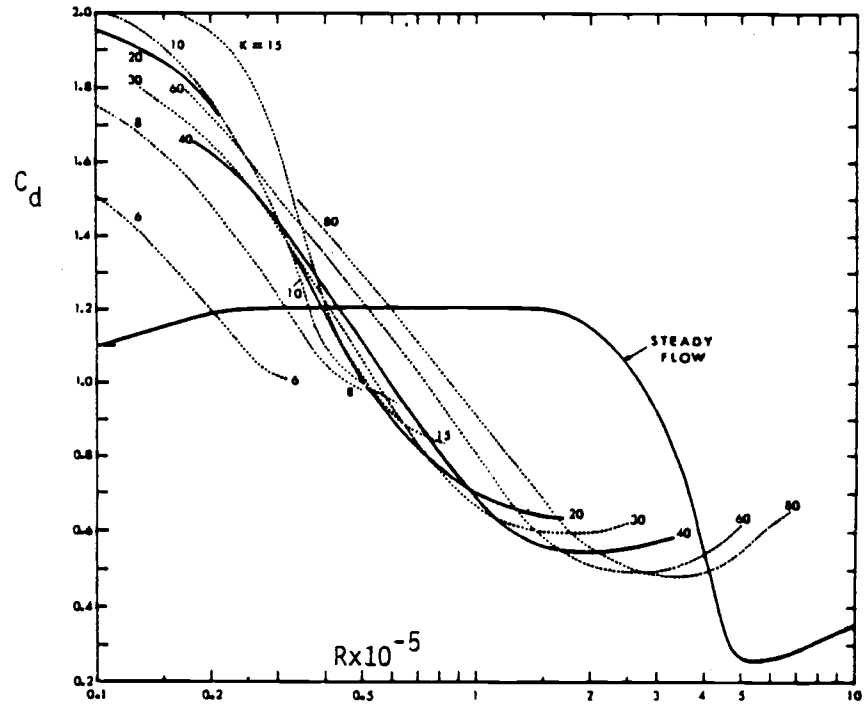

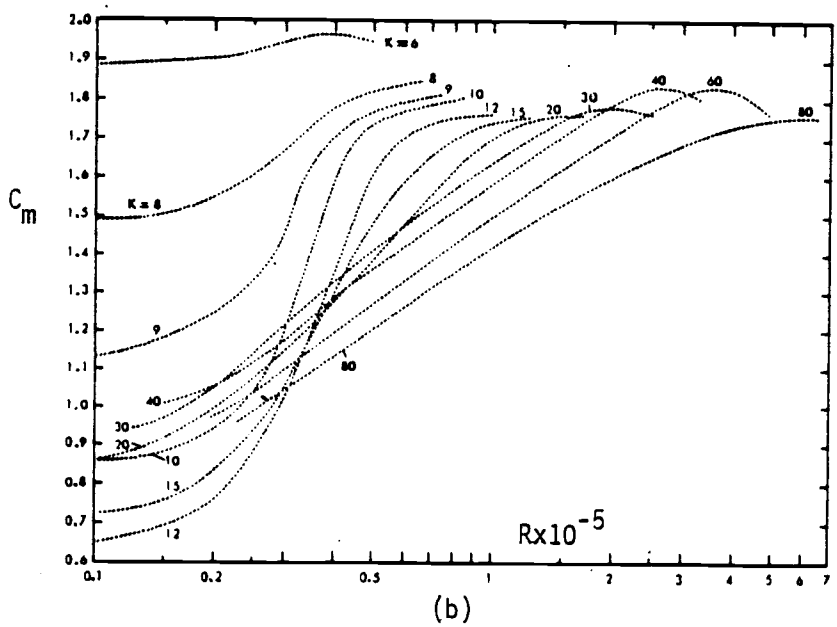

Fig. 2-6 (a)Drag and (b)Inertia Coefficients vs. Reynolds number for various values of K for planar oscillatory flow (From Sarpkaya 1976)

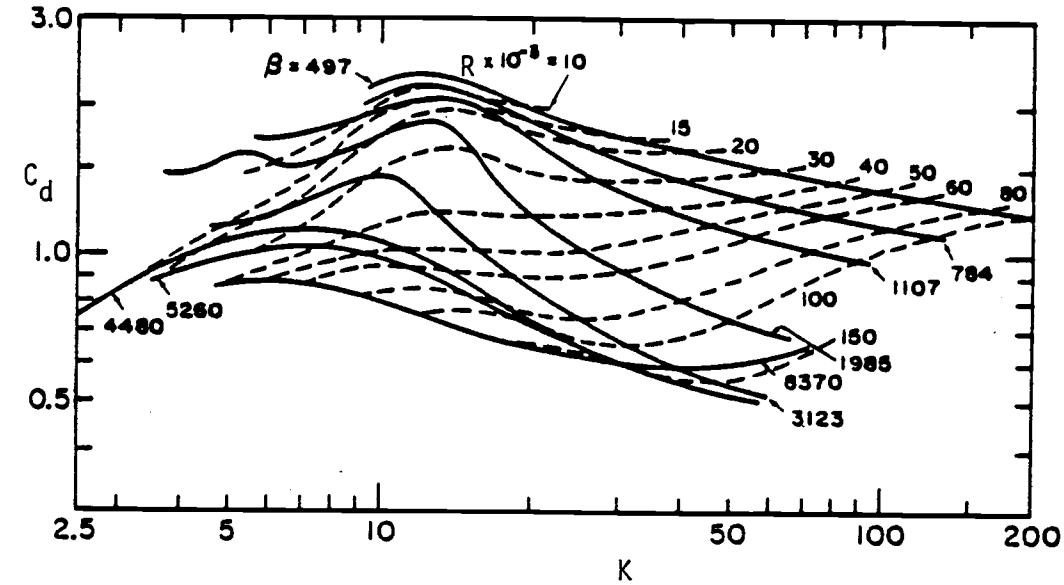

(a)

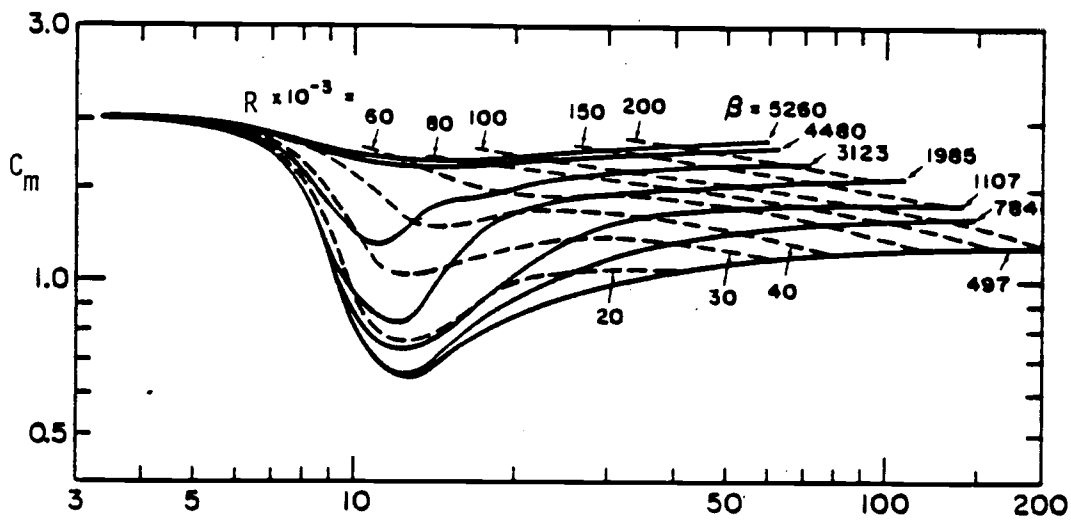

(b)

Fig. 2-7 (a)Drag and (b)Inertia Coefficients vs. K for various values of R and β (Planar Oscillatory Flow) (From Sarpkaya 1976)

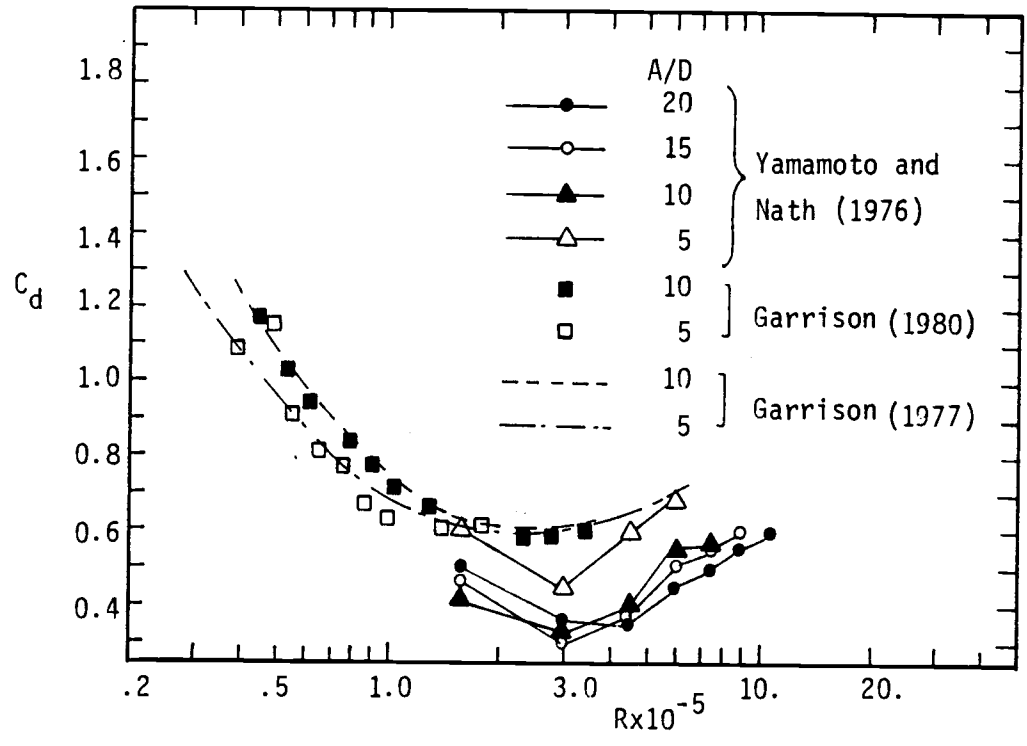

(a)

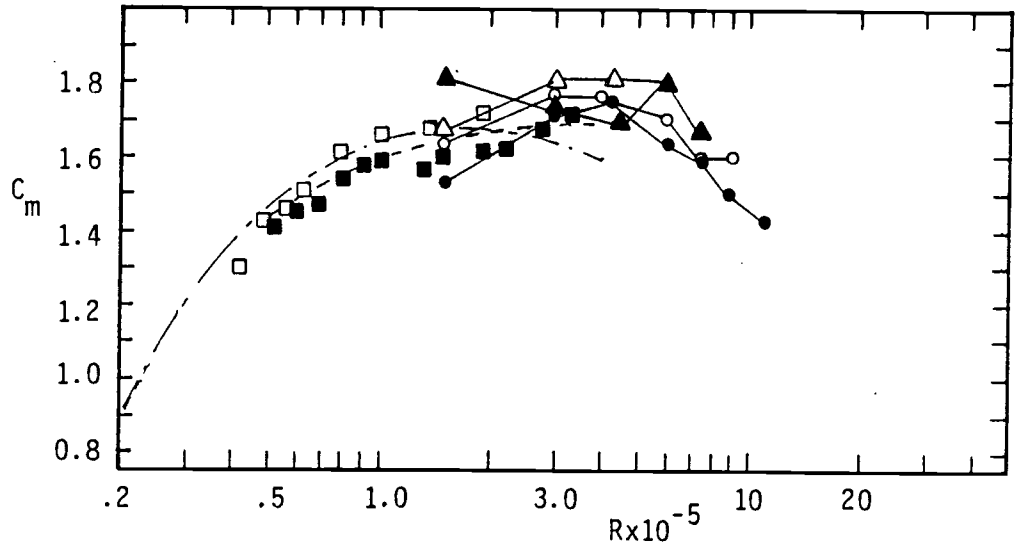

(b)

Fig. 2-8 (a)Drag and (b)Inertia Coefficients vs. Reynolds Number for Various K(=πA/D) by Oscillating a Cylinder in Still Water

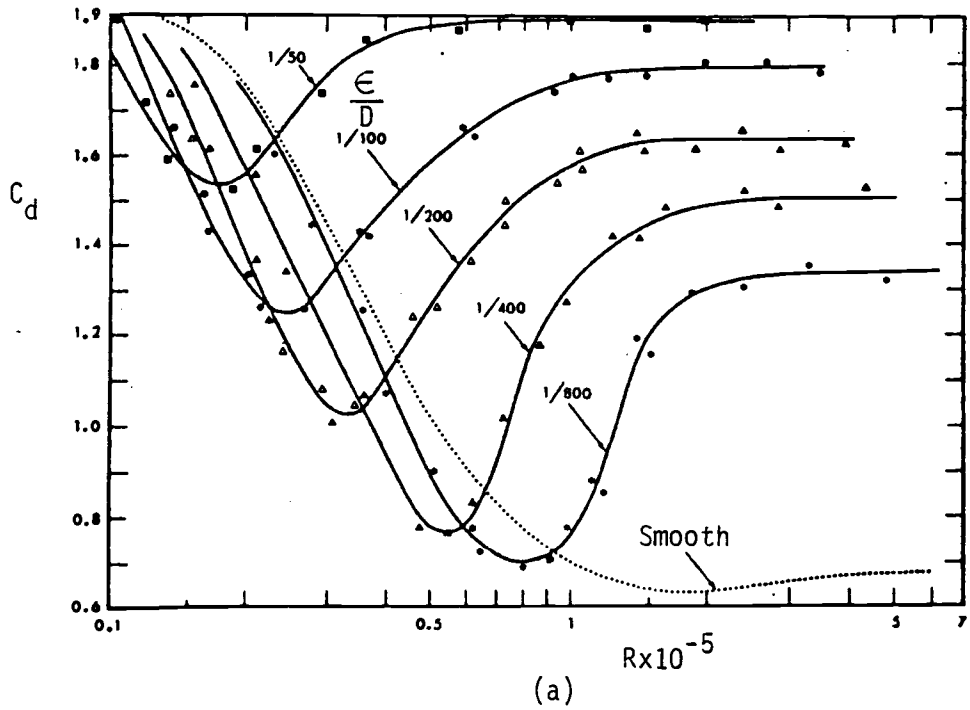

(a)

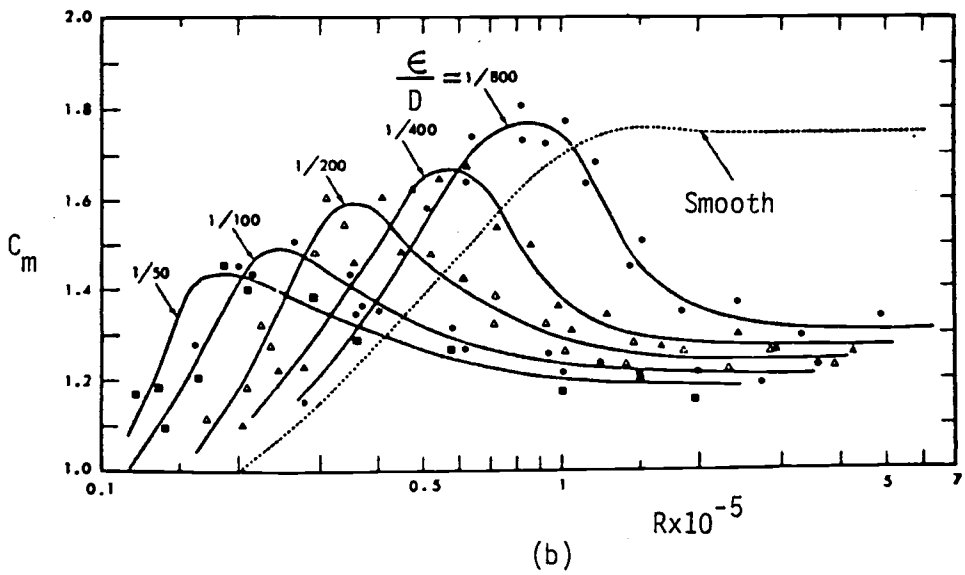

(b)

Fig. 2-9 (a)Drag and (b)Inertia coefficients vs. Reynolds number for various values of ϵ/D (From Sarpkaya 1976)

For a horizontal cylinder in waves, the force coefficient dependences are not quite the same as those for planar oscillatory flow because of the orbital motion of the water particle around the center of the horizontal cylinder. Ramberg and Niedzwecki (1982) presented C_d and C_m values as shown in Fig. 2-10, based on the vector form of Morison equation. They also examined the forces and force coefficients based on the Morison equation for each component of force using the corresponding component of velocity and acceleration, which are expressed in Eq. (2.31) and Eq. (2.32). As for the difference between the scalar form and the vector form, i.e., Eq. (2.14) and Eq. (2.15), they reported (i) the vector approach is indeed more appropriate, (ii) the drag coefficients obtained from the vector form are 5 -10% smaller than those for the scalar form, and (iii) the inertia coefficient is the same in each case.

$$F_x = C_d \frac{1}{2} \rho D \, u|u| + C_m \frac{\rho \pi D^2}{4} u' \tag{2.31}$$

$$F_z = C_d \frac{1}{2} \rho D \, w|w| + C_m \frac{\rho \pi D^2}{4} w' \tag{2.32}$$

Maull and Norman (1979) and Ramberg and Niedzwecki (1982) examined the forces on a horizontal cylinder by defining force coefficients based on root-mean-square values, averaging over time, as defined in Eq. (2.33) and Eq. (2.34), which are named the in-line

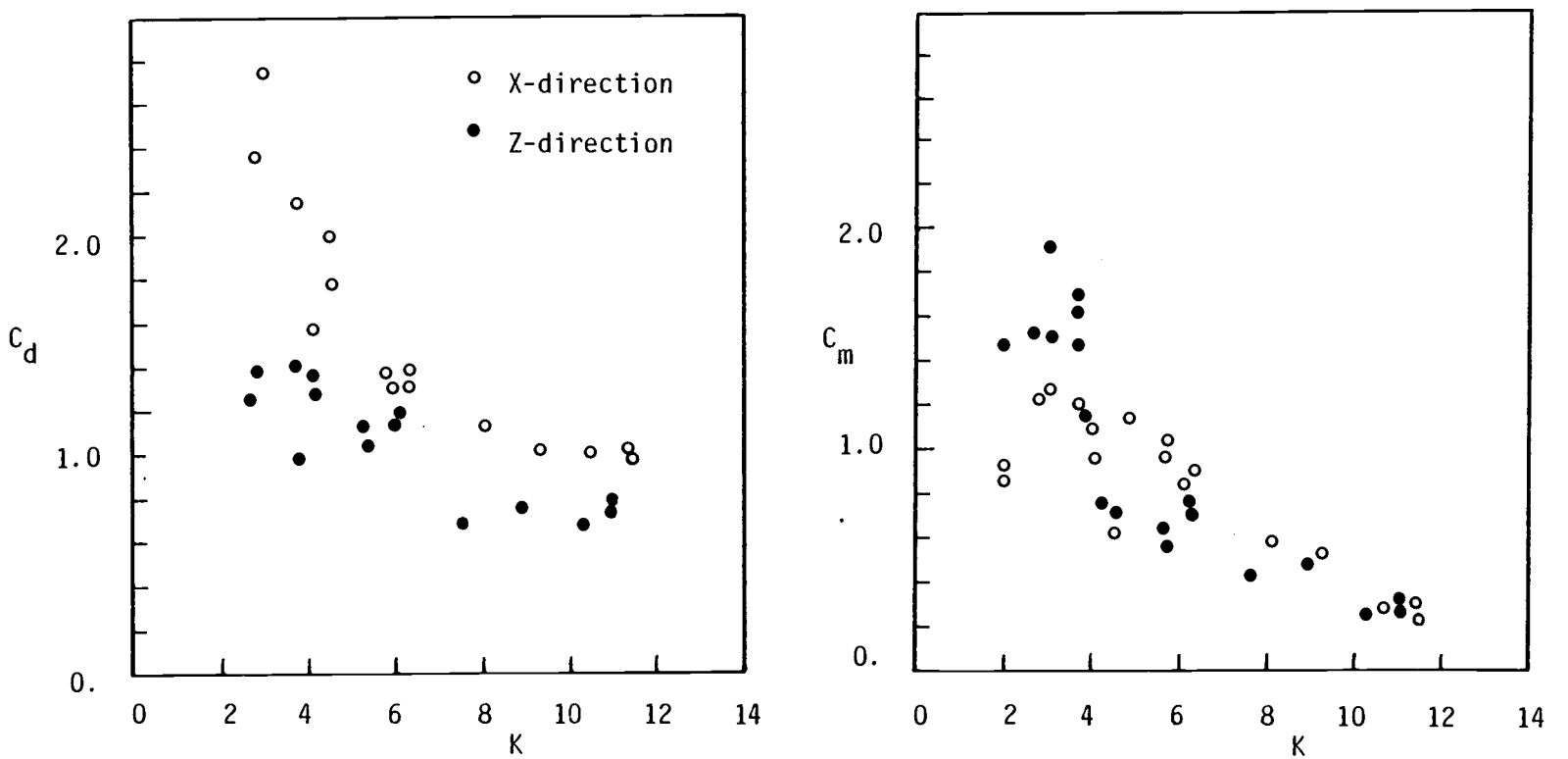

Fig. 2-10 (a)Drag and (b)Inertia Coefficients vs. Keulegan-Carpenter Number for a Horizontal Cylinder in Waves (From Ramberg and Niedzwecki 1982)

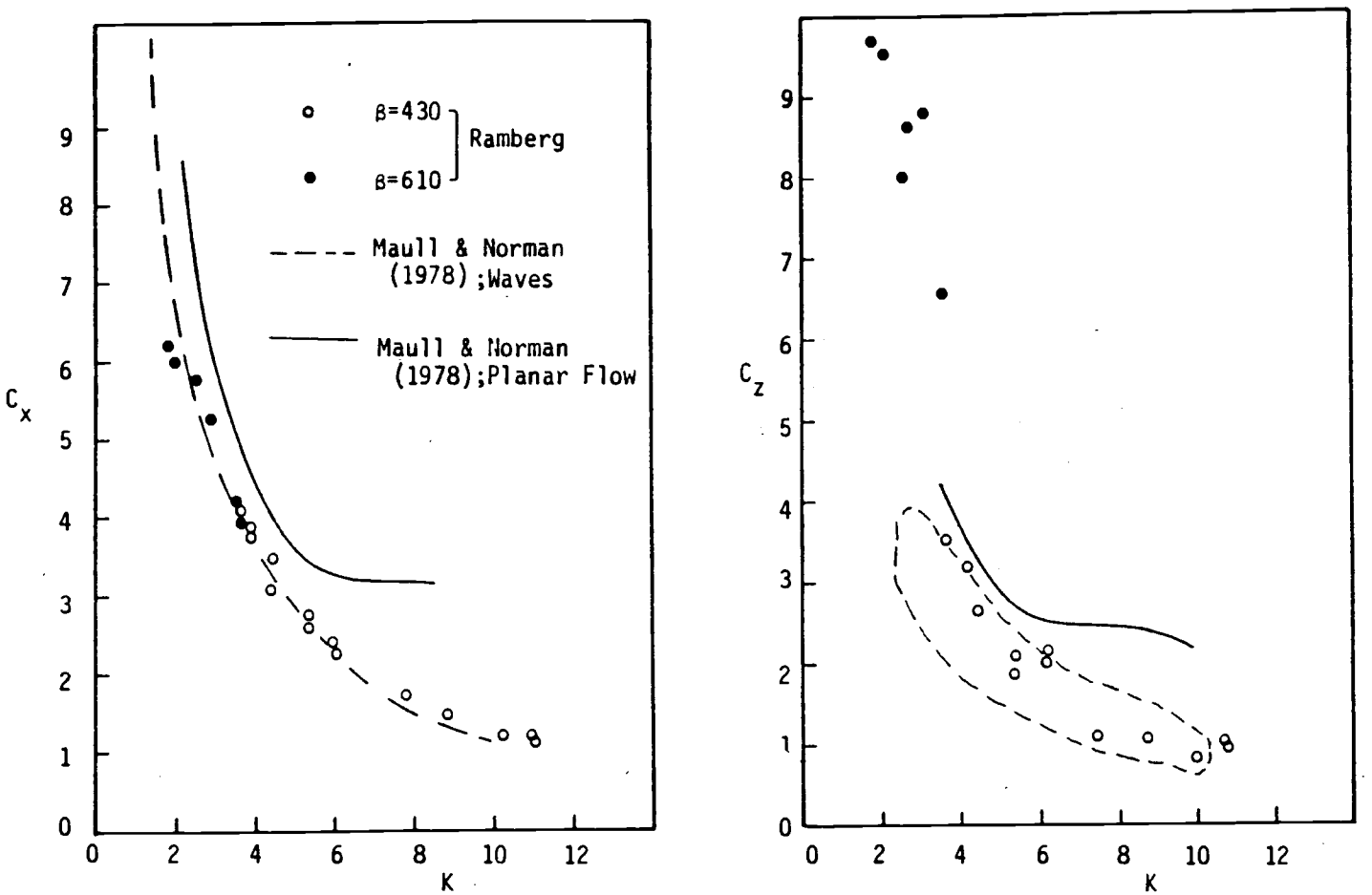

Fig. 2-11 (a)In-line and (b)Transverse Coefficients vs. Keulegan-Carpenter Number for a Horizontal Cylinder in Waves (From Ramberg and Niedzwecki 1982)

coefficient (C_x) and the transverse coefficient (C_z) respectively. Their results are shown in Fig. 2-11. The difference between planar oscillatory flow and wavy flow for the horizontal cylinder is evident from these plots. Thus,

$$C_x = \frac{(F_x)_{rms}}{\frac{1}{2}\rho D (u_{rms})^2} \tag{2.33}$$

and

$$C_z = \frac{(F_z)_{rms}}{\frac{1}{2}\rho D (w_{rms})^2} \tag{2.34}$$

The dependence of C_d and C_m on the water particle velocity ratio w_m/u_m was examined by Sarpkaya (1982) and is shown in Fig. 2-12. It can be seen that the C_d and C_m have high dependence on w_m/u_m for two-dimensional flow.

The results of the experiments for this study, plotted according to the parameters discussed here, will be presented in Section 5.1.

As mentioned before, the hydrodynamic forces on cylnders under waves and current are much more complicated than those in waves only and little research about this topic has been reported. Almost all of the former studies dealt with the forces under planar oscillatory flow and current only.

Verley and Moe (1978a, 1978b, 1979) conducted a sequence of experiments by oscillating a horizontal cylinder in a current where the plane of motion was parallel with the current flow line. In

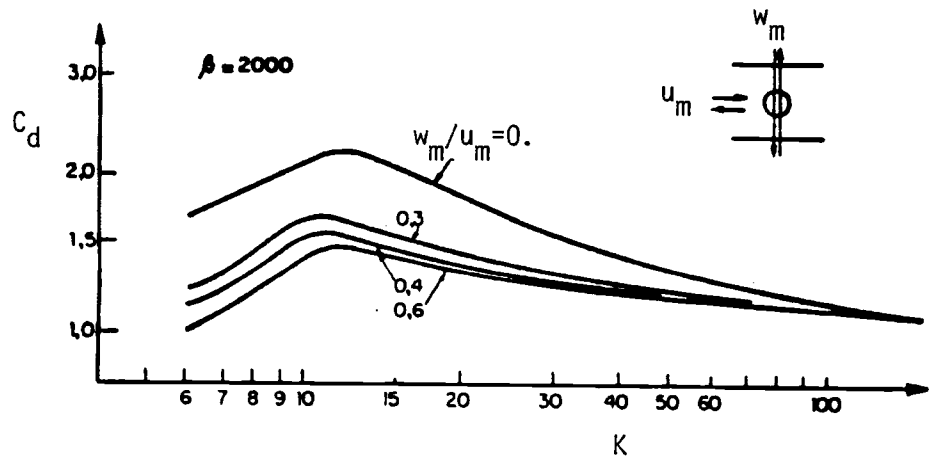

(a)

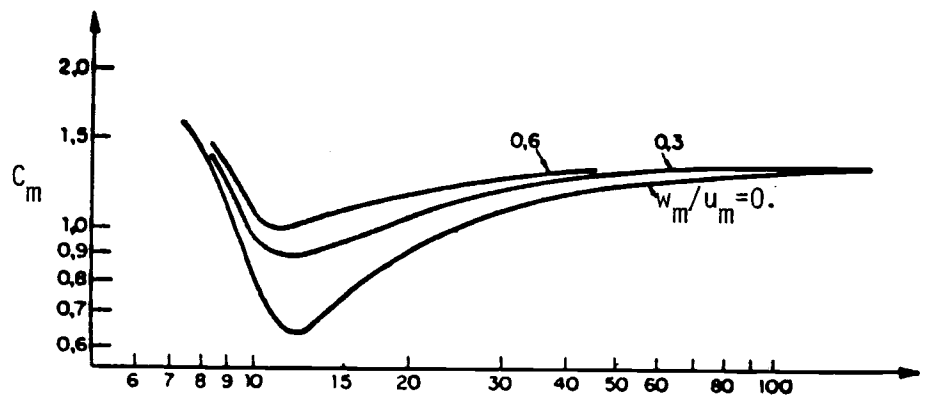

(b)

Fig. 2-12 (a)Drag and (b)Inertia Coefficients vs. K for various values of w_m/u_m for a Horizontal Cylinder in Waves (From Sarpkaya 1982)

their studies, the following two equations were used to analyze the data.

$$F = \frac{1}{2} \rho D C_d (U-\dot{x}) \mid U-\dot{x} \mid - \frac{1}{4} \rho \pi D^2 (C_m-1) \ddot{x} \qquad (2.35)$$

and

$$F = \frac{1}{2} \rho D C_{d1} U^2 - \frac{1}{2} \rho D C_{d2} \dot{x}|\dot{x}| - \frac{1}{4} \rho \pi D^2 (C_m - 1) \ddot{x} \qquad (2.36)$$

where x, $\dot{x}$ and $\ddot{x}$ are the displacement, velocity and acceleration of the cylinder. The added mass coefficient $C_a=C_m-1$ was used because the cylinder was oscillated instead of generating the planar oscillatory flow. They believed that Eq. (2.35) is the better formulation and Eq. (2.36) should be applied at low value of Verley and Moe number U/nD in which n(=1/T) is the wave frequency. The dependence of the force coefficients on VM number and velocity ratio U/u_{wm} were found in their studies.

Mercier (1973) also studied experimentally the forces on a cylinder oscillating with large amplitude in line with a steady stream. He found that the force coefficients are functions of VM number (which was called reduced velocity in his study) and Keulegan-Carpenter number.

Greenamyer (1973) investigated the forces on a cylinder immersed in a unidirectinal periodic flow which is characterized by

$U + u_m \sin 2\pi t$. He divided the total drag into steady state drag and oscillating drag. He defined the parameter $\lambda = nD/U$ which is the inverse of the VM number and found that the force coefficients obtained by him and others are functions of λ.

2.5. Accelerations in Inertia Term

Whether the inertia force term in the Morison equation should be taken as proportional to the total acceleration or to the local acceleration is debatable. Isaacson (1979) indicated that no formal justification exists for adopting one or the other even though these may differ significantly from each other in typical design waves.

At any point in a two-dimensional wave field, the relation between total and local acceleration in the horizontal and vertical direction can be expressed as

$$\frac{Du}{Dt} = \frac{\partial u}{\partial t} + u\frac{\partial u}{\partial x} + w\frac{\partial u}{\partial z} \tag{2.37}$$

$$\frac{Dw}{Dt} = \frac{\partial w}{\partial t} + u\frac{\partial w}{\partial x} + w\frac{\partial w}{\partial z} \tag{2.38}$$

In other words, the total acceleration is composed of a local acceleration and a convective acceleration.

Isaacson (1979) calculated the "effective inertia coefficient", C_m', which is defined in Eq. (2.39) by using Stokes fifth-order wave theory in the horizontal direction. He concluded that in deep water

the maximum values of total and local acceleration are equal. For finite depth water waves, the local acceleration will be larger than the total acceleration by comparing the C_m' and C_m theoretically. Thus,

$$C_m' = C_m \frac{(\frac{Du}{Dt})_{max}}{(\frac{\partial u}{\partial t})_{max}} \tag{2.39}$$

For two-dimensional wavy flow, the difference between total local acceleration in the vertical direction also should be examined. The results for this study obtained by using stream function wave theory are given in Section 5.4.

If a steady and uniform current, U, is introduced in a wave field, the total acceleration becomes

$$\frac{Du}{Dt} = \frac{\partial u_w}{\partial t} + (u_w + U)\frac{\partial u_w}{\partial x} + w_w \frac{\partial u_w}{\partial z} \tag{2.40}$$

$$\frac{Dw}{Dt} = \frac{\partial w_w}{\partial t} + (u_w + U)\frac{\partial w_w}{\partial x} + w_w \frac{\partial w_w}{\partial z} \tag{2.41}$$

Thus, the convective acceleration will be affected by the presence of the current and the influence varies linearly with the magnitude of the current velocity U. Because the local acceleration will not be affected by the presence of the current, the total acceleration gets smaller as U gets larger (if the current is in the direction of wave). In other words, the larger the current velocity is,

the bigger the difference between the total and the local acceleration.

When the current velocity is large, the drag force is much larger than the inertia force because the drag term is proportional to the square of relative velocity. Under these circumstances, the differences between using total acceleration and local acceleration are not important because of the small relative magnitude of the inertia term.

3. EXPERIMENT

3.1. Description of the Experiment

Wave Research Facility (OSU)

The experiments in this study were conducted at Oregon State University Wave Research Facility (WRF). The WRF is a large-scale wave channel 342 feet long, 12 feet wide and 15 feet deep in the test section. The hinged wave board is driven by an MTS Servo hydraulic piston. Periodic waves can be generated with wave periods of from about 1 to 8 seconds and wave heights of up to 5 feet high and breaking. Random waves can also be generated using the on-site PDP-11 computer to generate the wave spectrum and transfer function for the board motion.

Test Cylinder

The test cylinder is 0.719 feet in diameter and 8.7 feet long. The two feet long test section is located at the center portion of the cylinder and two sides (right and left) are dummy sections used to minimize end effects. Fig. 3-1 shows the arrangement of the specimen on the towing carriage in WRF.

The two-feet long test section is suspended from two 5/8-inch diameter aluminum rods that were milled on the ends to receive strain gauges in such a manner as to measure the total horizontal and vertical forces on the test section. The gauging length of each rod is 8

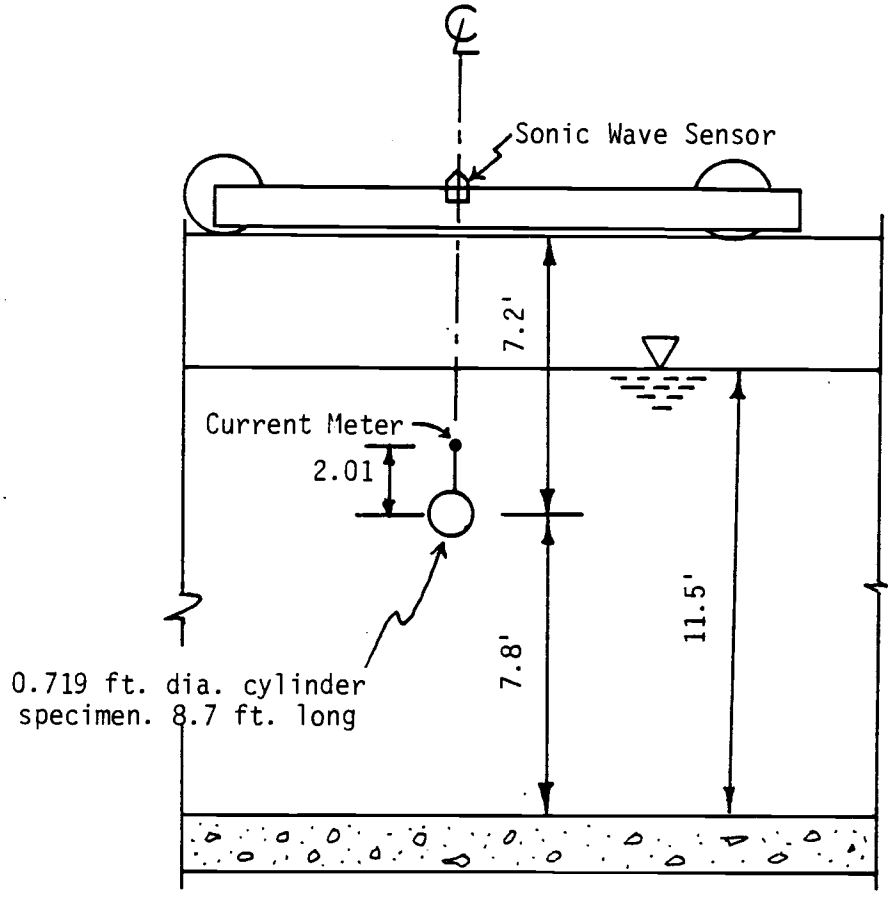

Fig. 3-1 Cross-section of Specimen Set-up in the OSU Wave Research Facility

inches, and the construction resulted with this gauge length being a fixed ended beam. There are four beams total and the strain gauges are arranged to eliminate any influences from torsion or from off-centered loadings of the hydrodynamic forces.

With the towing carriage stationary, waves are imposed on the cylinder so that hydrodynamic forces on test cylinder in wavy flow can be obtained. The towing carriage is powered with an electric motor which can control tow speed from 1 cm/sec to about 300 cm/sec. In this study, the combined effect of waves and current on the test cylinder is simulated by towing the test cylinder with the carriage into wavy flow. This simulation will be discussed in the following section.

Two kinds of cylinders are used in this study: a smooth cylinder and a sand roughened cylinder with relative roughness $\varepsilon/D = 0.02$.

Measurement and Calibration

Eleven channels of information were measured at times: the water surface elevation, three current meters with two directions each, the carriage speed, the horizontal acceleration of the cylinder, and two forces (horizontal and vertical) from the test section of the cylinder.

Wave heights (wave profiles) were measured with two sensors that measure the travel time of sound from gauge to the water surface and return. Nath (1981a) stated that static calibrations of the wave

profiler have been made in the past and they were quite linear. The water surface fluctuation should be measured directly above the test cylinder. Therefore, the wave sensor was mounted in an opening of the wave carriage at this location.

The water kinematics (velocities) were measured with Marsh-McBirney current meters. Through the steady state tow tests, Nath (1981a) reported the static sensitivity of the meter is 20.47, i.e., $u = 20.47 \times (\text{Volts})$. Obviously, with the cylinder present, it is impossible to measure water particle kinematics at the position of the center of the cylinder. The best that can be done under such circumstances is to measure the kinematics at some distance from the cylinder. However, some theories must then be used to account for the attenuation or phase shift of the kinematics due to differences in position. In present experiment, the current meter was placed 2.01 feet above the center of the test cylinder. The kinematics were measured together with wave profile and force data for each test run. The consistencies between measured and predicted kinematics for waves only were verified by Nath (1981a). The similarity between measured and predicted kinematics for waves plus towing will be examined in Section 5.3.

The force dynamometer was calibrated by means of providing known forces in each of four directions (up, down, south, north) using very low friction pulleys, weights, and buckets before and after the test. Table 3-1 gives the calibration constants for each test condi-

Cylinder	Run Number	Test Condition	Horizontal Direction		Vertical Direction		Actual Constants Used
			North	South	Up	Down	
Smooth	Waves: Run 278-305, Run 313-350; Waves + Towing Run 366-376	Before Test	31.95	33.64	31.95	31.95	32.55
		After Test	32.31	32.32	31.54	31.92	
Sand Roughened	Waves: Run 379-410; Waves + Towing Run 422-437	Before Test	32.14	32.31	31.22	31.79	32.14
		After Test	32.11	31.54	31.88	31.62	

Table 3-1

Summary of Force Dynamometer Calibration Constants

tion and actual calibration constants used for the data reduction. The details of the calibrations can be found in Nath (1981a).

Data Recording

Transducer outputs were recorded on digital magnetic tape and strip chart records. A PDP-11 minicomputer provided software for multiplexing and initial recording on disk. After an experiment, data were transferred from disk to tape.

The original approach to digitize the data is to keep the time interval small enough to avoid aliasing in the frequency domain with respect to the fundamental wave frequencies and the higher harmonics for any frequencies under consideration. Because the Fast Fourier Transform algorithm which was developed for processing the data was to be used, each wave fundamental period should be digitized at 2^N intervals for convenient use later. In this task, data were recorded at the rate of $2^{10} = 1024$ points per wave period for a total of four waves, starting at an arbitrary time during an experiment.

All of the digital recording data and strip chart records can be converted to data with physical units by multiplying respective scale constant.

Test Conditions

Both of the smooth and sand roughened cylinder were tested for the following conditions.

(I) Waves only: Wave periods were from 2.50 seconds to 6.00 seconds. Wave heights were from 0.8 feet to 4.7 feet.

(II) Waves plus towing: Wave periods were from 2.50 seconds to 6.00 seconds. Wave heights were from 3 feet to 4.6 feet. Towing speed was designated in two parts: (a) low range: U = 0.6 to 0.9 ft/sec. and (b) high range: U = 3.3 to 6.5 ft/sec.

3.2. Similarity between "Waves and Towing" and the Linear Superposition Principle.

To study the hydrodynamic forces on marine structures under waves and current, three possible kinds of experimental techniques can be used besides the one that generates waves and current simultaneously:

(I) By generating the flow characterized by $U + u_m \sin\theta$ in a water tunnel (e.g., See Greenamyer 1973).

(II) Oscillating a cylinder periodically in a uniform flow (e.g., see Verley and Moe 1978, 1979, Moe and Verley 1978, Mercier 1973).

(III) Towing a cylinder with uniform speed in a wave field.

The first two methods are for current superimposed onto planar oscillatory flow. That means the vertical component of kinematics

and forces are neglected. The third method can take account of the orbital motion of water particles for determining the hydrodynamic forces on cylinders. This method is used in the present study.

If a cylinder is towed with speed U in waves, the period experienced by the cylinder is different from the actual wave period T and is called the apparent period T_{ap}.

$$T_{ap} = \frac{T}{1 - \frac{U}{C}} \tag{3.1}$$

in which C is the wave velocity, and U is negative when the cylinder is towed opposite to the waves and is positive when towed in the same direction as the waves. Also, the time scale in one wave cycle can be related as

$$t_{ap} = \frac{t}{1\frac{U}{C}} \tag{3.2}$$

But the phase angle θ is still unchanged according to the following relation.

$$\theta = \frac{2\pi t}{T} = \frac{2\pi\, t_{ap}}{T_{ap}} \tag{3.3}$$

The instantaneous kinematics experienced by the towed cylinder are

$$u(\Theta) = \hat{u}\ (\Theta) + U \tag{3.4}$$

$$w(\Theta) = \hat{w}\ (\Theta) \tag{3.5}$$

where $\hat{u}(\Theta)$ and $\hat{w}(\Theta)$ are determined by a suitable wave theory using the actual wave period, wave height and water depth.

The conclusion can be drawn that the kinematics experienced by the towed cylinder in waves and those predicted by linear superposition are similar.

Because the period experienced by towing the cylinder is the apparent period, the apparent period should be used for all the dimensionless parameters, such as Reynolds number and Keulegan-Carpenter number, with the kinematics obtained from the actual wave period.

4. DATA ANALYSIS

4.1. Determination of Force Coefficients

The modified Morison equation Eq. (2.12) and Eq. (2.22) were used to predict hydrodynamic forces on the horizontal cylinder. Before using these equations, the diameter of the cylinder, the kinematics at the center of the cylinder if the cylinder was absent and the associated force coefficients must be known or estimated.

Nath (1981a) stated that the stream function theory compares quite well with the measured kinematics and is adequate for predicting the velocities and accelerations of water particles at the center of the cylinder. As mentioned in Section 2.1, the linear superposition principle is assumed to be valid for predicting the kinematics under waves and current. In the last section, the similarity of kinematics between the linear superposition principle and towing a cylinder in a wave field was described and examined. Therefore, the stream function theory with superposition principle is used to quantify the kinematics in this study. The total acceleration is used in the modified Morison equation.

With known cylinder diameter, water density, kinematics and measured force data, the force coefficients can be evaluted. Many techniques can be used to determine the force coefficients with given sets of known data, such as the least squares method, the Fourier averaging technique, the two points method (maximum velocity and

acceleration, maximum force and zero force), mean square method (Bishop, 1978), phase method (Nath, 1981a), drag and inertia dominate method (Kim and Hibbard, 1975), etc. The least square method is probably the most applicable and commonly used technique and is used in the present study.

Least Square Method

The least square method consists of the minimization of the error between the measured forces and calculated forces. The errors in the horizontal and vertical direction and total errors can be defined as follows:

$$E_x = F_{xm}-F_{xp} \tag{4.1}$$

$$E_z = F_{zm}-F_{zp} \tag{4.2}$$

$$E^2 = E_x^2+E_z^2 \tag{4.3}$$

Where F_{xm} and F_{zm} represent the instantaneous measured force in the x and z directions respectively, and F_{xp} and F_{zp} represent the predicted forces in x and z direction

The mean square error can be obtained by integrating Eq. (4.3) with respect to phase angle (θ) over one wave cycle, i.e., $o \leq \theta \leq 2\pi$, and then dividing by 2π.

$$\overline{E^2} = \frac{1}{2\pi} \int_0^{2\pi} E^2 \, d\theta \tag{4.4}$$

Because F_{xp} and F_{zp} are functions of C_d and C_m, $\overline{E^2}$ also is a function of C_d and C_m. The technique to determine the force coefficients C_d and C_m is to minimize the mean squre error by setting the derivative with respect to C_d and C_m equal to zero respectively. Then, two simultaneous equations with unknowns C_d and C_m can be obtained. The force coefficients C_d and C_m are obtained from Eqs. (4.5) and (4.6):

$$C_d = \frac{(AA)(BB)-(DD)(EE)}{\frac{1}{2}\rho DL[(CC)(BB)-(DD)^2]} \tag{4.5}$$

$$C_m = \frac{(CC)(EE)-(AA)(DD)}{\frac{1}{4}\pi\rho D^2 L[(CC)(BB)-(DD)^2]} \tag{4.6}$$

in which

$$AA = \int_0^{2\pi} [F_{xm}u + F_{zm}w]|\vec{q}|\,d\theta$$

$$BB = \int_0^{2\pi} |\vec{q}'|^2 \, d\theta$$

$$CC = \int_0^{2\pi} |\vec{q}|^4 \, d\theta$$

$$DD = \int_0^{2\pi} [uu' + ww']|\vec{q}|\,d\theta$$

$$EE = \int_0^{2\pi} [F_{xm}u' + F_{zm}w']d\theta \, .$$

Note that $u = u_w + U$ for waves and current. For waves only condition (U=o), $u = u_w$ and $u_m = u_{wm}$.

Three major computer programs, named WAVES, FDATA and LABTEST, are used to process the data obtained from the Wave Research Facility in OSU and recorded on magnetic tape. The procedure for data reduction and the listing of these programs can be found in Nath (1981a) and Wankmuller and Nath (1982).

4.2. Conditioning of Force Coefficients

Usually, force coefficients obtained from laboratory experiments or ocean field tests have a wide range of scatter. This will cause a major difficulty in applying the Morison equation to predict hydrodynamic forces on marine structures. The major factors that cause scatter are:

(I) Validity of the two term Morison equation: Although the Morison equation has been widely used to predict hydrodynamic forces since it was proposed in 1950, the applicability of this equation is still in question. The main reason caused this question is that Morison equation does not take into account the vortex shedding forces and time history of the fluid flow.

(II) Accuracy of fluid particle kinematics: The fluid particle kinematics are usually determined from some theory or from direct measurement. Existing wave theories always predict the velocity and acceleration with some errors. The difference between predicted

values and true values depend on both the quality of the theory used and the quality of the wave produced. If the kinematics are measured directly, there will also exist some error between the measurements and the actual kinematics.

(III) Experimental errors: Errors can result from instrumentation sensitivity, calibration of the transducers, measurement of the water surface or fluid particle kinematics, or other variables during periods of small waves, etc.

Dean (1976) showed that depending on the wave and cylinder characteristics, data can be well-conditioned or poorly-conditioned for resolving drag or inertia coefficients. It is believed that much of the scatter in the reported coefficients may be from data that were poorly conditioned for resolving them. In general, if the drag forces tend to dominate, then the data are better conditioned for determining the drag coefficient and the inertia coefficient would tend to be contaminated by the errors of various sources noted before. Conversely, if the inertia force dominates, then errors can contaminate the drag coefficient. If the drag and inertia forces are nearly the same magnitude, then a reasonable resolution for both coefficients can be expected.

Dean (1976) proposed the idea of an "error surface" to evaluate the suitability of wave and wave force data. His work was intended for a vertical cylinder wherein the flow is oscillatory. It's now extended to a horizontal cylinder in waves and current.

According to the Taylor expansion (to second order), the mean square error $\overline{E^2}$, which is defined in Eq. (4.4), associated with the minimum error value can be expressed as follows:

$$\overline{E^2} = (\overline{E^2})_{min} + \left.\frac{\partial \overline{E^2}}{\partial C_d}\right|_{min} \Delta C_d + \left.\frac{\partial^2 \overline{E^2}}{\partial C_d^2}\right|_{min} \frac{(\Delta Cd)^2}{2} + \left.\frac{\partial \overline{E^2}}{\partial C_m}\right|_{min} \Delta C_m$$

$$+ \left.\frac{\partial^2 \overline{E^2}}{\partial C_m^2}\right|_{min} \frac{(\Delta C_m)^2}{2} + \left.\frac{\partial^2 \overline{E^2}}{\partial C_d \partial C_m}\right|_{min} (\Delta C_d)(\Delta C_m) \qquad (4.7)$$

Because the minimum slope of the error surface is zero, the least square method gives $\left.\frac{\partial \overline{E^2}}{\partial C_d}\right|_{min} = 0$ and $\left.\frac{\partial \overline{E^2}}{\partial C_m}\right|_{min} = 0$, and Eq. (4.7) reduces to

$$\overline{E^2} = (\overline{E})^2_{min} + \left.\frac{\partial^2 \overline{E^2}}{\partial C_d^2}\right|_{min} \frac{(\Delta C_d)^2}{2} + \left.\frac{\partial^2 \overline{E^2}}{\partial C_m^2}\right|_{min} \frac{(\Delta C_m)^2}{2}$$

$$+ \left.\frac{\partial^2 \overline{E^2}}{\partial C_d \partial C_m}\right|_{min} (\Delta C_d)(\Delta C_m) \qquad (4.8)$$

From Eq. (4.4) (4.3) and Eq. (2.14), (2.15), the following relations can be obtained.

$$\frac{\partial^2 \overline{E^2}}{\partial C_d^2} = \frac{1}{2\pi} \cdot 2 \left(\frac{\rho D}{2}\right)^2 \int_0^{2\pi} \left[\left|\vec{q}\right|^4\right] d\Theta \qquad (4.9)$$

$$\frac{\partial^2 \overline{E^2}}{\partial C_m^2} = \frac{1}{2\pi} \cdot 2 \cdot \left(\frac{\rho\pi D^2}{4}\right)^2 \int_0^{2\pi} [u'^2 + w'^2] d\Theta \tag{4.10}$$

$$\frac{\partial^2 \overline{E^2}}{\partial C_d \partial C_m} = \frac{1}{2\pi} \cdot 2 \cdot \left(\frac{\rho D}{2}\right) \left(\frac{\rho\pi D^2}{4}\right) \int_0^{2\pi} [u\, u' \,|\vec{q}\,| + w w' |\vec{q}\,|] \, d\Theta \tag{4.11}$$

Eq. (4.11) is always zero if linear wave theory is applied. The analytical integration is tedious but results can be easily obtained numerically and graphically. Thus,

$$\overline{E^2} = (\overline{E^2})_{min} + \left(\frac{\rho D}{2}\right) \frac{1}{2\pi} \int_0^{2\pi} [\,|\vec{q}\,|^4] \, d\Theta \, (\Delta C_d)^2$$

$$+ \left(\frac{\rho\pi D^2}{4}\right)^2 \frac{1}{2\pi} \int_0^{2\pi} [u'^2 + w'^2] \, d\Theta \, (\Delta C_m)^2 \tag{4.12}$$

Regarding ΔC_d and ΔC_m as variables, the above equation forms an ellipse with

$$\sqrt{\frac{\overline{E^2} - (\overline{E^2})_{min}}{\left(\frac{\rho D}{2}\right)^2 \frac{1}{2\pi} \int_0^{2\pi} [\,|\vec{q}\,|^4] \, d\Theta}}$$

and $\sqrt{\dfrac{\overline{E^2} - (\overline{E^2})_{min}}{\left(\frac{\rho\pi D^2}{4}\right) \frac{1}{2\pi} \int_0^{2\pi} [u'^2 + w'^2] d\Theta}}$ as the length of the two axes of

the ellipse.

Defining RR as a measure of the relative suitability of data for determining force coefficients, this value is provided by the ratio of the axes of the ellipse.

$$RR = \frac{\Delta C_m}{\Delta C_d} = \frac{2}{\pi D} \sqrt{\frac{\int_0^{2\pi} [|\vec{q}|]^4 d\theta}{\int_0^{2\pi} [|\vec{q}'|]^2 d\theta}} \tag{4.13}$$

If linear wave theory and linear superposition principle are applied, we have the following relations

$$\begin{aligned} u &= u_{wm} \cos \omega t + U \\ w &= w_m \sin \omega t \\ q^2 &= u^2 + w^2 \\ u' &= -\omega u_{wm} \sin \omega t \\ w' &= \omega w_m \cos \omega t \\ q'^2 &= \omega^2 [u_{wm}^2 \sin \omega t + w_m^2 \cos^2 \omega t] \ . \end{aligned} \tag{4.14}$$

By substituting Eq. (4.14) into Eq. (4.13), RR becomes

$$RR = \frac{\Delta C_m}{\Delta C_d} = \frac{T}{D\pi^2} \sqrt{\frac{\frac{3}{8} u_{wm}^4 + \frac{3}{8} w_m^4 + \frac{1}{4} u_{wm}^2 w_m^2 + U^4 + 3u_{wm}^2 U^2 + w_m^2 U^2}{\frac{1}{2} [u_{wm}^2 + w_m^2]}}$$

If there is no current in the wave field, i.e. U=0, the ratio is for horizontal cylinder in waves only.

$$RR = \frac{T}{D\pi^2}\sqrt{\frac{\frac{3}{8}u_{wm}^4 + \frac{3}{8}w_m^4 + \frac{1}{4}u_{wm}^2 w_m^2}{\frac{1}{2}[u_{wm}^2 + w_m^2]}} \tag{4.16}$$

For deep water conditions, the water particle orbit is circular, i.e. $u_{wm} = w_m = u_m$, the ratio becomes

$$RR = \frac{1}{\pi^2}\frac{Tu_m}{D}$$

$$= 0.101\ K \tag{4.17}$$

where K is the Keulegan-Carpenter number associated with the maximum horizontal water particle velocity only.

For planar oscillatory flow, such as wavy flow near the bottom in shallow water, the vertical velocity w_m is zero. Thus,

$$RR = \frac{1}{\pi^2}\sqrt{\frac{3}{4}}\frac{Tu_m}{D}$$

$$= 0.088\ K \tag{4.18}$$

Equation (4.18) is the same as Dean's result (see Dean 1976, Eq. 34). Dean also suggested in his study that if RR is smaller than 1/4, the data are relatively well-conditioned to determine the inertia coefficient. Conversely, the data are relatively suitable for determining drag coefficient if RR is larger than 4. If the ratio is between 1/4 and 4, the data are well-conditioned for determining both C_d and C_m. A criterion for the smooth horizontal cylinder in waves (or waves and current) is proposed in Section 5.1.

5. RESULTS AND DISCUSSION

5.1 Hydrodynamic Forces on a Horizontal Cylinder in Waves

A summary of the test run and results for a smooth horizontal cylinder in waves is presented in Table 5-1. The force coefficients C_d and C_m are plotted against the Reynolds number in Fig. 5-1 with those data obtained under planar oscillatory flow by Sarpkaya (1976). Besides the variation due to the different Keulegan-Carpenter numbers K and different water particle ratio, w_m/u_m, there still exists some scatter in this figure. This scatter may be due to:

(1) The lack of a term accounting for vortex shedding in the Morison equation.

(2) The differences between actual water particle kinematics and the predicted kinematics obtained from stream function wave theory. Nath (1981a) reported the root-mean-square errors for the kinematics are from 8% to 22%. However, the wave test profile were excellent because the root-mean-square errors between measured profiles and those obtained by stream function wave theory were only from 2% to 7%.

(3) According to the report of Nath (1981a, 1982), a return current exists in the wave tank. This current will affect the real kinematics around the test cylilnder. An approximation was given for estimating the return flow, based on a limited amount of data. So,

Run No.	T(sec)	H(ft)	R	K	w_m/u_m	C_d	C_m	RR
278	2.50	1.18	0.38	2.59	0.916	0.54	0.96	0.253
280		1.75	0.56	3.84		1.39	1.65	0.375
283		3.79	1.18	8.06		0.52	1.22	0.812
284	3.70	0.99	0.38	3.86	0.681	0.53	0.97	0.343
285		2.16	0.84	8.52		0.61	1.18	0.749
286		3.35	1.31	12.24		0.55	0.79	1.162
287		4.59	1.78	17.95		0.27	1.17	1.592
288		4.64	1.80	18.13		0.35	1.13	1.609
289	4.61	1.03	0.42	5.32	0.552	0.57	0.93	0.455
290		1.85	0.78	9.76		0.67	1.11	0.818
291		3.57	1.53	19.20		0.58	0.73	1.578
292		4.40	1.88	23.63		0.40	0.99	1.945
293	5.29	0.88	0.37	5.36	0.482	0.94	0.89	0.452
294		1.59	0.69	9.95		0.51	0.79	0.818
295		2.98	1.34	19.28		0.31	0.81	1.532
296		3.71	1.67	24.16		0.53	0.87	1.908
297	6.00	1.18	0.52	8.51	0.426	1.04	1.26	0.696
298		2.01	0.92	1.506		0.67	1.00	1.186
299		2.66	1.24	20.31		0.64	1.07	1.569
300		3.01	1.41	23.14		0.63	1.22	1.776
301	3.13	3.84	1.39	11.82	0.788	0.54	1.14	1.101
302	4.17	3.85	1.58	17.99	0.609	0.58	1.18	1.524
303	5.00	4.04	1.78	24.34	0.510	0.46	0.99	1.953
304	5.56	2.86	1.30	19.77	0.459	0.60	1.12	1.553
305	3.13	4.03	.145	12.37	0.788	0.32	1.18	1.155
313	2.50	1.16	0.37	2.55	0.916	0.34	1.04	0.249
315		1.57	0.51	3.45		1.21	1.39	0.336
316		2.84	0.91	6.17		1.14	1.16	0.608
318		3.54	1.11	7.59		0.19	1.44	0.758
319	3.70	0.91	0.35	3.54	0.681	0.46	0.89	0.316
320		1.93	0.75	7.60		0.70	1.19	0.669
321	3.70	2.75	1.08	10.86	0.681	0.58	1.28	0.954
323		4.22	1.64	1.658		0.55	1.29	1.464
324	4.61	0.89	0.36	4.58	0.552	0.47	1.02	0.394
325		1.77	0.74	9.32		0.77	0.90	0.783
326		3.28	1.40	17.62		0.57	1.12	1.450
327		4.26	1.82	22.89		0.48	0.90	1.884
328	5.29	0.92	0.39	5.61	0.482	0.81	0.69	0.473
329		1.71	0.74	10.74		0.77	0.91	0.879
331		3.89	1.76	25.34		0.54	0.79	2.000
332	6.00	1.28	0.57	9.28	0.426	0.74	0.88	0.755

Table 5-1

Summary of Data for a Smooth Horizontal Cylinder in Waves

Run No.	T(sec)	H(ft)	R	K	w_m/u_m	C_d	C_m	RR
334		2.68	1.25	20.47		0.77	1.25	1.581
335		2.92	1.37	22.42		0.67	1.09	1.723
337	4.17	4.35	1.78	20.27	0.609	0.43	1.13	1.722
338	5.00	3.85	1.70	23.19	0.510	0.30	1.23	1.861
339	5.56	3.58	1.65	24.95	0.459	0.36	1.13	1.944
341	3.70	0.95	0.37	3.70	0.681	0.35	0.91	0.329
342	4.61	0.87	0.36	4.47	0.552	0.67	1.02	0.385
343	5.29	0.96	0.41	5.87	0.482	0.84	0.65	0.494
344	6.00	1.31	0.58	9.51	0.426	1.05	1.25	0.773
345	3.70	2.84	1.11	11.23	0.681	0.56	1.01	0.985
346	4.61	3.42	1.46	18.39	0.552	0.57	0.86	1.512
347	6.00	2.69	1.26	20.55	0.426	0.61	1.12	1.587
349	5.29	3.71	1.67	24.16	0.482	0.35	1.13	1.908
350	4.61	4.12	1.76	22.15	0.552	0.32	1.22	1.822

Table 5-1
(Continued)

Summary of Data for a Smooth Horizontal Cylinder in Waves

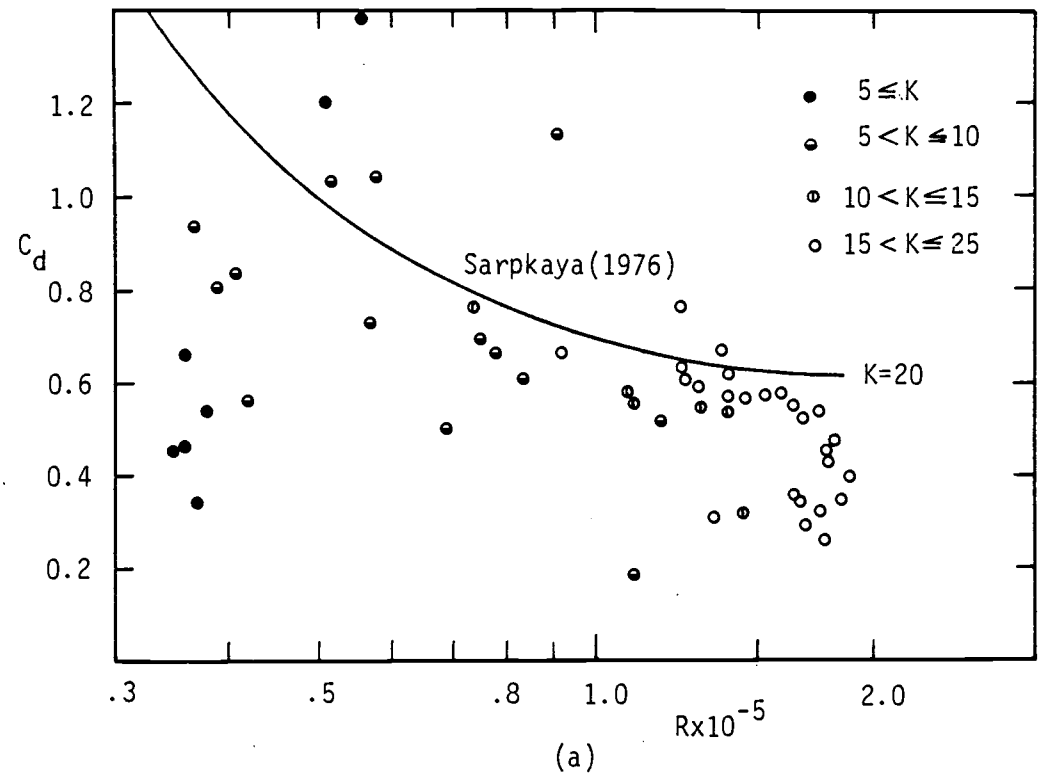

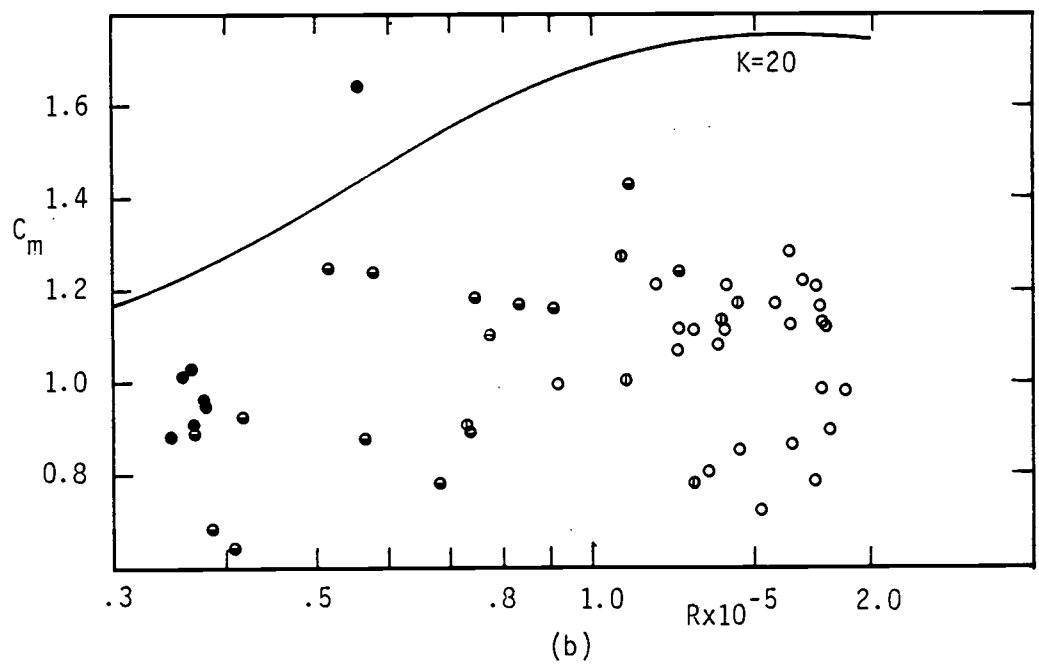

Fig. 5-1 (a)Drag and (b)Inertia Coefficients vs. Reynolds Number for a Smooth Horizontal Cylinder in Waves

the approximate nature of the return flow estimate may influence the scatter.

In spite of the scatter, it is evident that the force coefficients for a horizontal cylinder in waves are smaller than those for a cylinder under planar oscillatory flow. Thus, an over-estimate of forces can be expected if force coefficients obtained from planar oscillatory flow are used to predict the wave forces on a horizontal cylinder in waves.

The value of C_d and C_m with $25 \geq K \geq 18$ are plotted against Reynolds number in Fig. 5-2 [repeated from Fig. 25 of Nath (1982) with values multiplied by 1.03 for a calibration correction] with those obtained by Sarpkaya (1976) for K = 20 and Holmes and Chaplin (1978) for K = 24. Sarpkaya obtained his data by using the U-shape tube to generate planar oscillatory flow with $w_m/u_m = 0$. Holmes and Chaplin modelled experimentally circular orbital flow around a cylinder with $w_m/u_m = 1$ by moving a cylinder around a circular path in still water. The force coefficients obtained from the present study with $0.92 \geq w_m/u_m \geq 0.43$ almost fall between the values from Sarpkaya ($w_m/u_m = 0$) and Holmes and Chaplin ($w_m/u_m = 1$). This indicates the ratio w_m/u_m plays an important role in determining force coefficients for horizontal cylinder in waves and force coefficients could be functions of the ratio w_m/u_m, which will be further discussed later. There are two more reasons for the differences shown in Fig. 5-2: (1) different methods were applied to evaluate the water

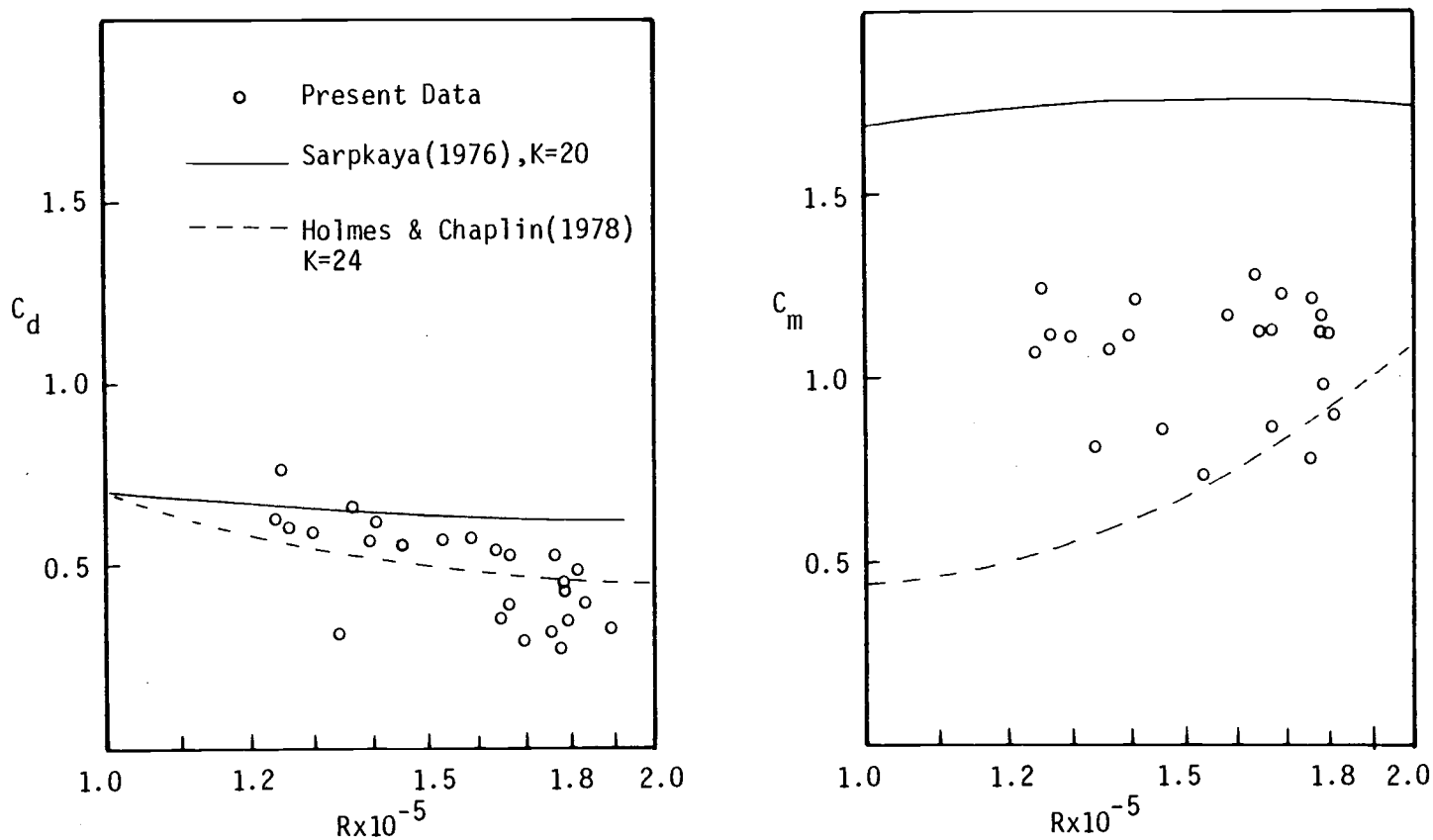

Fig. 5-2 C_d and C_m value for Smooth Cylinder in Waves for $25 > K > 15$

particle kinematics; and (2) different techniques were used to determine C_d and C_m.

To examine the dependence of C_d and C_m on the water particle velocity ratio w_m/u_m, data are plotted against K in Fig. 5-3. A trend is difficult to discern, nevertheless some similarity to the trend for a cylinder in planar oscillatory flow, noted by Sarpkaya (1982), does exist.

For small waves (or small K number), the wave forces are dominated by the inertia force and the test condition is not suitable for determining C_d values accurately. Thus, for small K value, C_d may not be accurate. It was considered by Nath (1981a, 1982) that the C_m could be low and inaccurate because the test cylinder was not solid and not sealed. For the unsealed cylinder, the water pressure could be transmitted to the inside of the cylinder through the gaps. It is still uncertain if the gaps affect the pressure transmission and the C_m values.

The present data with those obtained by Ramberg and Niedzwecki (1982) are plotted in Fig. 5-4. The C_d values obtained by Ramberg and Niedzwecki seem to form an upper bound for the present data for $12 \leq K$. One reason for this trend may be that the frequency parameter β ($=D^2/\nu T$) is an important parameter for evaluating force coefficients, as indicated by Sarpkaya (1976). The β for the present study is from 6110 to 14665 and is from 300 to 700 for Ramberg's study. It is on the order of 5×10^4 for prototype conditions (e.g.,

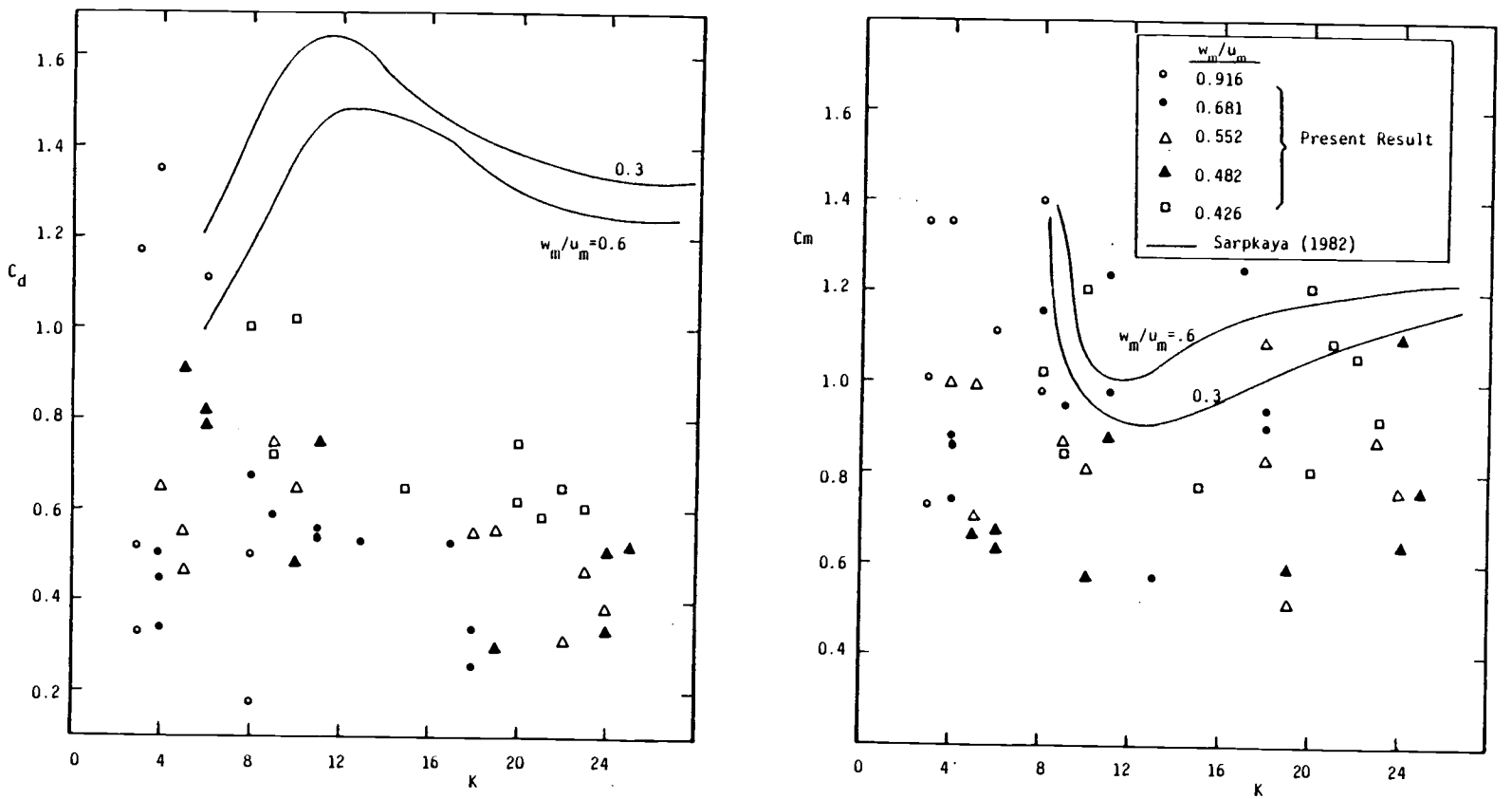

Fig. 5-3 (a)Drag and (b)Inertia Coefficients vs. Keulegan-Carpenter Number for Various Values of w_m/u_m for a Smooth Horizontal Cylinder in Waves

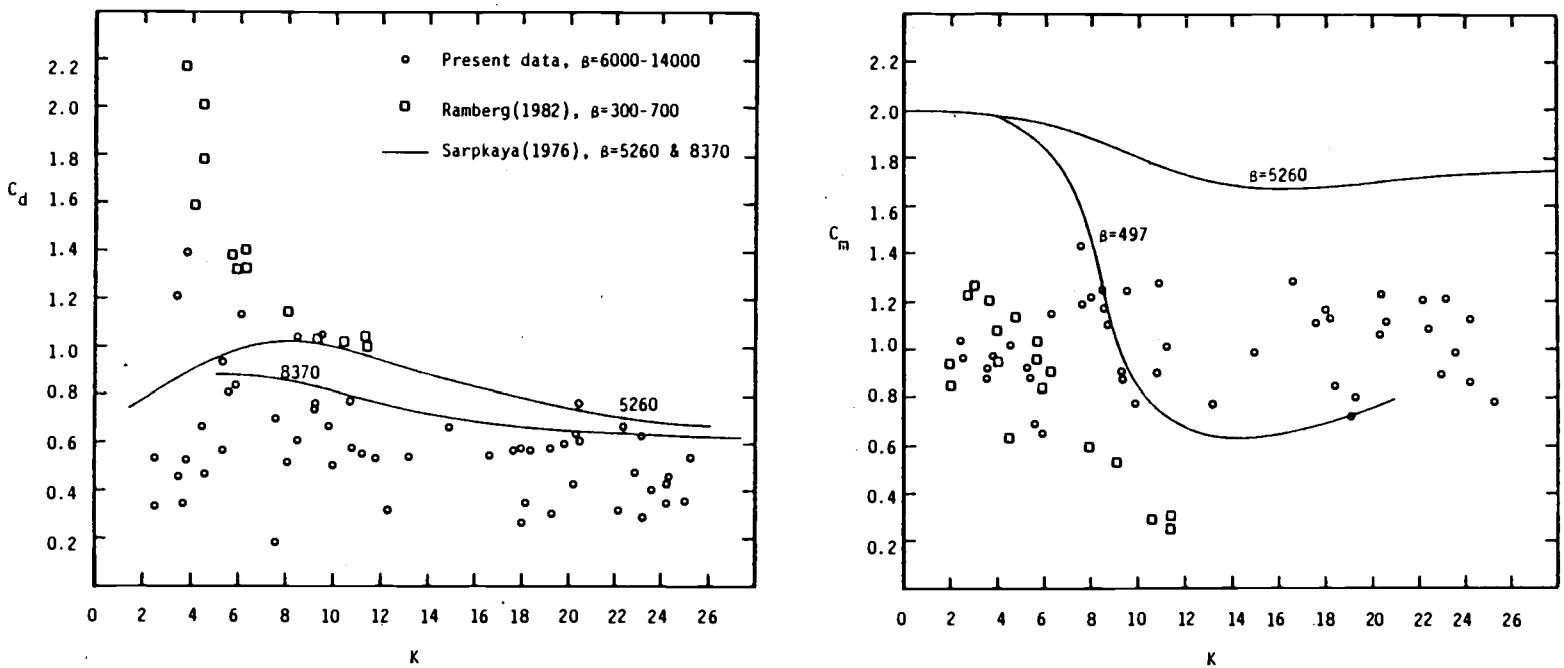

Fig. 5-4 (a)Drag and (b)Inertia Coefficients vs. Keulegan-Carpenter Number for a Smooth Horizontal Cylinder in Waves

T = 10 sec., D = 8 feet). As mentioned above, the data were not well-conditioned for determining C_d value for small K, so the data from Ramberg and Niedzwecki for K 4 vary from 1.6 to 2.2. Comparing with the results obtained by Sarpkaya (1976) for planar oscillatory flow, the present data are still reasonable in spite of the scatter. As for the C_m values, the present data and those of Ramberg and Niedzwecki seem to have the same order for $K < 6$. For $K > 6$, the differences between the present data and Ramberg's result are significant. Again, this phenomenon may be due to β values being different for these two experiments. It is observed that for both sets of data in waves the C_m values are smaller than those from planar oscillatory flow with the same order of β values. This again indicates that the force coefficients for a horizontal cylinder in waves are smaller than those for a vertical cylinder in waves (or horizontal cylinder in planar oscillatory flow).

Both Maull and Norman (1978) and Ramberg and Niedzwecki (1982) represented the hydrodynamic forces on a horizontal cylinder in waves by root-mean-square (r.m.s.) coefficients which are defined in Eq. (2.33) and Eq. (2.34). Comparisons between the data from their studies and the present results (re-computed) are presented in Fig. 5-5. The C_x values of these three sets of experiments agree quite well. For K>4, the present data are higher than those from the other two sets of experiments because of the higher β values. Except for the data with $w_m/u_m = 0.482$, the equal w_m/u_m values contours for C_z

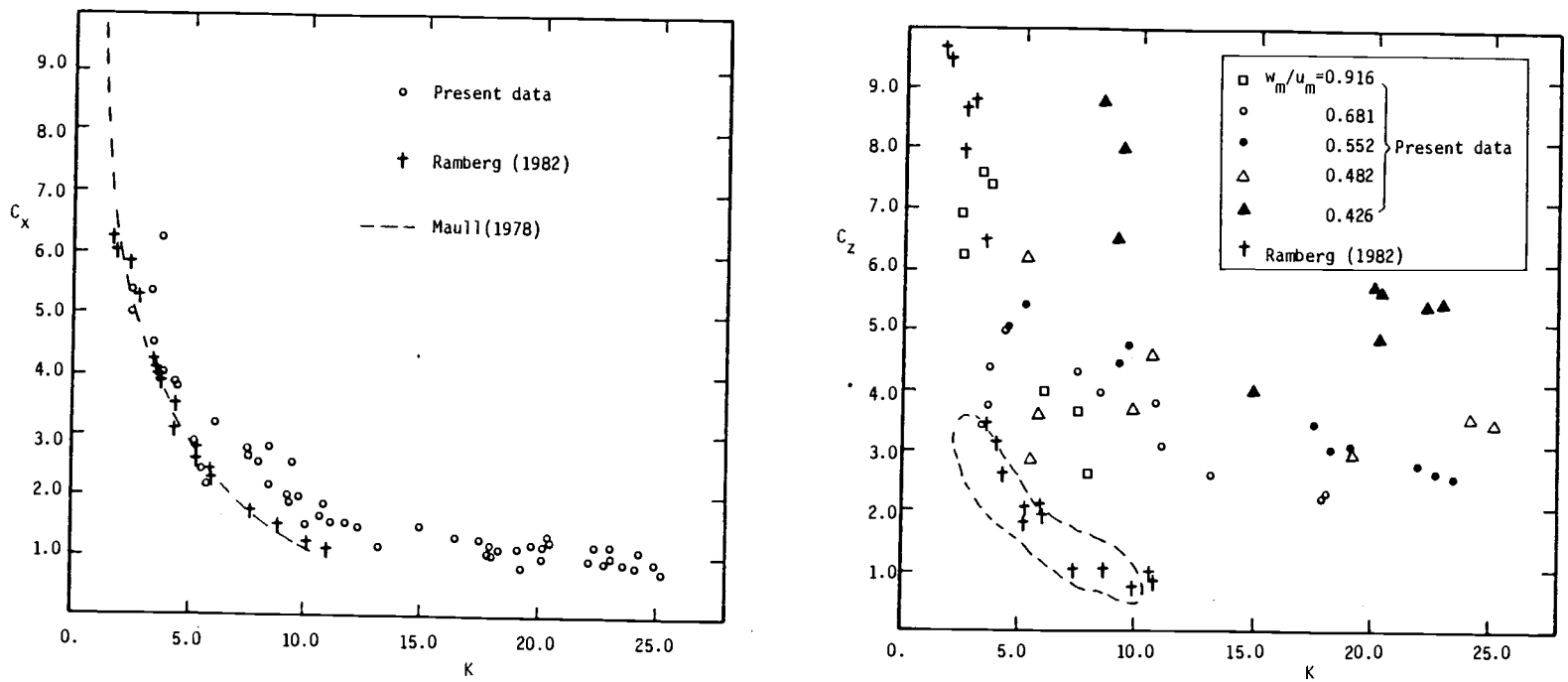

Fig. 5-5 (a)In-line and (b)Transverse Coefficients vs. Keulegan-Carpenter Number for a Smooth Horizontal Cylinder in Waves

seem not too difficult to trace. Comparing with Maull's and Ramberg's data, the present data appears to be anomalous. The reasons are (1) different β values as mentioned before, and (2) different w_m/u_m value as shown on the figure.

The results for the sand roughened cylinder with relative roughness $\varepsilon/D = 0.02$ are presented in Table 5-2. The force coefficients for $25 \geq K \geq 15$ are plotted against Reynolds number in Fig. 5-6 with present results for smooth cylinder. The results obtained by Sarpkaya (1976) for planar oscillatory flow with the same ε/D are also shown in this figure. As expected, C_d values for the horizontal cylinder in waves are smaller than those obtained in planar oscillatory flow. This trend is the same as that for the smooth cylinder.

Dean (1976) proposed a criterion for estimating the suitability of the data for determining C_d and/or C_m for a vertical cylinder in waves (neglecting w_m). An attempt is made here to propose a criterion for a horizontal cylinder in wavy flow. In Fig. 5-7, the RR values for a horizontal cylinder under wavy flow, as defined in Eq. (4,15), are plotted against the ratio of maximum drag force to maximum inertia force in one wave cycle, $(F_D)max/(F_I)max$. Because the calculated C_d and C_m values are used to determine the above maximum drag and inertia force, some errors will be introduced into the ratio $(F_D)max/(F_I)max$. If $(F_D)max$ is five times $(F_I)max$, it may be regarded that the drag force tend to dominate and the data are better conditioned for determining the C_d only. Conversely, if $(F_D)max = 5$

Run	T(sec)	H(ft)	w_m/u_m	C_d	C_m	R	K
379	2.50	1.14	0.916	1.47	1.02	0.37	3
381		2.94		1.05	0.63	0.94	6
382		3.74		0.19	0.31	1.17	8
384	3.70	0.95	0.681	1.35	0.94	0.37	4
385		2.27		1.31	1.05	0.89	9
386		2.95		0.94	0.73	1.16	12
387		4.02		1.06	0.80	1.57	16
388		4.44		0.94	0.88	1.72	17
389	4.61	0.88	0.552	0.96	0.90	0.36	5
390		1.92		0.60	0.73	0.81	10
391		3.55		0.74	1.12	1.52	19
392		4.24		0.93	1.15	1.81	23
393	5.29	0.92	0.482	0.83	0.76	0.39	6
394		1.64		0.77	0.84	0.71	10
395		3.00		0.83	1.33	1.35	19
396		3.83		0.88	1.06	1.73	25
397	6.02	1.28	0.426	1.11	1.38	0.57	9
399		2.83		1.04	0.90	1.33	22
400		3.20		1.02	0.88	1.51	25
401	3.70	2.98	0.681	0.93	0.74	1.17	12
402	5.29	3.03	0.482	0.82	1.32	1.36	20
403	3.13	4.44	0.788	1.02	0.64	1.58	14
404		3.09		0.80	0.77	1.12	10
405	4.17	4.43	0.609	0.99	0.65	1.81	21
406		2.81		1.07	1.45	1.15	13
407	5.00	4.32	0.510	0.67	0.81	1.91	26
408		3.32		0.76	0.63	1.46	20
409	5.56	3.62	0.459	0.88	0.48	1.66	25
410		3.00		0.94	0.81	1.37	21

Table 5-2

Summary of Data for a Sand Roughened Horizontal Cylinder in Waves

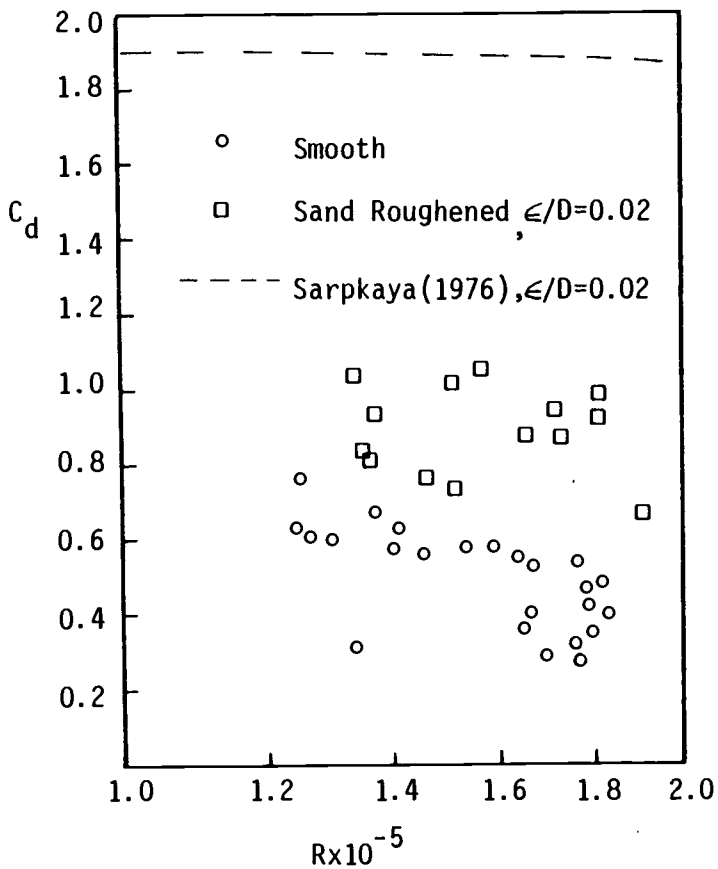

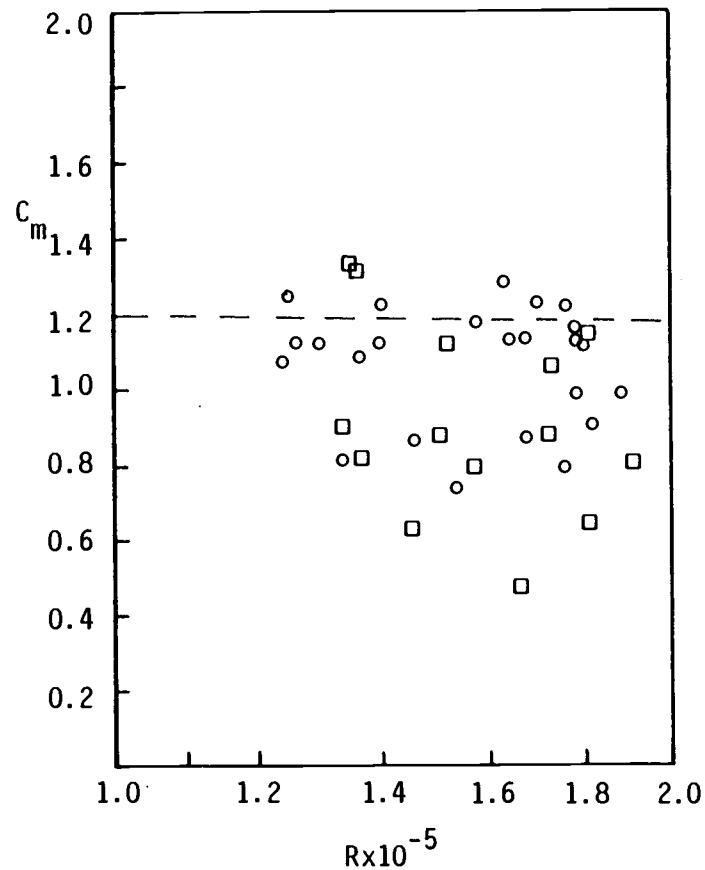

Fig. 5-6 Comparison of Force Coefficients between Smooth and Sand Roughened Cylinder in waves

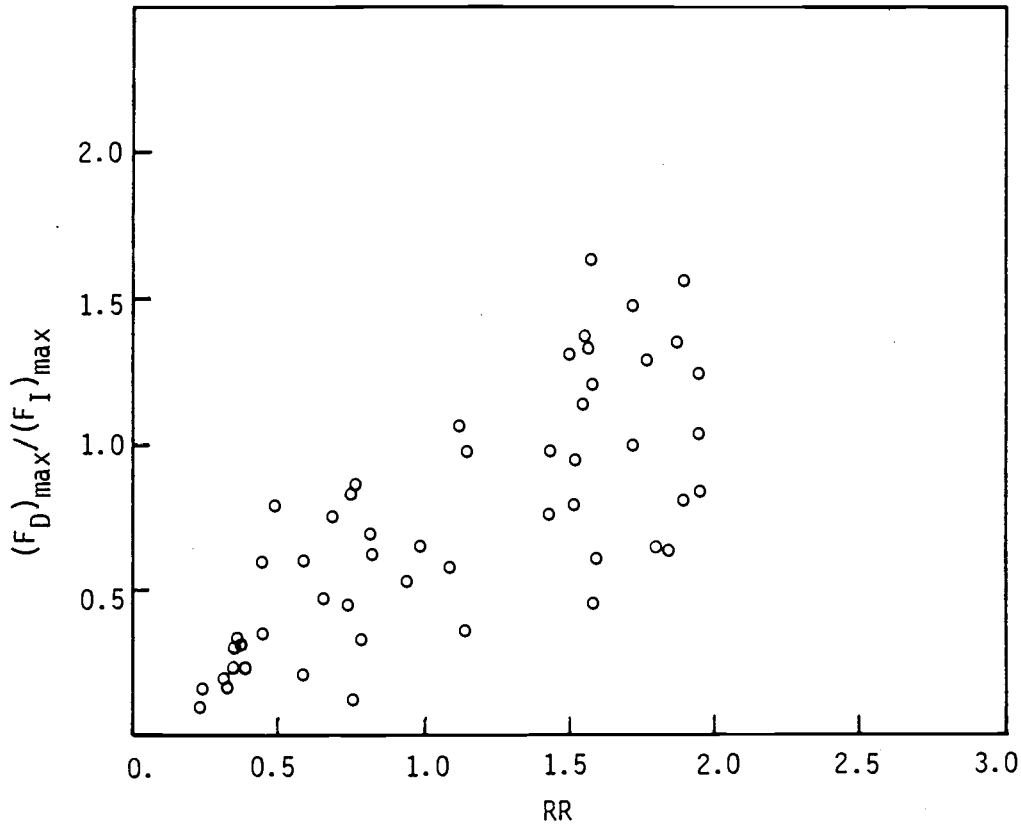

Fig. 5-7 RR Values vs. $(F_D)_{max}/(F_I)_{max}$

(F_I)max, the data are well-conditioned for determining C_m only. Based on above assumption and some conservative choices, the following criterion for a horizontal cylinder under wavy flow is suggested.

RR	Relatively better conditioned to determine
<0.4	C_m
0.4-8.0	C_d and C_m
>8.0	C_d

Because the roughness will affect the force coefficients, i.e. ususally C_d increases and C_m decreases as relative roughness ε/D increases (for relatively small values of ε/D), the $(F_D)_{max}$ and $(F_I)_{max}$ will change with respect to ε/D. This RR values vary with the roughness and the above criterion is appropriate for smooth cylinder only.

5.2 Hydrodynamic Forces on a Horizontal Cylinder under Waves Plus Towing (or under Waves and Current)

The summary of the test conditions and results for both smooth and sand roughened cylinder under waves plus towing is tabulated in Table 5-3. In this table, the R,K and VM are defined as

$$R = \frac{q_m D}{\nu} = \frac{u_m D}{\nu} = \frac{(u_{wm}+U)D}{\nu} \tag{5.1}$$

$$K = \frac{q_m T}{D} = \frac{u_m T}{D} = \frac{(u_{wm}+U)T}{D} \tag{5.2}$$

Run No.	U $\left(\frac{ft}{sec}\right)$	H(ft)	T(sec)	Tap (sec)	C_d	C_m	VM	R	K	RR	U/u_{wm}
Smooth Cylinder											
366	0.67	3.13	6.02	5.80	0.48	1.36	5.41	1.82	28.75	2.89	0.23
367	0.71	3.59	5.29	5.09	0.53	0.71	5.02	1.98	27.52	2.78	0.22
368	0.82	4.30	4.61	4.40	0.48	0.91	5.02	2.26	27.05	2.80	0.23
370	0.82	3.79	2.50	2.35	0.63	1.28	2.68	1.65	10.55	1.21	0.34
371	3.45	3.00	6.02	5.05	0.50	1.97	24.24	3.17	43.71	9.93	1.25
372	3.57	3.59	5.29	4.40	0.39	2.82	21.84	3.44	41.31	8.70	1.12
373	4.24	4.57	4.61	3.69	0.44	0.76	21.78	4.11	41.42	8.76	1.11
375	6.33	3.55	6.02	4.45	0.42	0.75	39.20	4.91	59.66	12.29	1.18
376	6.33	3.76	5.29	3.89	0.43	2.38	34.26	4.93	52.31	17.38	1.90
Sand Roughened Cylinder											
422	4.07	3.87	2.50	1.89	1.05	1.43	10.69	3.28	16.89	4.14	1.72
423	4.03	4.48	2.50	1.89	0.79	0.71	10.61	3.40	17.53	4.00	1.53
424	3.33	3.20	6.02	5.08	0.97	1.69	23.43	3.21	44.46	9.46	1.13
425	3.40	3.56	5.29	4.43	1.04	0.27	20.97	3.34	40.41	8.26	1.08
430	6.25	3.91	5.29	3.91	0.87	1.71	33.94	4.95	52.75	16.86	1.81
431	6.25	3.24	6.02	4.47	0.79	0.81	38.84	4.72	57.50	20.89	2.08
432	4.15	4.52	3.70	2.94	1.07	0.50	16.94	3.87	30.99	6.58	1.21
433	0.71	3.31	6.02	5.79	0.73	0.15	5.72	1.93	30.46	3.06	0.23
434	0.71	3.91	5.29	5.09	0.64	1.16	5.02	2.13	29.50	2.94	0.21
435	0.89	4.39	4.61	4.38	0.69	0.72	5.42	2.33	27.86	2.93	0.24

Table 5-3

Summary of Data for a Horizontal Cylinder under Waves and Current (Smooth and Sand Roughened)

$$VM = \frac{UT}{D} \tag{5.3}$$

Hogben et al. (1977) indicated that the Keulegan-Carpenter number, K, represents the relative magnitude of drag to inertia force for planar oscillatory flow. He suggested that the vector sum for the velocity should be used although the meaning and evaluation of the K number is uncertain when a current is introduced into the flow field. Sarpkaya and Isaacson (1981 pp. 323) also suggested using Eq. (5.1) and Eq. (5.2) as the definition of R and K for waves and current.

In the next section, it will be shown experimentally that the kinematics for towing a cylinder in a wave field are the same as those under waves and current if the superposition principle is assumed.

For the smooth cylinder, the data are well-conditioned for determining both C_d and C_m values for waves with low tow speed ($U < 1.0$) whether present criterion (proposed in Section 5.1) or Dean's criterion (1976) is used. For the high tow speed case, the data are suitable for determining drag coefficient only, and the inertia coefficient values obtained under this circumstance are not reliable. As mentioned in Section 5.1, the criterion for RR values varies for the sand roughened cylinder, so both sets of criteria are no longer useful. But, it still can be said that the data are suitable for determining C_d only when the RR value is large.

The force coefficients for a smooth cylinder under waves and current are plotted against Reynolds number in Fig. 5-8 with those obtained under planar oscillatory flow and the present results for waves only. The dependence of C_d on R can be roughly observed. In the present study for waves plus towing, the detail of C_d vs. R can not be established because the data are insufficient. However, the drag coefficients for waves and current are less than those for planar oscillatory flow because the vertical component of water particle velocity is still present. As expected, the inertia coefficients are scattered because the data are not well-conditioned for C_m values.

For a horizontal cylinder under waves and current, the drag coefficients for the sand roughened cylinder are greater than those for the smooth one as shown in Fig. 5-9. This trend is the same as that for planar oscillatory flow and that for waves only. From Table 5-3, it shows the runs for sand roughened cylinder proceeded from high tow speed. It is possible, but not proven, that some sand could have been lost, which could account for some of the lower C_d value, especially for later runs.

The drag coefficient for both smooth and sand roughened cylinders under waves and current, together with those for steady flow obtained by Nath (1983), are plotted in Fig. 5-10. The value near the point represents the ratio of current velocity (or tow speed) to the maximum horizontal wave-induced velocity U/u_{wm}. From

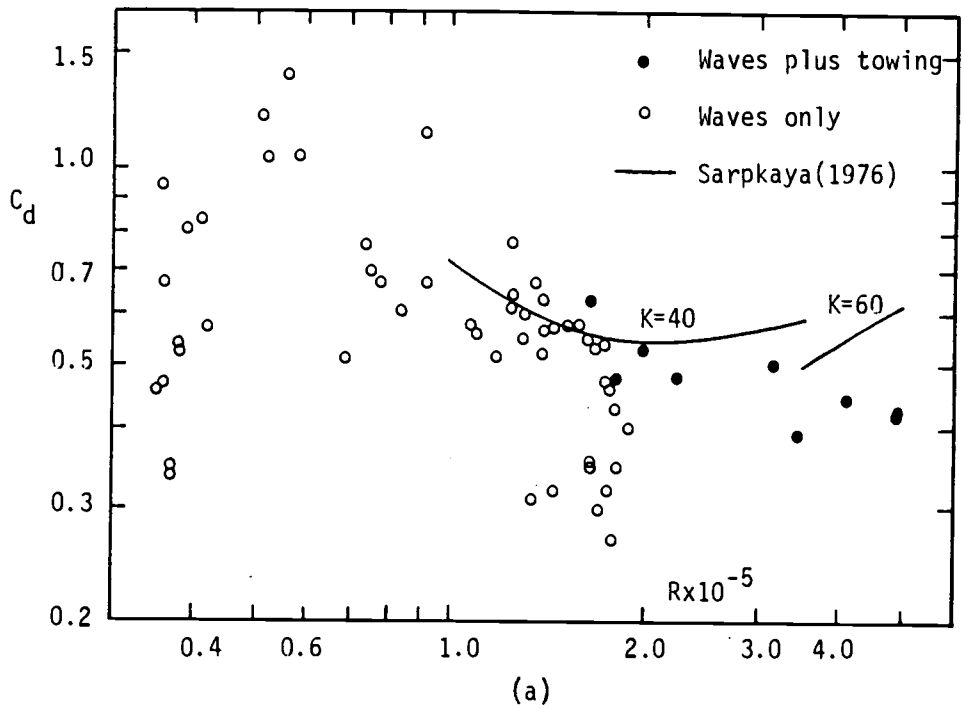

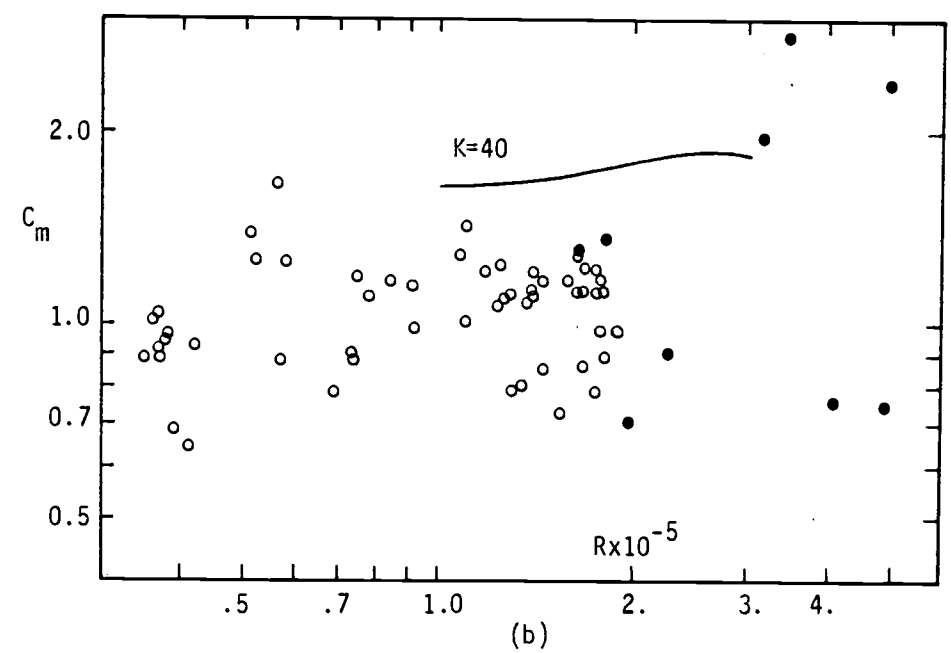

Fig. 5-8 (a)Drag and (b)Inertia Coefficients vs. Reynolds Number for a Smooth Cylinder under Waves and Towing

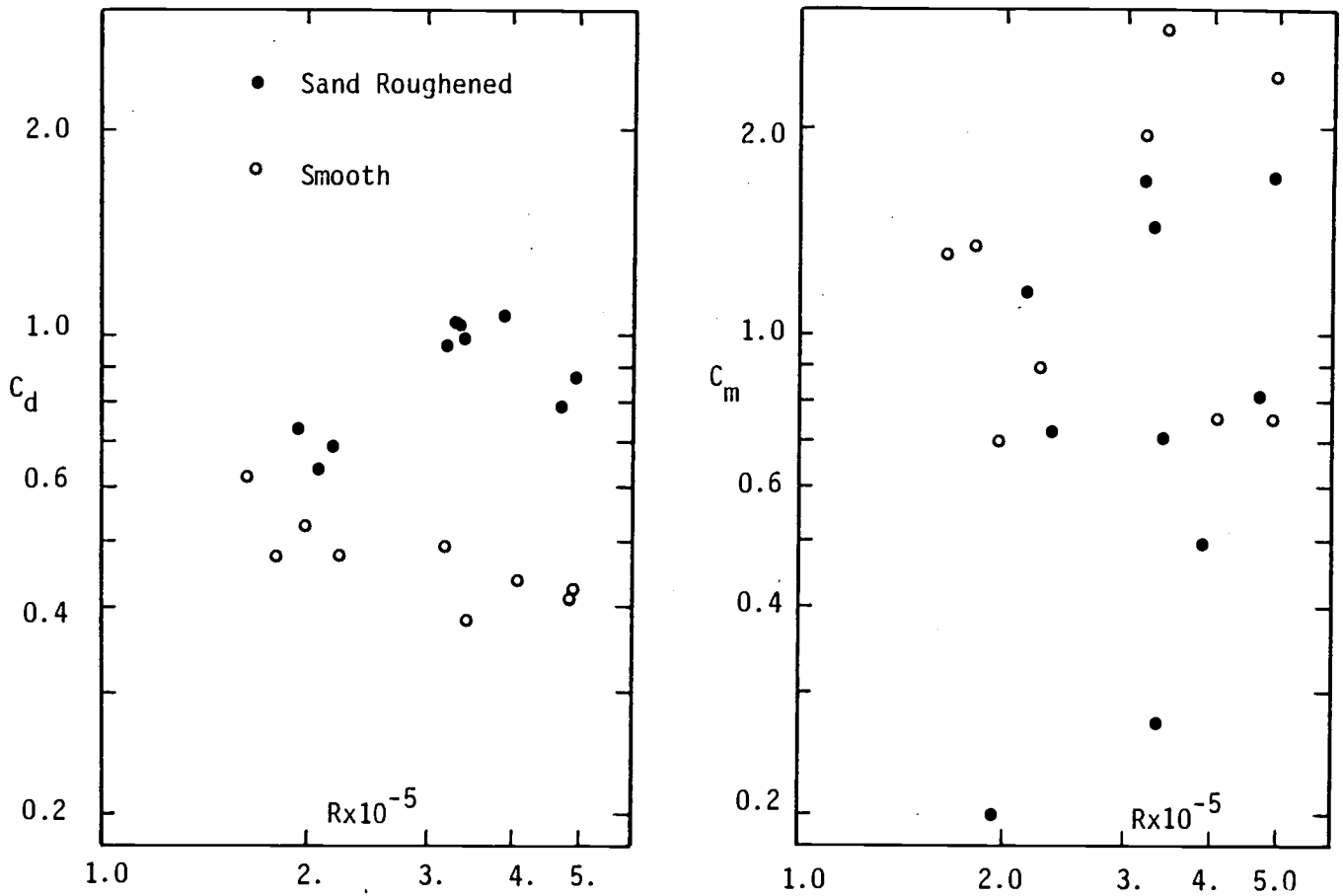

Fig. 5-9 (a)Drag and (b)Inertia Coefficients vs. Reynolds Number for a Sand Roughened Cylinder under Waves and Towing(current)

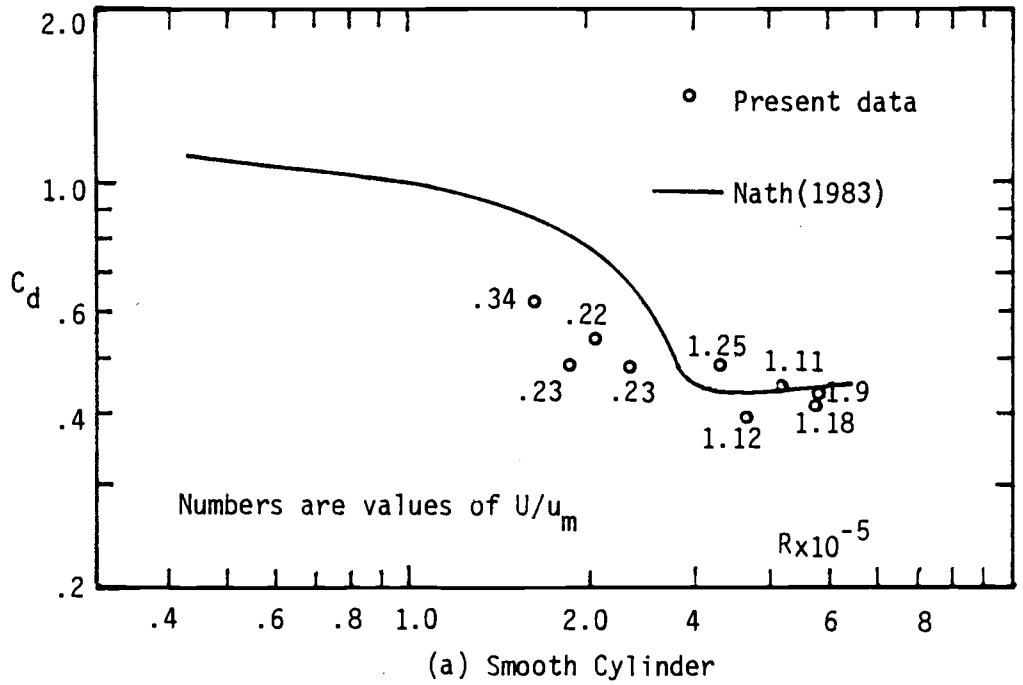

(a) Smooth Cylinder

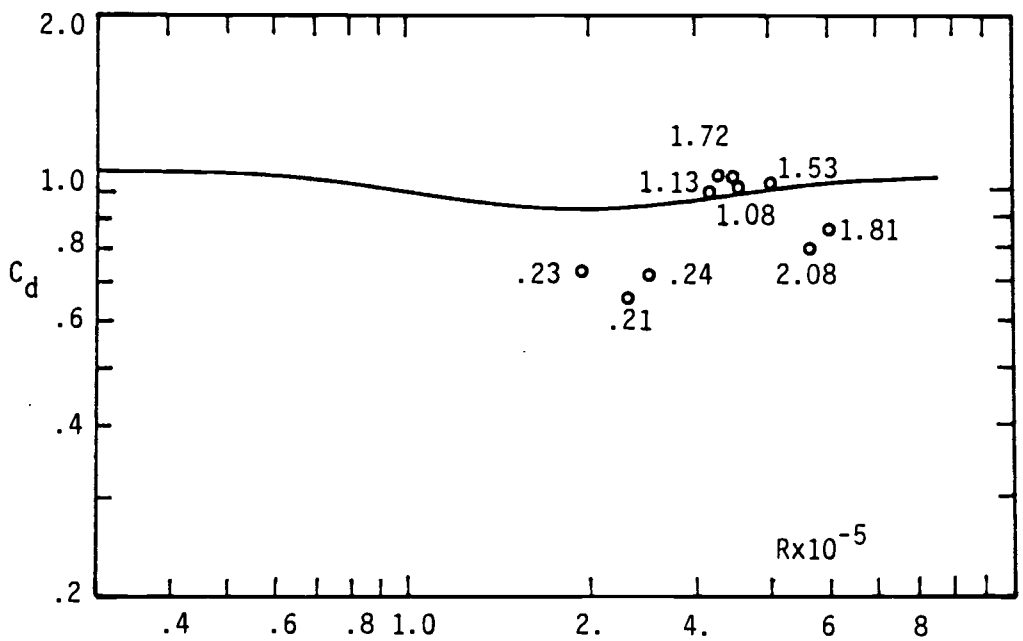

(b) Sand Roughened Cylinder

Fig. 5-10 Comparison between Drag Coefficients Obtained from Steady Flow and Those under Waves plus Towing

the figure, it can be interpreted that the drag coefficients for waves and current approach the data for steady flow when U/u_{wm} = 1.0. A conclusion can be drawn that the drag coefficient for waves and current tends to approach the drag coefficient for steady current as the current speed U (or U/u_{wm}) increases. If U (or U/u_{wm}) is large enough, these two sets of data will coincide with each other. In Fig. 5-10(b), the two points with high tow speed are away from steady state flow result is inexplicable. One possible reason is that some sand could have been removed during the first few runs (as mentioned before).

The dependence of C_d on VM number can be observed in Fig. 5-11. For the smooth cylinder, C_d approaches a constant 0.42 as VM increases. For the sand roughened cylinder, the C_d are higher than those for the smooth cylinder. These values reach 1.1 for $20 > VM > 10$ and then decrease as VM increases. Again, C_m values are distributed randomly against VM.

As shown in Fig. 5-12, the dependence of the force coefficients on K, which is defined in Eq. (5.2), is not as evident as the other parameters (R and VM).

The r.m.s. in-line and transverse force coefficients C_x and C_z are evaluated for a horizontal cylinder under waves and current. The results are presented in Fig. 5-13 together with the results for waves only. The in-line force coefficients, C_x, are consistent for

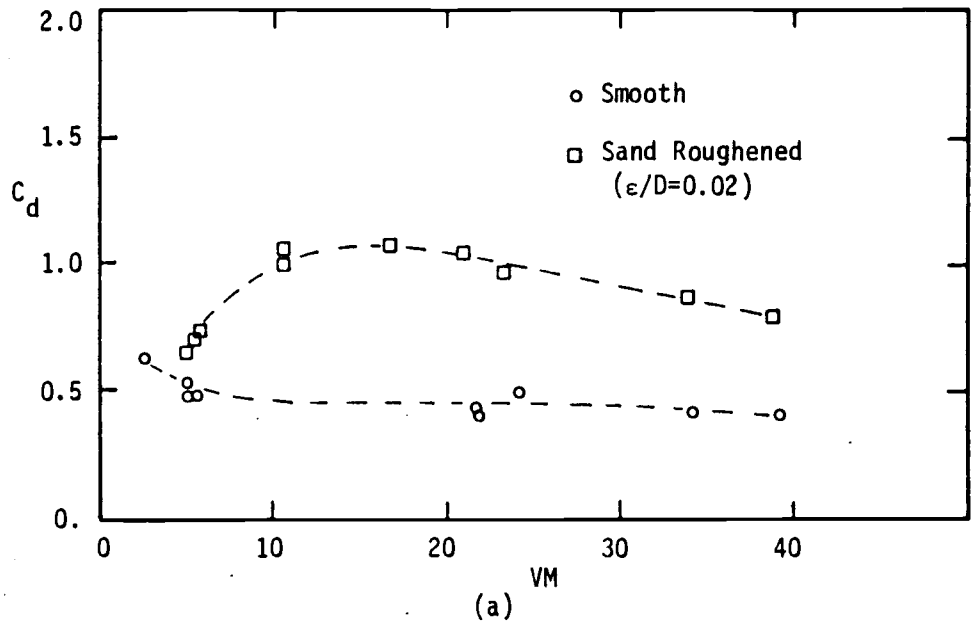

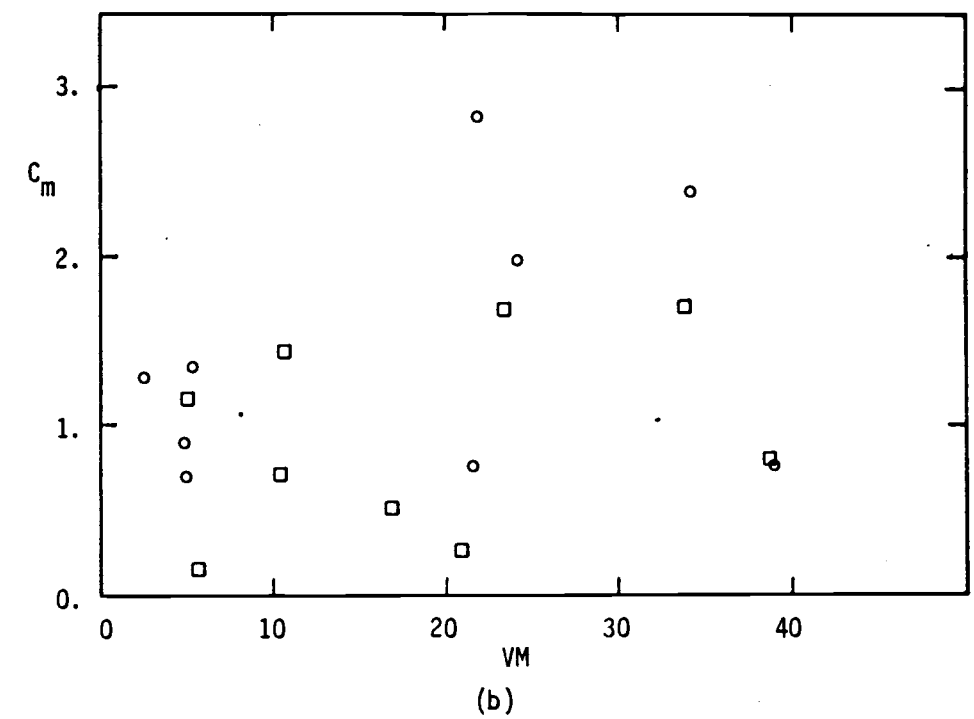

Fig. 5-11 (a)Drag and (b)Inertia Coefficients vs. Verley and Moe Number for a Cylinder under Waves and Towing

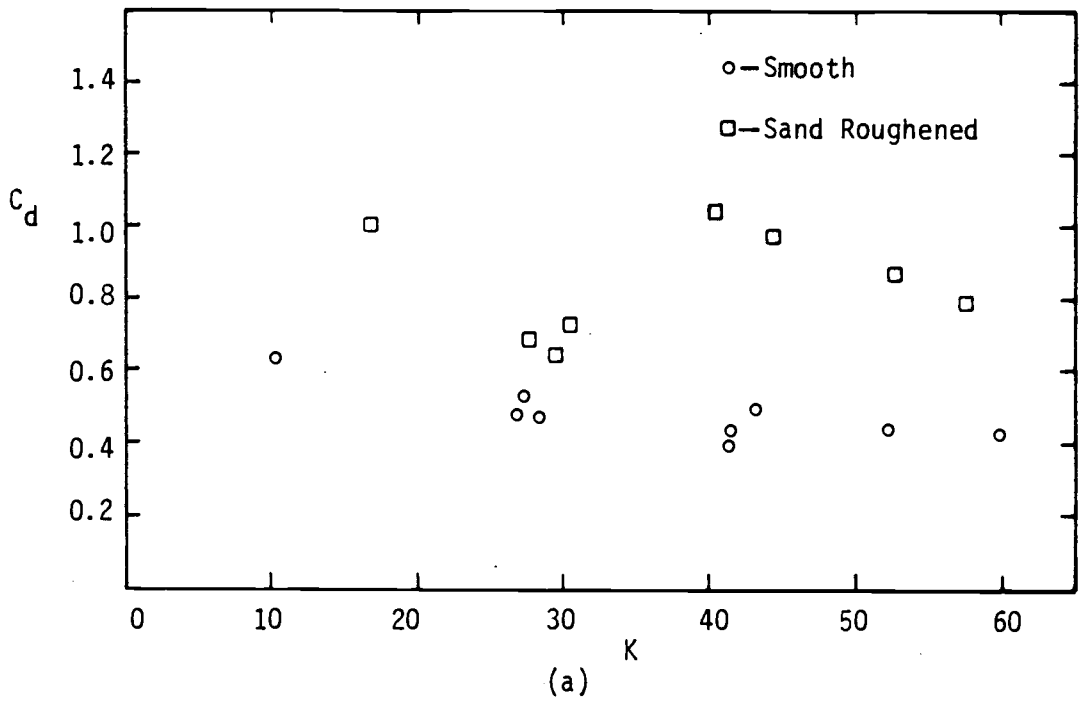

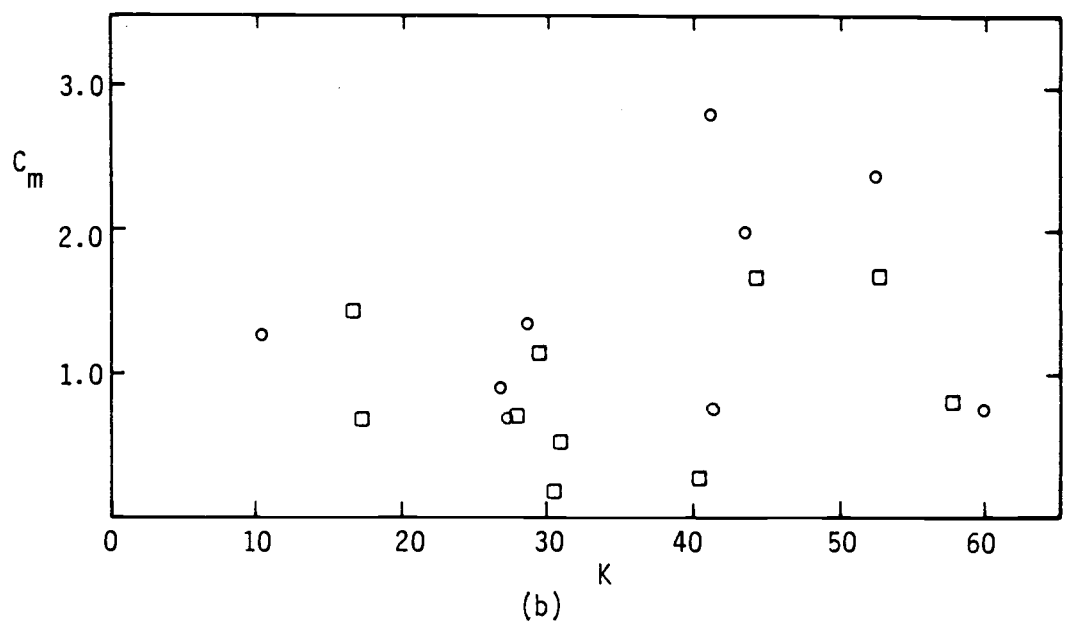

Fig. 5-12 (a) Drag and (b) Inertia Coefficients vs. Keulegan-Carpenter Number for a Smooth and a Sand Roughened Cylinder under Waves and Towing

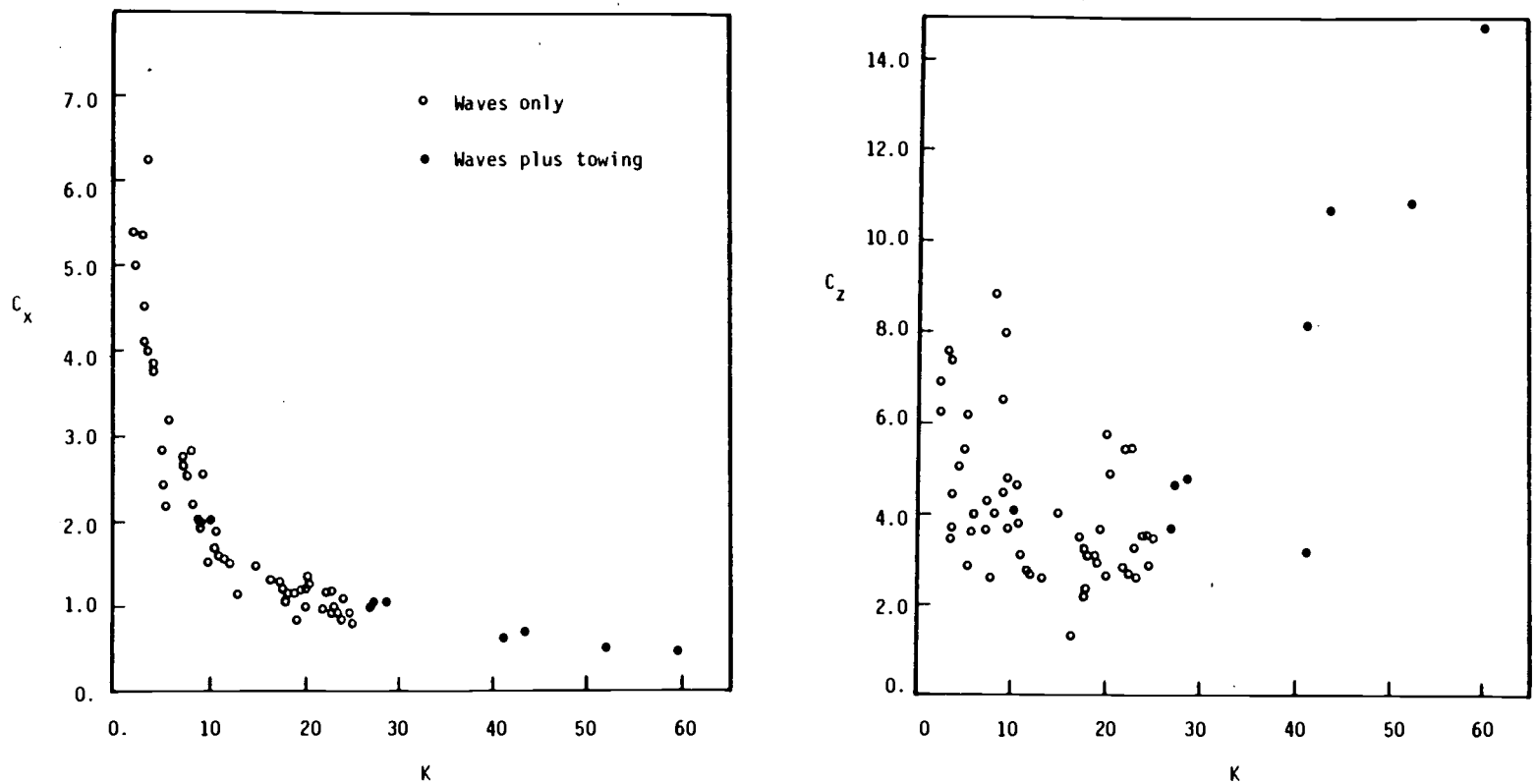

Fig. 5-13 (a)In-line and (b)Transverse Coefficients vs. Keulegan-Carpenter Number for a Smooth Horizontal Cylinder under Waves Plus Towing

both sets of data. For K>50, the C_x values seem to approach a constant value of 0.5. For K<30, both sets of C_z values seem to have the same order of magnitude. For K>30, the C_z values increase rapidly. In this region, the influence on vertical forces F_z from vortex shedding is stronger than that for the vertical velocity.

5.3 Similarity Between "Waves and Towing" and "Linear Superposition Principle"

For the laboratory tests, the current meters were towed with the test cylinder in a wave field to obtain the measured kinematics. To avoid the flow around the meters from being affected by the cylinder the two current meters were placed 2.01 feet above the center line of the test cylinder (See Fig. 3-1). Each component of measured water particle velocity was recorded for both digital tape and strip chart.

The predicted kinematics under waves and current are obtained by using the seventh order stream function wave theory with superimposing the tow speed U onto the wave-induced velocity. That is,

$$u(x,z) = \sum_{n=1}^{7} X(n) \left[\frac{2\pi}{L}n\right] \cosh\left[\frac{2\pi}{L}n(h+z)\right]\cos\left[\frac{2\pi n}{L}x\right]+U \qquad (5.4)$$

$$w(x,z)=-\sum_{n=1}^{7} X(n) \left[\frac{2\pi}{L}n\right]\sinh\left[\frac{2\pi}{L}n(h+z)\right]\sin\left[\frac{2\pi n}{L}x\right] \qquad (5.5)$$

Two typical measurements for horizontal water particle velocity with associated measured wave profile are shown in Fig. 5-14. One is

for the cylinder with low tow speed and the other is for the high tow speed. By examining the difference between measured value and predicted value for one wave cycle, i.e., 33 points for one wave, it can be said that the predicted horizontal velocity fits the measured one quite well except for a few runs. Two examples of comparison betwen predicted values and measured data are shown in Fig. 5-15, one is for the low tow speed case and the other is for the high tow speed. The root-mean-square error defined in the following equation is used as one indicator to compare the predicted and measured horizontal water particle velocity.

$$E_{rms} = \frac{\left[\sum_{1}^{N} (u_{measured} - u_{predicted})^2\right]^{\frac{1}{2}}}{\frac{N}{(u_{measured})_{max}}} \qquad (5.6)$$

The second indicator is the ratio of maximum predicted horizontal velocity to the maximum measured horizontal velocity, $(u_p)_{max}/(u_m)_{max}$. Actually, the mean horizontal velocity for one whole wave cycle can be defined as the current velocity. The ratio of the mean predicted horizontal velocity to the mean measured horizontal velocity is used as the third indicator. The summary of the results is presented in Table 5-4. From the comparisons of the plots and these three indicators, it is believed that the horizontal velocity "felt" by a towing cylinder in a wave field can be predicted by using linear superposition principle. The root-mean-square error for the

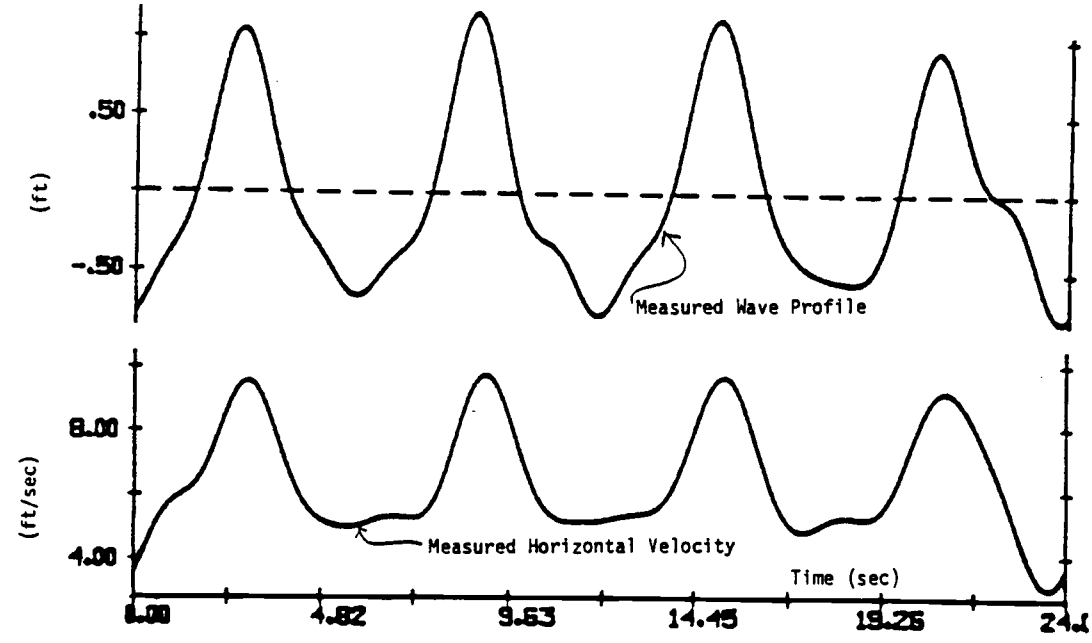

(a) High Tow Speed: U=6.25 ft/sec

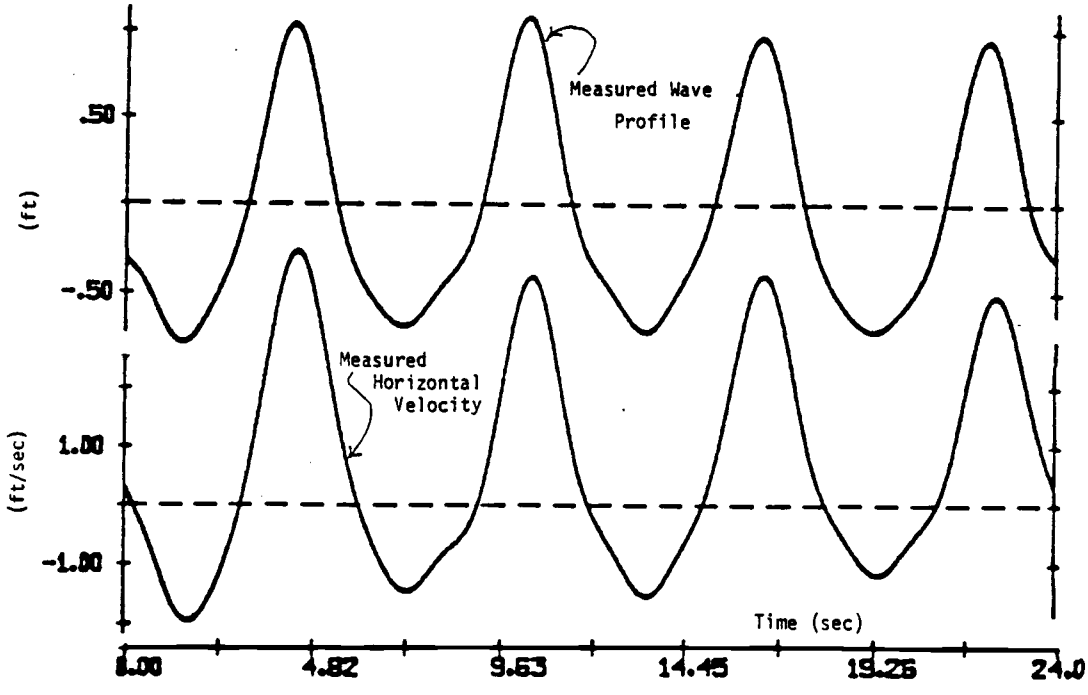

(b) Low Tow Speed: U=0.71 ft/sec

Fig. 5-14 Measurements of Horizontal Velocity under Waves and Towing

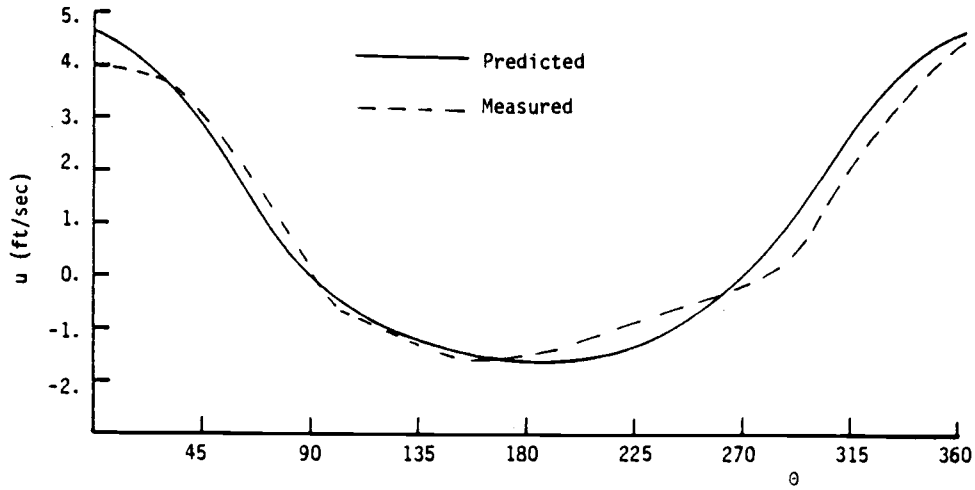

(a) Low Tow Speed: T=5.29 sec., H=3.91 ft., U=0.71 ft/sec (Run 434)

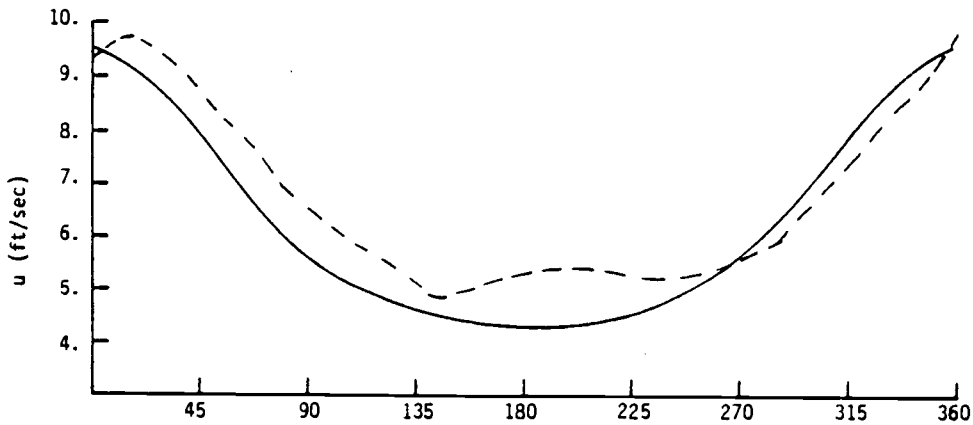

(b) High Tow Speed: T=6.02 sec., H=3.24 ft., U=6.25 ft/sec (Run 431)

Fig. 5-15 Comparison between Predicted values and Measured Oata for Horizontal Velocity under Waves and Towing (a) U=0.71 and (b) U=6.25

Run No.	T (sec)	H (ft)	U (ft/sec)	H/T^2	h/T^2	$E_{rms}(u)$	$E_{rms}(F)$	$\frac{(u_p)_{max}}{(u_m)_{max}}$	$\frac{u_p}{u_m}$
422*	2.50	3.87	4.07	0.6192	1.8400	0.2185	0.0489	1.108	1.227
423	2.50	4.48	4.03	0.7168	1.8400	0.0315	0.0569	0.997	1.029
424	6.02	3.20	3.33	0.0883	0.3173	0.0503	0.0483	0.969	1.007
425	5.29	3.56	3.40	0.1272	0.4110	0.0373	0.0515	1.024	1.066
430	5.29	3.91	6.25	0.1397	0.4110	0.0855	0.0344	1.048	0.930
431	6.02	3.24	6.25	0.0894	0.3173	0.0476	0.0331	0.971	0.934
432	3.70	4.52	4.15	0.3302	0.8400	0.0349	0.0533	1.006	0.997
433	6.02	3.31	0.71	0.0913	0.3173	0.0664	0.1180	0.975	1.116
434	5.29	3.91	0.71	0.1397	0.4110	0.0354	0.0862	1.045	1.080
435	4.61	4.39	0.89	0.2066	0.5411	0.1265	0.1339	1.029	0.784
Mean Value (Except Run 422)						0.0573	0.0684	1.007	0.999
Standard Deviation						0.0313	0.0363	0.031	0.108

*It is obvious that there is something wrong with at least $E_{rms}(u)$ for Run 422. Therefore it is excluded as calculating mean value and standard deviation.

Table 5-4

Summary of Error Indicators for Horizontal Velocity under Waves and Towing

horizontal velocity, $E_{rms}(u)$ in Table 5-4, is the same order as that for force, $E_{rms}(F)$. That means the small error due to the horizontal velocity, as calculated will not have a large influence on forces and force coefficients.

For the vertical water particle velocity, the trend between measured record and predicted value is compared. Fig. 5-16 and Fig. 5-17 show two typical examples of vertical velocity for low tow speed and high tow speed respectively. No major phase shift can be observed. The magnitude of vertical velocity seems to be overpredicted by up to 20% at some points for both high tow speed and low tow speed case. It can be concluded that the vertical velocity is more or less unchanged during towing.

5.4. Total and Local Acceleration for Force Prediction

The total and local accelerations of the water particle for all test runs in the present study were calculated by using the seventh order stream function wave theory. In one wave cycle, the phase between the total acceleration and the local acceleration is unchanged, but the magnitudes will be different. To examine the magnitude difference between total and local acceleration, the following three parameters are used.

$$\frac{(Dq/Dt)_{max}}{(\partial q/\partial t)_{max}} = \alpha_q = \text{gross acceleration rato} \qquad (5.7)$$

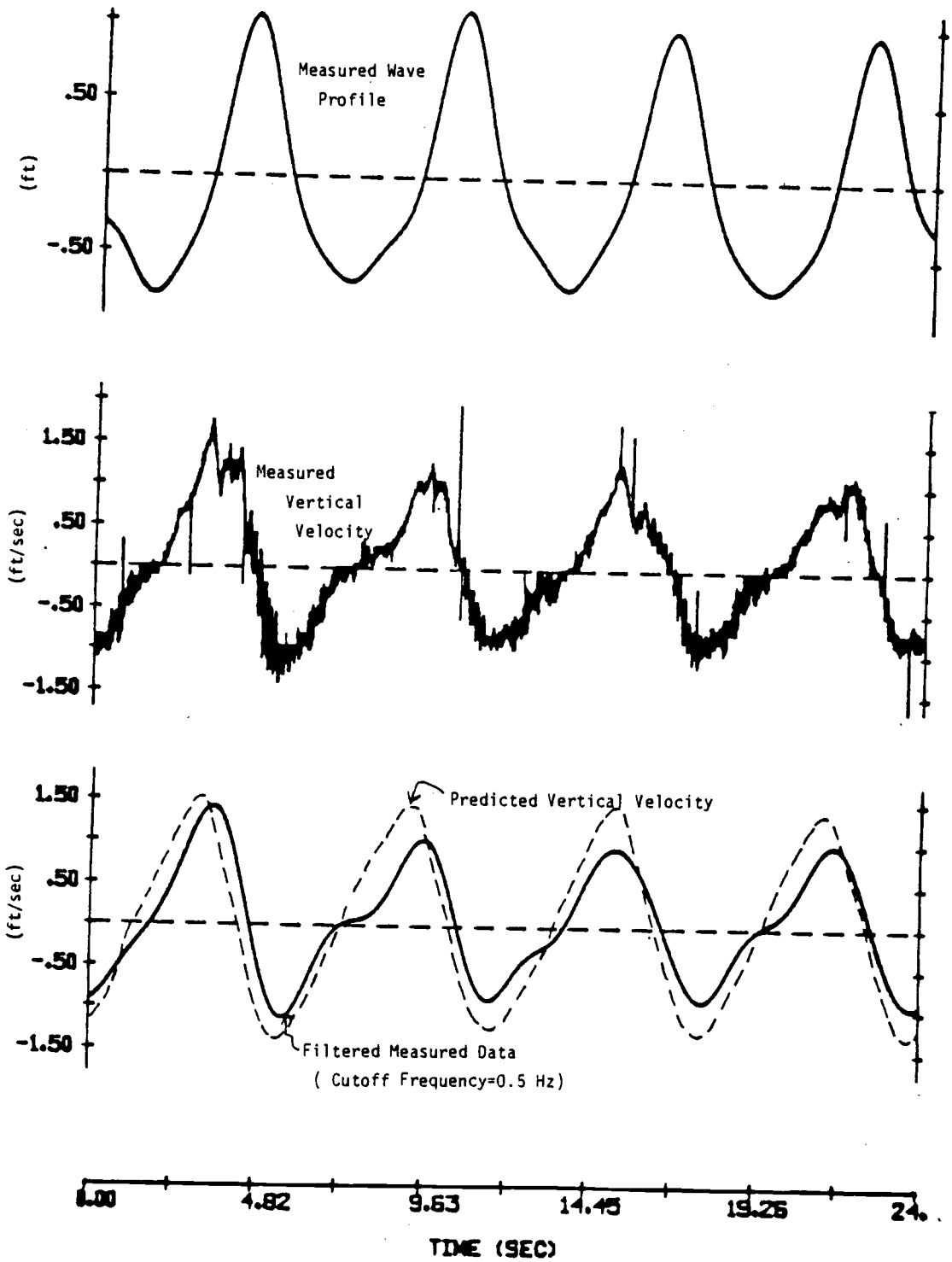

Fig. 5-16 Comparison between Predicted Values and Measured Data for the Vertical Velocity under Waves and Towing at Low Tow Speed (U=0.71 ft/sec,T=6.02 sec)

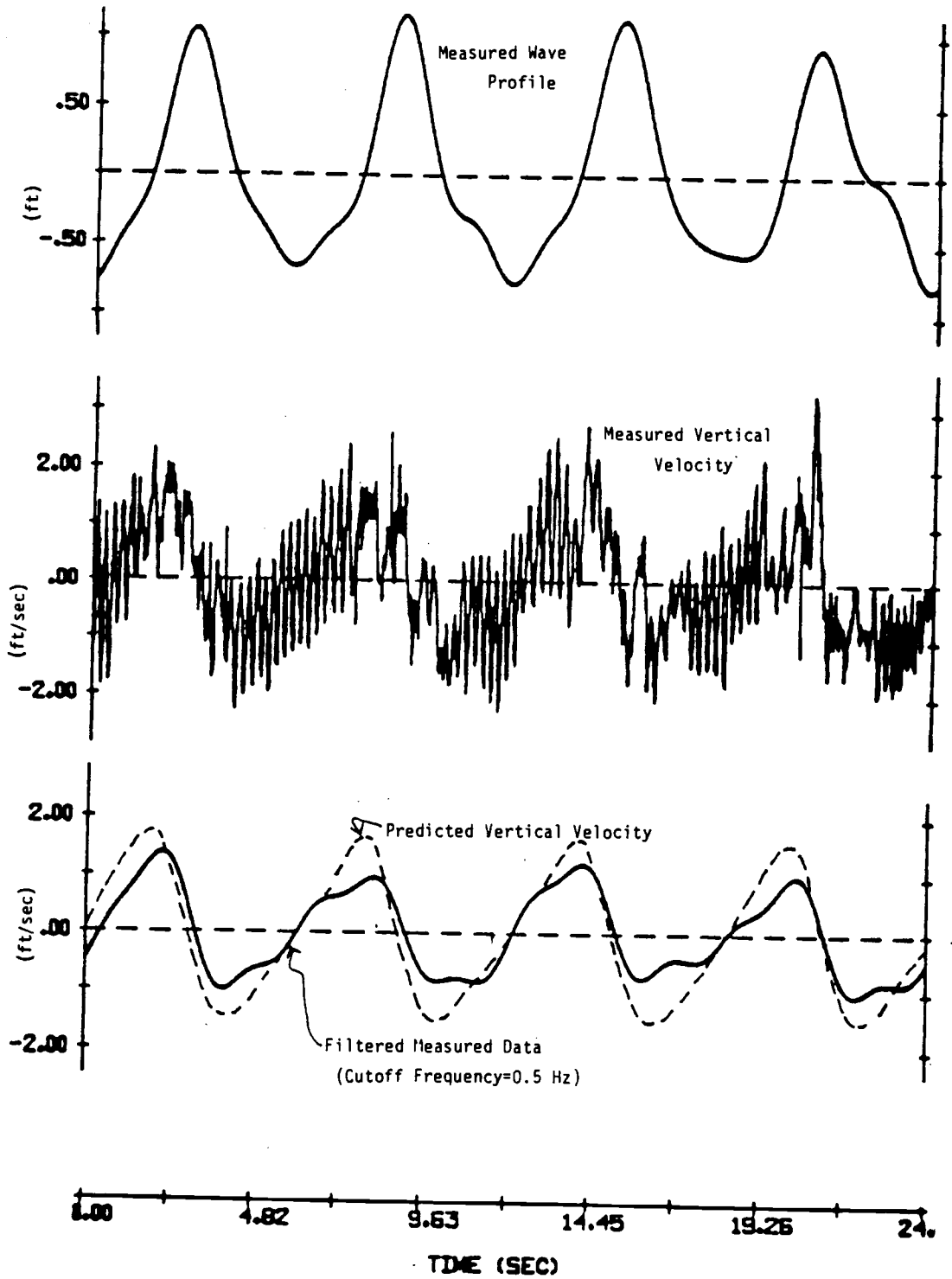

Fig. 5-17 Comparison between Predicted Values and Measured Data for the Vertical Velocity under Waves Plus Towing at High Tow Speed (U=6.25 ft/sec, T=6.02 sec)

$$\frac{(Du/Dt)\ max}{(\partial u/\partial t)\ max} = \alpha_x = \text{horizontal acceleration ratio} \qquad (5.8)$$

$$\frac{(Dw/Dt)\ max}{(\partial w/\partial t)\ max} = \alpha_z = \text{vertical acceleration ratio} \qquad (5.9)$$

The α_x and α_z together with the associated steepness parameter H/T^2 and depth parameter h/T^2 are plotted in Fig. 5-18. From this figure, it can be seen that both the horizontal and vertical maximum acceleration ratios, α_x and α_z are smaller than or equal to one. These two ratios decrease as steepness parameter increases and depth parameter decreases. In other words, the difference between total and local acceleration in both horizontal and vertical component become significant for shallow water waves and for steeper waves. This trend is the same as that indicated by Isaacson (1979) for planar oscillatory flow by using Stokes fifth-order wave theory. If linear wave theory is applied, the gross maximum acceleration ratio, α_q, will not be greater than one because the maximum horizontal acceleration occurs as the vertical acceleration is zero.

If a current is present in the wave field, the convective acceleration is affected by the current. The convective acceleration increases as the current follows the waves and decreases as the current opposes the waves. Thus, the total acceleration will be changed and the local acceleration remains unchanged. According to Eq. (2.40) and (2.41), the changes of convective acceleration are linearly proportional to the current velocity U, so the ratios α_x and α_z are also linearly proportional to the current under the same wave

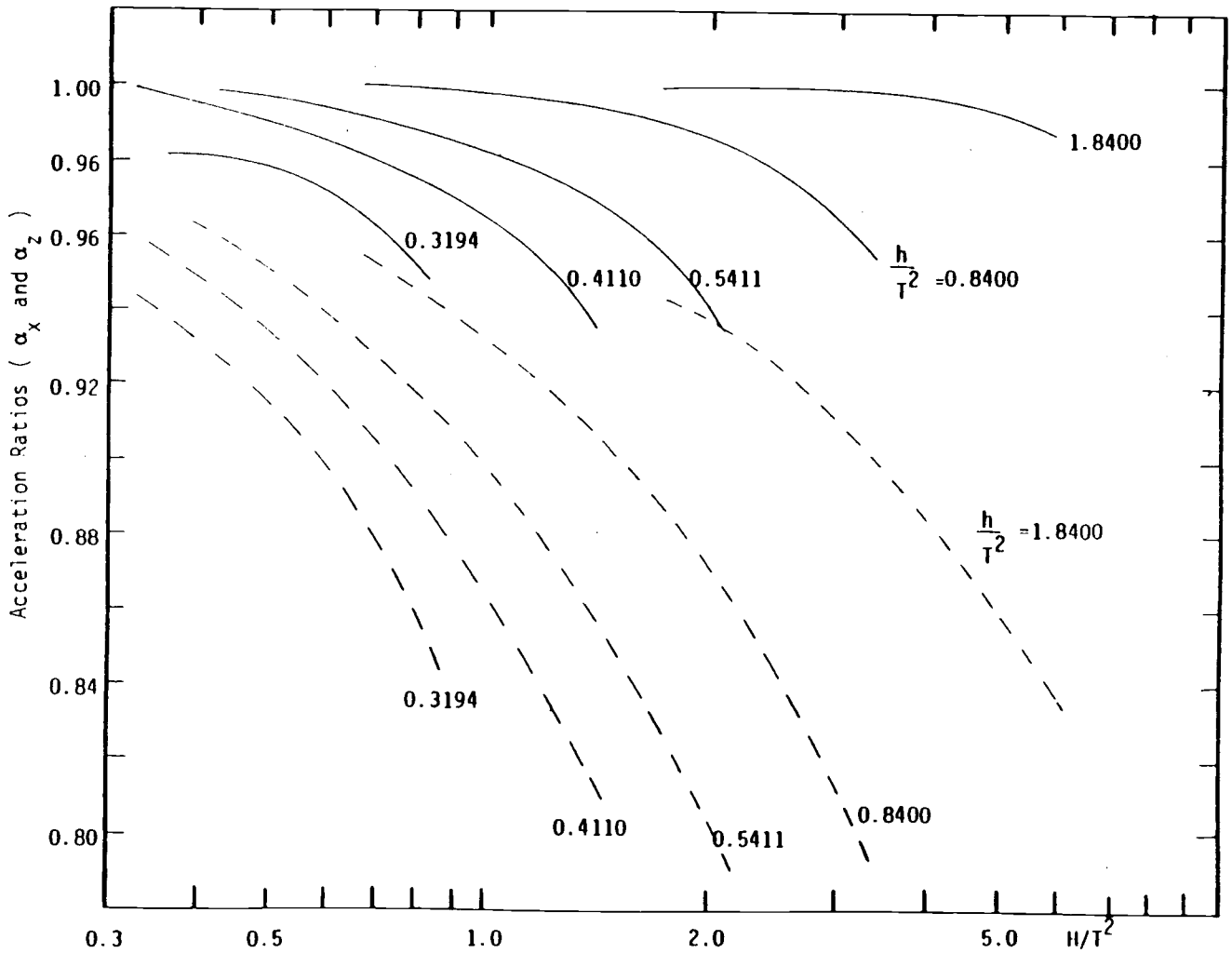

Fig. 5-18 Ratios of Total Acceleration to Local Acceleration (----: vertical; ——: horizontal)

(1) Run No.	(2) T (sec)	(3) H (ft)	(4) $\frac{Dq}{Dt}/\frac{aq}{at}$	(5) $(C_d)_{total}$	(6) $(C_m)_{total}$	(7) $(C_d)_{local}$	(8) $(C_m)_{local}$	(9) $\frac{(C_m)_{total}}{(C_m)_{local}}$	(10) RMS error		(11) $\frac{(F_p)_{max}}{(F_m)_{max}}$	
									Total	Local	Total	Local
278	2.50	1.18	1.008	0.54	0.96	0.54	0.96	1.00	0.16	0.15	0.87	0.87
280		1.75	1.015	1.39	1.65	1.39	1.64	1.01	0.19	0.21	0.81	0.80
283		3.79	1.004	0.52	1.22	0.52	1.23	0.99	0.25	0.24	0.72	0.74
284	3.70	0.99	1.001	0.53	0.97	0.53	0.97	1.00	0.21	0.22	0.74	0.73
285		2.16	0.992	0.61	1.18	0.61	1.19	0.99	0.27	0.26	0.69	0.71
286		3.35	0.980	0.55	0.79	0.55	0.80	0.99	0.38	0.37	0.70	0.73
287		4.59	0.966	0.27	1.17	0.27	1.17	1.00	0.30	0.26	0.80	0.85
288		4.64	0.966	0.35	1.13	0.35	1.13	1.00	0.34	0.30	0.80	0.86
289	4.61	1.03	0.993	0.57	0.93	0.57	0.72	1.01	0.31	0.32	0.71	0.71
290		1.85	0.989	0.67	1.11	0.67	1.10	1.01	0.31	0.31	0.31	0.68
291		3.57	0.960	0.58	0.73	0.58	0.72	1.01	0.44	0.44	0.72	0.75
292		4.40	0.943	0.40	0.99	0.40	0.96	1.03	0.40	0.39	0.85	0.90
293	5.29	0.88	0.994	0.94	0.89	0.94	0.89	1.00	0.28	0.28	0.77	0.78
294		1.59	0.984	0.51	0.79	0.51	0.78	1.01	0.34	0.34	0.68	0.70
295		2.98	0.959	0.31	0.81	0.31	0.76	1.06	0.37	0.39	0.75	0.77
296		3.71	0.939	0.53	0.87	0.53	0.83	1.05	0.30	0.29	0.92	0.95
297	6.00	1.18	0.987	1.04	1.26	1.04	1.24	1.02	0.38	0.38	0.80	0.82
298		2.01	0.975	0.67	1.00	0.67	0.98	1.02	0.32	0.32	0.86	0.88
299		2.66	0.952	0.64	1.07	0.64	1.03	1.09	0.30	0.30	0.75	0.77
300		3.01	0.949	0.63	1.22	0.63	1.16	1.05	0.29	0.29	0.87	0.89
301	3.13	3.84	0.992	0.54	1.14	0.54	1.16	0.98	0.33	0.30	0.74	0.79
302	4.17	3.85	0.963	0.58	1.18	0.58	1.16	1.02	0.37	0.36	0.94	0.98

Table 5-5

Summary of Data for a Smooth Horizontal Cylinder in Waves by Using Different Accelerations

(1) Run No.	(2) T (sec)	(3) H (ft)	(4) $\frac{Dq}{Dt}/\frac{\partial q}{\partial t}$	(5) $(C_d)_{total}$	(6) $(C_m)_{total}$	(7) $(C_d)_{local}$	(8) $(C_m)_{local}$	(9) $\frac{(C_m)_{total}}{(C_m)_{local}}$	(10) RMS error		(11) $\frac{(F_p)_{max}}{(F_m)_{max}}$	
									Total	Local	Total	Local
303	5.00	4.04	0.940	0.46	0.99	0.46	0.91	1.09	0.42	0.43	0.67	0.68
304	5.56	2.86	0.955	0.60	1.12	0.60	1.09	1.03	0.29	0.28	0.92	0.95
305	3.13	4.03	0.989	0.32	1.18	0.32	1.22	0.97	0.39	0.35	0.77	0.80
313	2.50	1.16	1.008	0.34	1.04	0.34	1.04	1.00	0.14	0.14	0.86	0.85
315		1.57	1.013	1.21	1.39	1.21	1.37	1.01	0.21	0.25	0.75	0.73
316		2.84	1.017	1.14	1.16	1.14	1.17	0.99	0.29	0.28	0.70	0.70
318		3.54	1.009	0.19	1.44	0.19	1.46	0.99	0.27	0.24	0.73	0.73
319	3.70	0.91	1.001	0.46	0.89	0.46	0.89	1.00	0.29	0.30	0.62	0.62
320		1.93	0.993	0.70	1.19	0.70	1.21	0.98	0.30	0.29	0.64	0.66
321	3.70	2.75	0.988	0.58	1.28	0.58	1.28	1.00	0.33	0.32	0.76	0.79
323		4.22	0.971	0.55	1.29	0.55	1.30	0.99	0.33	0.30	0.79	0.85
324	4.61	0.89	0.994	0.47	1.02	0.47	1.01	1.01	0.31	0.31	0.69	0.69
325		1.77	0.991	0.77	0.90	0.77	0.89	1.01	0.37	0.37	0.68	0.69
326		3.28	0.965	0.57	1.12	0.57	1.09	1.03	0.38	0.38	0.82	0.85
327		4.26	0.946	0.48	0.90	0.48	0.88	1.02	0.36	0.36	0.88	0.92
328	5.29	0.92	0.994	0.81	0.69	0.81	0.69	1.00	0.30	0.30	0.70	0.70
329		1.71	0.980	0.77	0.91	0.77	0.90	1.01	0.28	0.28	0.73	0.75
331		3.89	0.937	0.54	0.78	0.54	0.75	1.04	0.31	0.30	1.02	1.05
332	6.00	1.28	0.983	0.74	0.88	0.74	0.87	1.01	0.47	0.47	0.81	0.82
334		2.68	0.951	0.77	1.25	0.77	1.21	1.03	0.23	0.22	0.87	0.89
335		2.92	0.950	0.67	1.09	0.67	1.05	1.04	0.30	0.30	0.87	0.90
337	4.17	4.35	0.953	0.43	1.13	0.43	1.09	1.04	0.45	0.45	0.84	0.88
338	5.00	3.85	0.944	0.30	1.23	0.30	1.17	1.05	0.38	0.38	0.81	0.86
339	5.56	3.58	0.942	0.36	1.13	0.36	1.09	1.04	0.27	0.26	0.90	0.94
341	3.70	0.95	1.001	0.35	0.91	0.35	0.90	1.01	0.26	0.27	0.69	0.69

Table 5-5
(Continued)

(1) Run No.	(2) T (sec)	(3) H (ft)	(4) $\frac{Dq}{Dt}/\frac{\partial q}{\partial t}$	(5) $(C_d)_{total}$	(6) $(C_m)_{total}$	(7) $(C_d)_{local}$	(8) $(C_m)_{local}$	(9) $\frac{(C_m)_{total}}{(C_m)_{local}}$	(10) RMS error		(11) $\frac{(F_p)_{max}}{(F_m)_{max}}$	
									Total	Local	Total	Local
342	4.61	0.87	0.994	0.67	1.02	0.67	1.01	1.01	0.28	0.29	0.71	0.71
343	5.29	0.96	0.994	0.84	0.65	0.84	0.64	1.02	0.35	0.35	0.83	0.85
344	6.00	1.31	0.982	1.05	1.25	1.05	.124	1.01	0.39	0.37	0.74	0.78
345	3.70	2.84	0.986	0.56	1.01	0.56	1.02	0.99	0.48	0.48	0.93	0.96
346	4.61	3.42	0.963	0.57	0.86	0.57	0.83	1.03	0.31	0.31	0.86	0.89
347	6.00	2.69	0.951	0.61	1.12	0.61	1.08	1.04	0.29	0.30	0.83	0.86
349	5.29	3.71	0.939	0.35	1.13	0.35	1.07	1.05	0.32	0.32	0.84	0.88
350	4.61	4.12	0.949	0.32	1.22	0.32	1.16	1.05	0.31	0.31	0.75	0.76

Table 5-5
(Continued)

(1) Run No.	(2) T (sec)	(3) H (ft)	(4) U $\left(\frac{ft}{sec}\right)$	(5) $\frac{Dq/Dt}{\partial q/\partial t}$	(6) $(C_d)_{total}$	(7) $(C_m)_{total}$	(8) $(C_d)_{local}$	(9) $(C_m)_{local}$	(10) $\frac{(C_m)_{total}}{(C_m)_{local}}$	(11) RMS error Total	(11) RMS error Local	(12) $\frac{(F_p)_{max}}{(F_m)_{max}}$ Total	(12) $\frac{(F_p)_{max}}{(F_m)_{max}}$ Local
366	6.02	3.13	0.67	0.913	0.48	1.36	0.48	1.26	1.08	0.21	0.20	0.85	0.88
367	5.29	3.59	0.71	0.904	0.53	0.71	0.53	0.69	1.03	0.45	0.44	0.90	0.92
368	4.61	4.30	0.82	0.901	0.48	0.91	0.48	0.89	1.02	0.47	0.45	0.93	0.96
370	2.50	3.79	0.82	0.948	0.63	1.28	0.63	1.22	1.05	0.46	0.45	0.72	0.75
371	6.02	3.00	3.45	0.763	0.50	1.97	0.50	1.42	1.39	0.22	0.22	0.86	0.86
372	5.29	3.59	3.57	0.753	0.39	2.82	0.39	2.05	1.37	0.26	0.27	0.88	0.89
373	4.61	4.57	4.24	0.713	0.44	0.76	0.44	0.42	1.82	0.21	0.22	1.04	1.03
375	6.02	3.55	6.33	0.605	0.42	0.75	0.42	--	--	0.24	0.24	0.97	0.97
376	5.29	3.76	6.33	0.606	0.43	2.38	0.43	1.09	2.17	0.20	0.21	0.99	0.98

Table 5-6

Summary of Data for a Smooth Horizontal Cylinder under Waves and Current by Using Different Accelerations

Although the depth and the wave height effects are not considered, the effects of current on the acceleration ratios α_x and α_z still can be easily observed in Fig. 5-19.

For comparison, the C_d and C_m values are determined from the least squares technique by using the total and local acceleration in inertia term respectively. It can be observed from Table 5-5 that all of the C_d values remain unchanged no matter which acceleration is used. This phenomenon also holds for the waves and current condition (see Table 5-6). The C_m values have a small variation up to 9% for waves only. From an engineering design point of view, this small variation may make no difference due to the use of a safety factor. From Fig. 5-20, if α_q is near 1.0, the C_m values obtained by using the total acceleration are almost the same as those using the local acceleration. When α_q decreases, i.e., for shallow waters waves and steeper waves, the C_m value obtained by using the total acceleration are larger than those obtained with the local acceleration.

As a current is introduced into the wave field, the signficant difference of the C_m values, between using the two different accelerations, can be found in Table 5-6. From Fig. 5-21, it is evident that the difference between the two sets of C_m values becomes larger as the current velocity increases. As stated in Section 2.5, the inertia term compared with the drag term may be neglected if the current velocity is large enough. Under this circumstance, it is not very important to quantify the inertia coefficient precisely. In

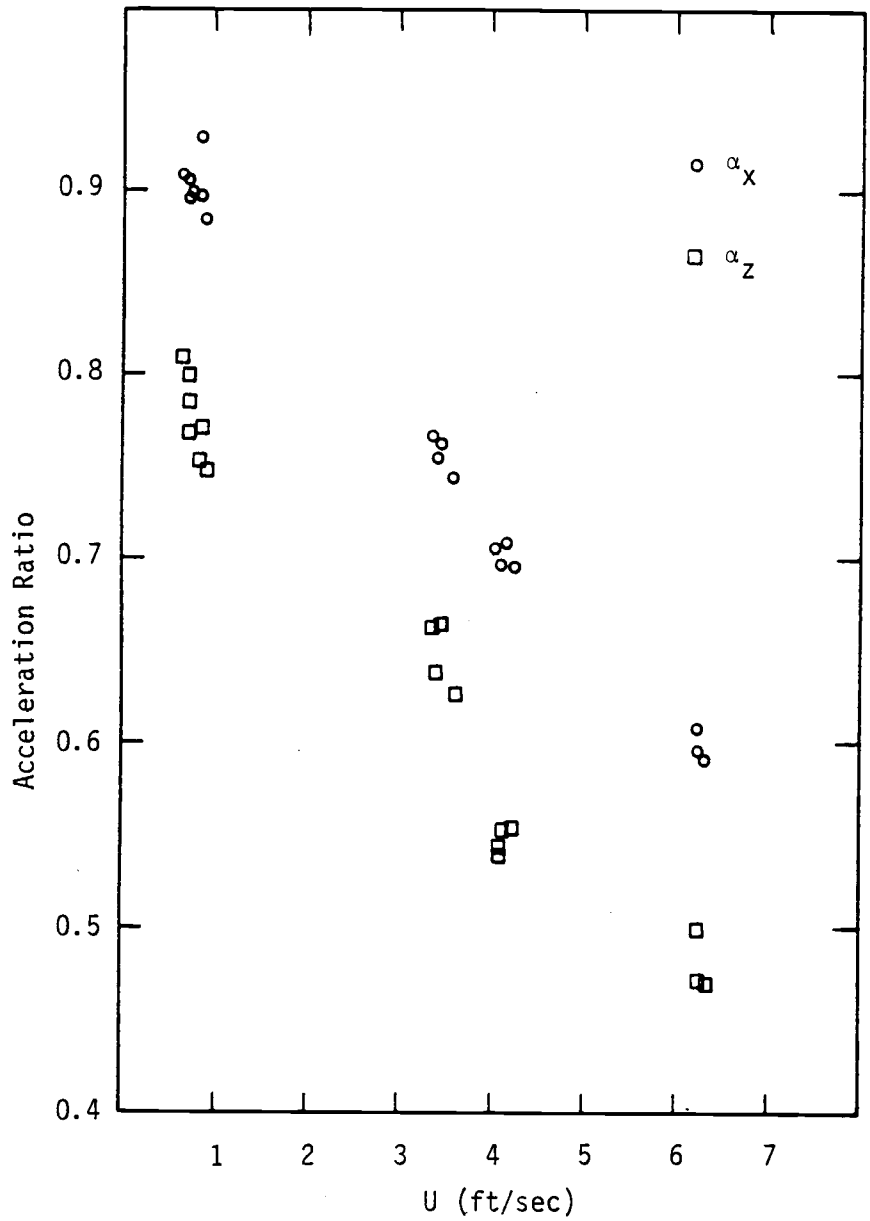

Fig. 5-19 Influence of current velocity on acceleration ratio α_x and α_z

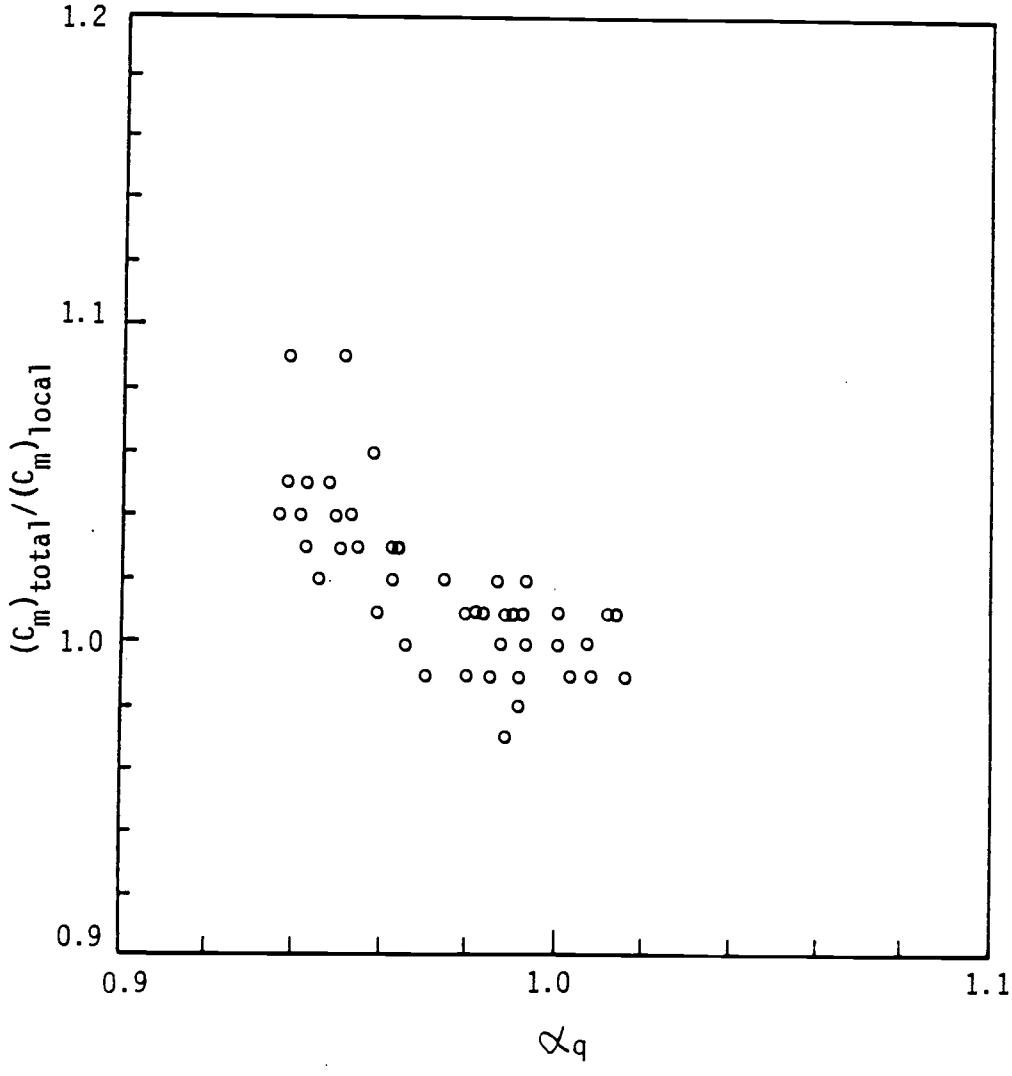

Fig. 5-20 Acceleration Ratio vs. C_m's Ratio

(Waves only)

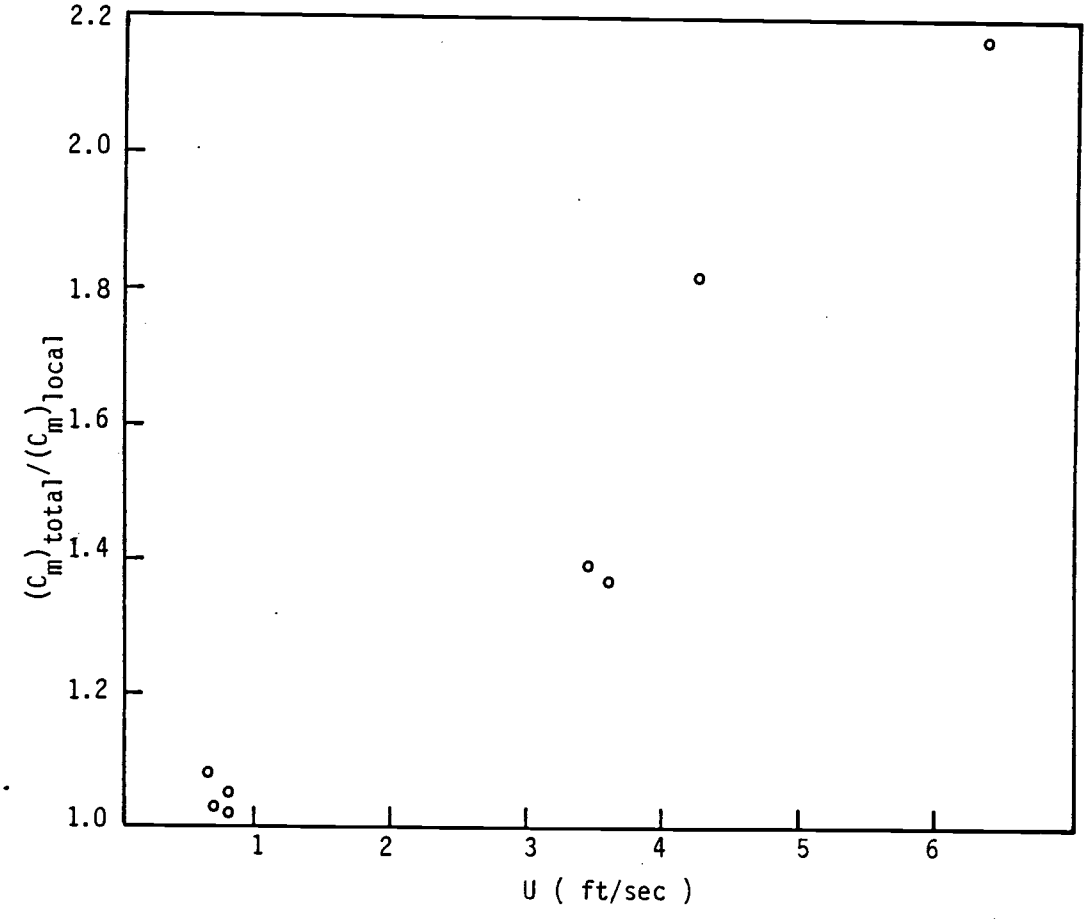

Fig. 5-21 Effect of Current on C_m's Ratio

Table 5-7, with the same wave period (T=6.02 sec.) and wave height (H=3.10 ft), the ratio of drag and inertia component of maximum predicted force $(Fmax)_D/(Fmax)_I$ increases from 1.30 to 27.11 as current velocity increases from 0 ft/sec to 6.33 ft/sec. This shows the inertia term becomes less important as the current velocity increases. For U = 6.33, the ratio of the maximum drag force to the maximum force is 1.00 and the ratio of the total drag force to the total force is 1.00. In other words, the total force can be predicted by using the drag force only for a large current velocity and the inertia force is negligible.

To compare the predicted force obtained by using the total acceleration with that obtained by using the local acceleration, two indicators are used: (1) The root-mean-square error between measured force and predicted force for the whole wave cycle, and (2) the ratio of maximum predicted force to maximum measured force in one wave cycle. These two indicators for all of the test runs are shown in Table 5-5 (Column 10 and 11) and Table 5-6 (Column 11 and 12). It can be observed that force predictions by using the local acceleration seem a little bit better than those from using the total acceleration for most of the runs in the present study. However, there is no significant difference between using the total acceleration and using the local acceleration for force prediction through the detailed check of the force data.

Run No.	T (sec)	H (ft)	U ($\frac{ft}{sec}$)	$(F_{max})_D$ (lbs)	$(F_{max})_I$ (lbs)	F_{max} (lbs)	$\frac{(F_{max})_D}{(F_{max})_I}$	$\frac{(F_{max})_D}{F_{max}}$	$(F_D)_{total}$ (lbs)	$(F_I)_{total}$ (lbs)	F_{total} (lbs)	$\frac{(F_D)_{total}}{(F_I)_{local}}$	$\frac{(F_D)_{total}}{F_{total}}$
300	6.00	3.01	0	6.59	5.08	8.27	1.30	0.80	90.42	106.69	146.11	0.85	0.62
366	6.02	3.13	0.67	8.24	5.71	8.90	1.44	0.93	85.54	118.62	153.46	9.72	0.56
371	6.02	3.00	3.45	26.32	6.59	26.59	3.99	0.99	351.83	138.84	360.64	2.53	0.98
375	6.02	3.55	6.33	56.12	2.07	56.13	27.11	1.00	752.85	41.77	753.08	18.02	1.00

Table 5-7

Influence of Current on the Force Prediction

6. CONCLUSIONS

The force coefficients for a horizontal cylinder in waves or under waves and current are smaller than those obtained for a horizontal cylinder under planar oscillatory flow due to the orbital motion of water particles around the centerline of the cylinder. That implies that the vertical component of water particle velocity and the ratio w_m/u_m play an important role in determining the force coefficients for the horizontal cylinder. This trend holds for both smooth and sand roughened cylinders.

The drag coefficient for sand roughened cylinder is larger than that for smooth cylinders in waves or in waves and current.

Except for Reynolds number, the dimensionless parameters VM and U/u_m are very important for determining the force coefficients under waves plus towing (or waves and current). The definition of Keulegan-Carpenter number for waves and towing is still questionable. For large VM number or U/u_{wm}, i.e., for large current velocity (or towing speed), the drag coefficient for waves and current is the same as that for steady flow.

An indicator, RR, with associated criteria, is proposed to examine whether the test condition is suitable for determining the force coefficients of a smooth horizontal cylinder in wavy flow. For the sand roughened cylinder, the criterion may vary with the relative roughness ε/D.

Through theoretical and experimental examination of the kinematics acting on a horizontal cylinder, it is concluded that the forces from waves and current can be simulated by those from towing a horizontal cylinder in a wave field if the linear superposition principle is assumed.

There is little difference between the total and local acceleration in deep water. The difference becomes significant for shallow water and steeper waves. The drag coefficients are unchanged no matter whether the total acceleration or local one is used. The difference between C_m's obtained by using these two different accelerations is small for waves only and increases as the current velocity (or towing speed) increases. However, there is no evident difference for the force prediction.

REFERENCES

1. Achenback, E., (1971), "Influences of Surface Roughness on the Cross-Flow around a Circular Cylinder," J. of Fluid Mechanics, Vol. 46, Pt. 2, pp:321-336.

2. Bernitsas, M. M. (1979), "Analysis of the Hydrodynamic Force Exerted on a Harmonically Oscillating Circular Cylinder in any Direction with Respect to a Uniform Current," BOSS'79, pp:323-338.

3. Bishop, J. R. (1978), "The Mean Square Value of Wave Force Based on the Morison Equation," National Maritime Institute Report, No. 40, January, OT-R-7811.

4. Dalrymple, R. A. (1973), "Water Wave Models and Wave Forces with Shear Current," Tech. Report No. 20, Coastal Oceanography Engr. Lab., U. or Florida, Gainesville, Florida.

5. Dean, R. G. (1976), "Methodology for Evaluating Suitability of Wave and Wave Force Data for Determining Drag and Inertia Coefficients," BOSS'76, pp:40-64.

6. Dean, R. G. (1979), "Kinematics and Forces Due to Wave Groups and Associated Second-Order Currents," BOSS'79, pp:87-94.

7. Garrison, C. J., Field, J. B., and May, M. D. (1977), "Drag and Inertia Forces on a Cylinder in Periodic Flow," J. of Waterways, ASCE, May, WW2, pp:193-204.

8. Garrison, C. J. (1980), "A Review of Drag and Inertia Forces on Circular Cylinders," OTC No. 3760, pp:205-218.

9. Greenamyer, R. D. (1973), "Unidirectional Periodic Flow about Circular Cylinders," Master Thesis, Naval Postgraduate School, Monterey, CA.

10. Hedges, T. S. (1979), "Measurement and Analysis of Waves on Currents," Mechanics of Wave-Induces Forces on Cylinders (ed. by T.L. Shaw), pp:249-259, Pitman Co.

11. Hogben, N., Miller, B.L., Searle, J. W. and Ward, G. (1977), "Estimation of Fluid loading on Offshore Structures," Proc. Institute Civil. Engr., Part 2, 63, Sept., pp: 515-562.

12. Holmes, P., and Chaplin, J. R. (1978), "Wave Loads on Horizontal Cylinders," 16th of Coastal Engineering, August, Hamburg, Germany.

13. Isaacson, M. (1979), "Nonlinear Inertia Forces on Bodies," J. of Waterway, ASCE, Aug., WW3, pp:213-227.

14. Kim, Y. Y., Hibbard, H. C. (1975), "Analysis of Simultaneous Wave Force and Water Particle Velocity Measurements," OTC No. 2192, pp. 461.

15. Longuit-Higgins, M.S., and Stewart, R. W. (1960), "Changes in the Amplitude of Short Gravity Waves on Steady Non-uniform Currents," J. of Fluid Mechanics, Vol. 10, pp:529-549.

16. Maull, D. J., and Norman, S. G. (1978), "A Horizontal Circular Cylinder Under Waves," Mechanics of Wave-Induced Forces on Cylinders (ed. by T. L. Shaw), Pitman Co., pp:359-378.

17. Mercier, J. A. (1973), "Large Amplitude Oscillations of a Circular Cylinder in Low-Speed Stream," Ph.D. Dissertation, Stevens Institute of Technology, Castle Point, Hoboken, N.J.

18. Miller, B. L. (1977), "The Hydrodynamic Drag of Roughened Circular Cylinder," Jour. Royal Institute of Naval Architects, RINA, Vol. 119, pp:65-70.

19. Moe, G., and Verley, R. L. P. (1978), "An Investigation into the Hydrodynamic Damping of Cylinders Oscillated in Steady Currents of Various Velocities," VHL Report STF 60 A 78049, Norwegian Institute of Technology.

20. Morison, J. R., O'Brien, M. P., Johnson, J. W., and Schaaf, S. A. (1950), "The Force Exerted by Surface Wave on Piles," Petroleum Transactions, AIME, Vol.189, pp:149-157.

21. Nath, J. H., and Yamamoto, T. (1974), "Forces from Fluid Flow around Objects," 14th Coastal Engr. Conference, Copenhagen, Denmark, Chap. 106, pp:1808-1827.

22. Nath, J. H. (1981a), "Hydrodynamic Coefficients for Cylinders with Pronounced Marine Growths," Final Report to API.

23. Nath, J. H. (1981b), "Hydrodynamic Coefficients for Macro-Roughnesses," OTC No. 3989, pp:189-208.

24. Nath, J. H. (1982), "Heavily Roughened Horizontal Cylinders in Waves," BOSS'82, M. I. T.

25. Nath, J. H. (1983), "Hydrodynamic Coefficients for Cylinders with Pronounced Marine Growths," A Final Report to API.

26. Peregrine, D. H. (1976), "Interaction of Water Waves and Currents," Advances in Applied Mechanics, Vol. 16, pp:9-117.

27. Ramberg, S. E., and Niedzwecki, J. M. (1982), "Horizontal and Vertical Cylinders in Waves," Ocean Engr., Vol. 9, No.1, pp:1-15.

28. Sarpkaya, T. (1976), "Vortex Shedding and Resistance in Harmonic Flow about Smooth and Rough Cylinders at High Reynolds Numbers," Report No. NPS-59 SL76021, U.S. Naval Post Graduate School, Monterey, CA.

29. Sarpkaya, T. (1977), "In-line and Transverse Forces on Cylinders near a Wall in Oscillatory Flow at High Reynolds Numbers," OTC No. 2898, pp. 161-166.

30. Sarpkaya, T, and Isaacson, M. (1981), "Mechanics of Wave Forces on Offshore Structures," Van Nostrand Reinhold Co.

31. Sarpkaya, T. (1982): Personal Communication

32. Tung, C. C., and Huang, N. E. (1973), "Combined Effects of Current and Waves on Fluid Force," Ocean Engr., Vol 2, pp:183-193.

33. Verley, R. L. P., and Moe, G. (1978), "The Effect of Cylinder Vibration on the Drag Force and the Resultant Hydrodynamic Damping," Mechanics of Wave-Induced Forces on Cylinders (ed. by T. L. Shaw).

34. Verley, R. L. P., and Moe, G. (1979), "The Forces on a Cylinder Oscillating in a Current," VHL Report STF60 A79061, Norwegian Institute of Technology.

35. Wankmuller, R. N. and Nath, J. H. (1982), "Wave and Current Forces on Kelp Covered Cylinder," A Final Report to the OSU Seat Grant College Program.

36. Yamamoto, T., and Nath, J. H. (1976), "High Reynolds Number Oscillating Flow by Cylinders,"15th Coastal Engr. Conference, Honolulu, Hawaii, Chap. 136, pp:2321-2340.

APPENDIX A.

Comparison of Force Coefficients Obtained through Different Techniques

Consider the Morison equation for one-dimensional flow.

$$\frac{F}{L} = C_d \frac{\rho}{2} D u|u| + C_m \frac{\rho \pi D^2}{4} \frac{\partial u}{\partial t} \tag{A.1}$$

If linear wave theory is used, we have the following relations:

$$u = u_m \cos\omega t \tag{A.2}$$

$$\frac{\partial u}{\partial t} = -u_m w \sin\omega t \tag{A.3}$$

In which u_m is the maximum horizontal velocity and $\omega = 2\pi/T$ is the angular wave frequency.

Substituting Eq. (A.2) and Eq. (A.3) into Eq. (A.1), we have

$$F = C_d \frac{\rho D}{2} \cdot L \cdot u_m^2 \cos\omega t|\cos\omega t| - C_m \frac{\rho \pi D^2}{4} L \omega u_m \sin\omega t \tag{A.4}$$

Because the total force is composed of drag force and inertia force, the following expression can be used if linear wave theory is used.

$$F = F_{Dm} \cos\omega t \ |\cos\omega t| + F_{Im} \sin\omega t \tag{A.5}$$

in which F_{Dm} is the maximum drag force in one wave cycle and F_{Im} is the maximum inertia force.

Three different techniques for determining the force coefficients C_d and C_m are discussed: (i) Fourier-averaged method, (ii) Least square method, and (iii) Maximum kinematics and dynamics method.

(I) Fourier-averaged Method:

Multiplying both sides of Eq. (A.4) by $\cos\omega t$ and integrating over one wave cycle (from 0 to 2π), the C_d can be obtained.

$$C_d = \frac{3}{4} \int_0^{2\pi} \frac{F \cos\omega t}{\rho L u_m{}^2 D} d\omega t \tag{A.6}$$

Again, multiplying Eq. (A.4) by $\sin\omega t$ and integrating from 0 to 2π, the C_m value is determined

$$C_m = \frac{-2u_m T}{\pi^3 D} \int_0^{2\pi} \frac{F \sin\omega t}{\rho L u_m{}^2 D} d\omega t \tag{A.7}$$

If Eq. (A.5) is introduced into Eq. (A.6) and Eq. (A.7), we have

$$C_d = \frac{3}{4} \frac{1}{\rho L u_m{}^2 D} \int_0^{2\pi} [F_{Dm} \cos\omega t \, |\cos\omega t| + F_{Im} \sin\omega t] \cos\omega t \, d\omega t$$

$$= \frac{2}{\rho L u m^2 D} F_{Dm} \tag{A.8}$$

$$C_m = \frac{-2u_m T}{\pi^3 D} \frac{1}{\rho L u_m^2 D} \int_0^{2\pi} [F_{Dm}\cos\omega t\ |\cos\omega t| + F_{Im}\sin\omega t]\ \sin\omega t\ d\omega t$$

$$= \frac{2T}{\pi^2 D^2 \rho L u_m} F_{Im} \qquad ((A.9)$$

(II) Least Square Method:

The mean square error betwen the measured and predicted force is defined as

$$\overline{E^2} = \frac{1}{2\pi} \int_0^{2\pi} (F-F_p)^2\ d\omega t \qquad (A.10)$$

where the predicted force F_p is evaluated by Eq. (A.4).

To determine C_d and C_m, the $\overline{E^2}$ is minimized by taking the derivative with respect to each coefficient. That is

$$\frac{\partial \overline{E^2}}{\partial C_d} = 0 \qquad (A.11)$$

and

$$\frac{\partial \overline{E^2}}{\partial C_m} = 0 \qquad (A.12)$$

Through some calculations, the following results are obtained.

$$C_d = \frac{8}{3\pi} \int_0^{2\pi} \frac{F\ \cos\omega t\ |\cos\omega t|}{\rho D L u_m^2}\ d\omega t \qquad (A.13)$$

and

$$C_m = \frac{-2u_m T}{\pi^3 D} \int_0^{2\pi} \frac{F \sin\omega t}{\rho u_m^2 LD} \, dwt \qquad (A.14)$$

Again, substituting Eq. (A.5) into Eq. (A.13) and Eq. (A.14), we have

$$C_d = \frac{8}{3\pi} \frac{1}{\rho D L u_m^2} \int_0^{2\pi} [F_{Dm} \cos\omega t \, |\cos\omega t| + F_{Im} \sin\omega t] \cos\omega t \cos\omega t \, d\omega t$$

$$= \frac{2}{\rho D L u_m^2} F_{Dm}$$

$$C_m = \frac{-2u_m T}{\pi^3 D} \frac{1}{\rho L u_m^2 D} \int_0^{2\pi} [F_{Dm} \cos\omega t \, |\cos\omega t| + F_{Im} \sin\omega t] \sin\omega t \, d\omega t$$

$$= \frac{2T}{\pi^2 D^2 \rho L u_m} F_{Im} \qquad (A.16)$$

(III) Maximum Kinematics and Dynamics Method:

This method assumes that when the velocity is maximum (acceleration is zero according to linear wave theory), only drag force exists. And only inertia force exists when acceleration is maximum (velocity is zero).

When velocity is maximum ($\theta = 0^o$ in our case),

$F = C_d \frac{\rho D}{2} \cdot L \cdot u_m^2$ and $F = F_{Dm}$. Thus

$$C_d = \frac{2}{\rho D L u_m^2} F_{Dm} \tag{A.17}$$

When acceleration is maximum ($\theta=90^o$ in our case),

$F= C_m \frac{\rho \pi D^2}{4} LWu_m$ and $F = F_{Im}$. Thus

$$C_m = \frac{4}{\rho \pi D^2 L u_m W} F_{Im}$$

$$= \frac{2T}{\rho \pi^2 D^2 L u_m} F_{Im} \tag{A.18}$$

Comparing the C_d values [Eq. (A.8), (A.15) and (A.17)] and C_m values [Eq. (A.9), (A.16),(A.18)], conclusion can be drawn that although these three different techniques are used, the C_d and C_m values should be the same if linear wave theory is used.

APPENDIX B

LIST OF NOTATIONS

a	Wave amplitude
a_o	Wave amplitude in quasi-still water
C_d	Drag coefficient
C_m	Inertia coefficient
C_r	Relative wave velocity with respect to coordinates moving with U
C_x	In-line force coefficient [Eq. (2.33)]
C_z	Transverse force coefficient [Eq. (2.34)]
C	Wave celerity ($C=\omega/K$)
C_g	Group velocity ($C_g = d\omega/dk$)
D	Diameter of circular cylinder
d	Distance between water surface and upper face of cylinder
E	Total error
E	Wave energy
E rms	Root-mean-square error [Eq.(5.6)]
E_x	Error is x direction
E_z	Error in z direction
$\overline{E^2}$	Mean square error
e	Distance between bottom and lower face of cylinder
F	Wave force
F_x, F_z	Wave force in horizontal and vertical direction
F_D	Drag force

F_{Dx}, F_{Dz}	Drag force in horizontal and vertical direction
F_I	Inertia force
F_{Ix}, F_{Iz}	Inertia force in horizontal and vertical direction
F_{xm}, F_{zm}	Measured force in horizontal and vertical direction
F_{xp}, F_{zp}	Predicted force in horizontal and vertical direction
f	Wave frequency
g	Gravitational acceleration
H	Wave height
h	Water depth
K	Keulegan-Carpenter number $(= \frac{u_{mT}}{D})$
k	Wave number $(= 2\pi/L)$
L	Wave length
L_o	Wave length in deep water
NN	The order of stream function wave theory
n	Wave frequency $(=1/T)$
OF	Objective function [Eq. (2.6)]
P	Pressure
Q	Bernoulli constant
q	Total velocity
q'	Total acceleration
R	Reynolds number $(=uD/\nu)$
RR	Ratio to examine the suitability of data for determining force coefficients
T	Wave period
Tap	Apparent wave period [Eq. (3.1)]

t	Time scale
t_{ap}	Apparent time scale [Eq. (3.2)]
$U(z)$	Horizontal current at vertical elevation
U_b	Current velocity at the bottom
U_s	Current velocity at the free surface
u	Horizontal component of water particle velocity
u_m	Maximum horizontal velocity
u_w	Horizontal velocity induced by waves only
u_{wm}	Maximum wave-induced horizontal velocity
u'	Horizontal component of water particle acceleration
VM	Verley and Moe number (= UT/D)
w	Vertical component of water particle velocity
w_m	Maximum vertical velocity
w_w	Vertical velocity induced by waves only
w_{wm}	Maximum wave-induced vertical velocity
w'	Vertical component of water particle acceleration
x	Horizontal Coordinate
$X(n)$	Stream function coefficients
z	Vertical coordinate, direction measured positive upwards from still water level
α_q	Gross acceleration ratio [Eq. (5.7)]
α_x	Horizontal acceleration ratio [Eq. (5.8)]
α_z	Vertical acceleration ratio [Eq. (5.9)]
β	Frequency parameter ($=D^2/\nu T$)

γ	Specific weight of water
ε	Surface roughness of the cylinder
η	Water surface elevation
Θ	Phase angle ($=2\pi t/T$)
λ	Parameter (inversion of VM)
λ_1, λ_2	Lagrangian multipliers
ν	Kinematic viscosity
ρ	Density of water
Φ	Velocity potential
Ψ	Stream function
σ	Relative wave frequency
ω	Angular wave frequency ($=2\pi/T$)
μ	Dynamic viscosity